SISSA
Scuola
Internazionale
Superiore di
Studi Avanzati

Neuroscience Area – PhD course in

Molecular Biology

SERPINA3/SerpinA3n role in prion diseases

Candidate:

Marco Zattoni

Advisor:

Professor Giuseppe Legname

Academic Year 2020-21

ABSTRACT

Prion diseases are a family of rare and fatal neurodegenerative disorders, characterized by the accumulation of abnormally folded prion protein. Previous data suggested that SERPINA3/SerpinA3n might be involved in the pathogenesis and the progression of prion diseases.

Serpins represent the most broadly distributed superfamily of proteases inhibitors. They contribute to a variety of physiological functions and any alterations of the serpin-protease equilibrium can lead to pathological consequences. Besides prion diseases, SERPINA3 dysregulation has been associated with other neurodegenerative disorders, such as Alzheimer's disease.

The hypothesis supporting SERPINA3/SerpinA3n involvement in prion diseases could reside in its upregulation upon prion inoculation, which will be responsible to a decrease activity of the protease(s) involved in the clearance of the pathological prion aggregates.

The differential expression of other serpin superfamily members has been investigated in human frontal cortex samples of sporadic cases of Creutzfeldt-Jakob disease and in an animal models of prion disease. Besides the already observed *SERPINA3* upregulation, *SERPINB1*, *SERPINE1*, *SERPINB6*, *SERPING1*, *SERPINH1* and *SERPINI1* were dysregulated in prion-infected individuals compared to age-matched controls. Together with the previously known *SerpinA3n* increased expression, prion-infected mice showed the upregulation of *SerpinF2*. Therefore, among the differentially regulated serpins, SERPINA3/SerpinA3n is the only member highly dysregulated in both prion-infected human and murine samples, suggesting its potential role in diseases progression.

SerpinA3n protein and transcript expression has been confirmed in chronically prion-infected immortalized cells. Interestingly, slight changes in prion levels have been observed upon SerpinA3n modulation in infected cells. Finally, prion inoculation of SerpinA3n depleted mice has been performed to observe their survival and incubation period compared to prion inoculated wild type mice. Although no differences have been observed between transgenic and wild-type mice, possible compensatory effects given by the upregulation of another serpins' member, *SerpinI1*, would explain the unaltered prion clearance.

However, these results suggest SERPINA3/SerpinA3n as a novel potential therapeutic target, opening the way for future therapies aimed to boost the clearance of protein aggregates responsible for prion and other neurodegenerative diseases.

List of publications

Original Articles

1) Vanni S, Moda F, **Zattoni M**, Bistaffa E, De Cecco E, Rossi M, Giaccone G, Tagliavini F, Haïk S, Deslys JP, Zanusso G, Ironside JW, Ferrer I, Kovacs GG, Legname G. Differential overexpression of SERPINA3 in human prion diseases. Sci Rep. 2017 Nov 15;7(1):15637. doi: 10.1038/s41598-017-15778-8
2) Vanni S*, **Zattoni M***, Moda F, Giaccone G, Tagliavini F, Haïk S, Deslys J-P, Zanusso G, Ironside JW, Carmona M, Ferrer I, Kovacs GG and Legname G (2018) Hemoglobin mRNA Changes in the Frontal Cortex of Patients with Neurodegenerative Diseases. Front Neurosci. 12:8. doi: 10.3389/fnins.2018. 00008

   * These authors have contributed equally to this work
3) **Zattoni M**, Garrovo C, Xerxa E, Spigolon G, Fisone G, Kristensson K, Legname G. NMDA Receptor and L-Type Calcium Channel Modulate Prion Formation. Cell. Mol Neurobiol. 2021 Jan;41(1):191-198. doi: 10.1007/s10571-020-00834-1
4) Scialò C, Celauro L, **Zattoni M**, Tran T H, Bistaffa E, Moda F, Kammerer R, Buratti E, Legname G. The Cellular Prion Protein Increases the Uptake and Toxicity of TDP-43 Fibrils. *Viruses* 2021,*13*,1625. https://doi.org/ 10.3390/v13081625

Review

1) Vanni S, Colini Baldeschi A, **Zattoni M**, Legname G. Brain aging: A Ianus-faced player between health and neurodegeneration. J Neurosci Res. 2019 Jan 11. doi: 10.1002/jnr.24379.
2) Colini Baldeschi A, Vanni S**, Zattoni M**, Legname G. Novel regulators of PrPC expression as potential therapeutic targets in prion diseases. Expert Opin Ther Target. 2020 Aug; 24(8):759-776.doi: 10.1080/14728222.2020.1782384.
3) **Zattoni M** & Legname G (2021) Tackling prion diseases: a review of the patent landscape, Expert Opin Ther Pat, DOI: 10.1080/13543776.2021.1945033

List of abbreviations

COVID-19: coronavirus disease 2019

AD: Alzheimer's disease

CNS: central nervous system

Aβ: amyloid-β

PD: Parkinson's disease

MSA: multiple system atrophy

TDP43: TAR DNA-binding protein 43

ALS: Amyotrophic Lateral Sclerosis

FTD: Frontotemporal Dementia

SCA: Spinocerebellar Ataxia

TSEs: Transmissible Spongiform Encephalopathies

PrP^{C}: cellular prion protein

PrP^{Sc}: "scrapie" prion protein

GPI: glycosylphosphatidylinositol

ADAM: disintegrins and metalloproteinases

CSF: cerebrospinal fluid

KO: knockout

NMDAR: N-methyl-d-aspartate receptor

NCAM: neural cell adhesion molecule

LPR: laminin precursor receptor

PK: proteinase K

WB: Western Blot

4RβS: 4-rung β solenoid

PIRIBS: parallel in-register intermolecular β sheets

cryo-EM: cryogenic electron microscopy

BSE: Bovine Spongiform Encephalopathy

vCJD: variant Creutzfeldt-Jakob disease

CWD: Chronic Wasting Disease

SNP: single nucleotide polymorphism

VPSPr: Variably Protease-Sensitive Prionopathy

OPRI: octapeptide repeat insertion

OPRD: octapeptide repeat deletion

gCJD: genetic CJD

FFI: Fatal Familial Insomnia

GSS: Gerstmann–Sträussler–Scheinker Syndrome

iCJD: iatrogenic CJD

EEG: electroencephalography

hGH: human pituitary-derived growth hormones

PSWCs: periodic short-wave complexes

MRI: magnetic resonance imaging

PMCA: Protein Misfolding Cyclic Amplification

RT-QuIC: Real-time Quaking Induced Conversion

ThT: thioflavin-T

NMR: nuclear magnetic resonance

N2a: neuroblastoma-derived cells

GT1: hypothalamic gonadotropin-releasing hormone immortalized neuronal cells

RML: Rocky Mountain Laboratory

RT-qPCR: reverse transcription quantitative polymerase chain reaction

RCL: reactive centre loop

HSP47: heat-shock protein 47

RT: room temperature

CM: conditioned medium

t-PA: tissue-type plasminogen activator

Table of contents

1. INTRODUCTION

Despite the coronavirus disease 2019 (COVID-19) pandemic, global life expectancy is showing a sustained increase over the last four decades (Andrasfay and Goldman 2021, Ritchie and Barria 2021). According to World Population Prospects 2019, the number of people above age 65 is projected to double by 2050 (United Nations 2019).

With an increase in the elderly population, the number of people affected by age-related health disorders will also increase. Unfortunately, together with the common changes, including hearing loss, visual acuity decrease and muscle mass and strength decline, aging is accompanied by an increased risk for the development of different conditions such as cardiovascular diseases, cancer and dementia (Jaul and Barron 2017).

Nowadays, around 50 million people suffer from dementia and this number is projected to increase to 152 million by 2050 (Patterson 2018). Dementia is defined by chronic, acquired loss of cognitive abilities beyond what might be expected from normal aging. Pathologically, dementia is frequently caused by a combination of cerebrovascular and neurodegenerative diseases (Arvanitakis, Shah et al. 2019).

1.1 Neurodegenerative diseases

The aging process itself has the most impact among the many risk factors for neurodegenerative diseases (Hou, Dan et al. 2019), such as Alzheimer's disease (AD) and Lewy body disease, which are the most common cause of dementia (Arvanitakis, Shah et al. 2019). Neurodegenerative diseases are incurable debilitating conditions mainly characterized by the accumulation of misfolded proteins in the central nervous system (CNS) (Peng, Trojanowski et al. 2020). Abnormal processing of misfolded proteins can lead to their accumulation in the form of amyloids, defined as fibrillar, proteinaceous, congophilic deposits that birefringe in cross-polarized light (Iadanza, Jackson et al. 2018). They are able to alter the physiological neuronal function, leading to the clinical manifestation of neurodegenerative disease (Walker and Jucker 2015) (**Figure 1.1**).

The accumulation of amyloidogenic proteins results in a loss-of-function and, more importantly, gain-of-toxic-function phenotypes. The former is attributed to the sequestration and the consequent inability of the aggregating protein to ensure its physiological role, whereas the latter is evident in tissue damaged by these proteinaceous deposits (Denny, Gavrin et al. 2013).

The protein aggregates involved in AD are mainly amyloid-β (Aβ) (Glenner and Wong 1984) and tau (Kosik, Joachim et al. 1986). Misfolded α-synuclein has been found in the brain of patients affected by Parkinson's disease (PD), dementia with Lewy bodies and Multiple System Atrophy (MSA) (Spillantini, Crowther et al. 1998). TAR DNA-binding protein 43 (TDP43)-related pathology characterize lesions found in Amyotrophic Lateral Sclerosis (ALS) and Frontotemporal Dementia (FTD) (Arai, Hasegawa et al. 2006, Neumann, Sampathu et al. 2006). In addition, inclusions of mutant SOD1 protein have been found in tissues from ALS patients (Bruijn, Houseweart et al. 1998). Mutated huntingtin and Spinocerebellar Ataxia (SCA) gene, with several polyglutamine repeats responsible for the formation of aggregates, has been associated to Huntington disease (DiFiglia, Sapp et al. 1997) and SCA (Orr, Chung et al. 1993), respectively.

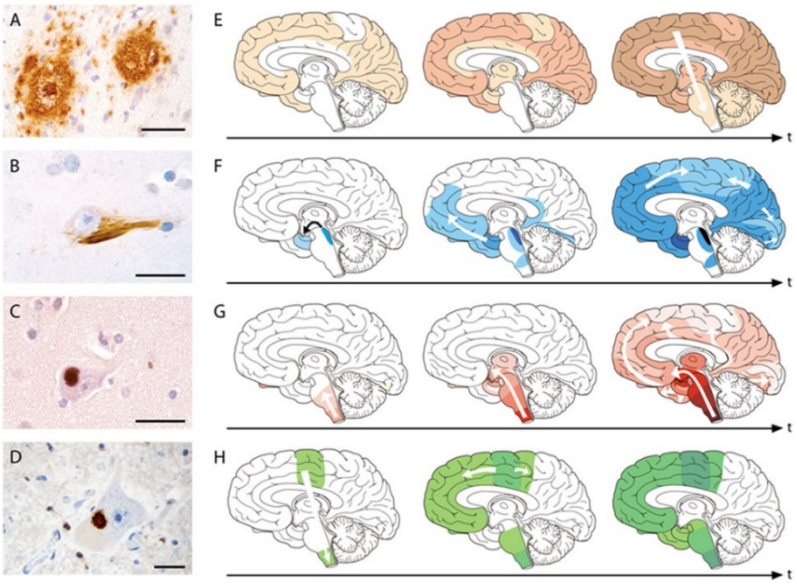

Figure 1.1. Commonalities among age-related neurodegenerative diseases. The deposited proteins assume amyloid conformation and show prion-like mechanism of propagation and spreading. **A** Aβ deposits (senile plaques) in the neocortex of an Alzheimer's disease patient. **B** Tau inclusions in a neocortical neuron Alzheimer's disease patient. **C** α-Synuclein inclusion (Lewy body) in a neocortical neuron from a patient with Parkinson's disease/Lewy body dementia. **D** TDP-43 inclusion in a motoneuron of the spinal cord from a patient with amyotrophic lateral sclerosis. Scale bars are 50μm in **A** and 20μm in **B, D.** Characteristic progression of specific proteinaceous lesions in neurodegenerative diseases over time (*t*, black arrows), from post-mortem analyses of brains is shown. Three stages of Alzheimer's disease (**E**, **F**), Parkinson's disease (**G**), amyotrophic lateral sclerosis (**H**) are shown, with arrow indicating the spread of the lesions (from Jucker and Walker 2013).

1.2 Prion diseases as model for neurodegenerative diseases

The archetypal model proposed for the replication and spread of the above mentioned misfolded protein aggregates is well described in prion diseases (Ritchie and Barria 2021).

Prion diseases, also called Transmissible Spongiform Encephalopathies (TSEs), are a rare class of uniformly fatal brain diseases affecting humans and non-human species (Prusiner 1991). Etiological agent responsible for TSEs are infectious prions; alternative protein conformation isoforms (called PrP^{Sc}) of the cellular prion protein (PrP^{C}) (Prusiner 1998). Neuropathologically, these diseases are characterized by neuronal loss, spongiform degeneration of brain tissue, astrogliosis and accumulation of PrP^{Sc} plaques (Brown and Mastrianni 2010). The pathological mechanism is based on the conformational change of the properly-folded physiological form, PrP^{C}, to disease-causing isoforms, PrP^{Sc}. The latter in turn recruits PrP^{C} molecules to convert into aberrant forms, leading to accumulation of PrP^{Sc} molecules (Colby and Prusiner 2011, Atkinson, Zhang et al. 2016).

The disease agents that proliferate in prion and non-prion brain disorders are abnormally folded proteins, called "seeds" (Jucker and Walker 2018).

According to the prion paradigm, a misfolded protein is able to self-assemble and spread through the CNS inducing conformational changes into like molecules (Jucker and Walker 2018). Pathogenic molecules bind to one another and, in a crystallization-like process, the assemblies grow, fragment in more seeds, and in this way proliferate in the brain of an affected individual (Walker and Jucker 2015).

Spatial distribution of the pathological proteins in diseased brains follows stereotypical patterns (Thal, Rüb et al. 2002, Braak, Del Tredici et al. 2003, Braak, Alafuzoff et al. 2006), which can be explained by the cell-to-cell transmission of aggregates (Jucker and Walker 2013) (**Figure 1.1**).

Following transmission to the recipient cell, pathological proteins are able to induce their normal endogenous counterpart protein to misfold, in a corruptive templating amplification process (Peng, Trojanowski et al. 2020).

Intra- and extracellular aggregates, progressively involving different CNS regions, lead to structural and functional neuronal loss, causing both cognitive and motor dysfunctions commonly observed in neurodegeneration-affected individuals (Peng, Trojanowski et al. 2020).

Differently from prion diseases, other neurodegenerative disorders are not considered contagious. However, many non-PrP misfolded proteins have demonstrated their transmissibility *in vivo* (Kane, Lipinski et al. 2000, Kordower, Chu et al. 2008, Li, Englund et al. 2008, Clavaguera, Bolmont et al. 2009). It is still unknown whether these proteins, exhibiting prion-like features, are infectious in the

same way as prions are, since there is no direct evidence supporting their infectivity in human-human transmission (Stopschinski and Diamond 2017).

1.3 Historical perspective on prion diseases

First reports of what are now called prion diseases dates back to 1700 when "scrapie", the name given to a pathological condition affecting *Caprinae* subfamily, was observed on British farms. Although hypothetical viral nature of the infectious agent responsible for scrapie was initially proposed in the 19th, the cause of this disorder remained unknown. The transmissible nature of prion diseases was first demonstrated experimentally in 1936 when two French veterinarians, Cuillé and Chelle, transmitted scrapie to a healthy goat by intraocular administration of scrapie-infected spinal cord (Liberski 2012). Thirty years later, Dr. Clarence Joseph Gibbs and Dr. Daniel Carleton Gajdusek performed the first transmission of a human prion disease, called "kuru", to chimpanzees, providing direct evidence for the infectious nature of this pathology (Gajdusek, Gibbs et al. 1966). Having demonstrated the transmissibility of scrapie and Kuru, what remained was to prove the nature of the infectious agent able to induce these diseases. The long incubation period led to hypothesize that the infectious agent was a slow virus (Cho 1976). However, Tikvah Alper and colleagues observed that the scrapie agent appeared uncommonly resistant to nuclease activity, UV treatment and ionizing radiation ruling out the hypothesis of viral or bacterial nature of this infectious agent (Alper, Cramp et al. 1967), although treatment with protein denaturing agents (such as urea or phenol) reduced its infectivity. In the same year, the mathematician John S. Griffith, proposed an innovative model in which the pathological agent of prion disorders was a protein able to self-replicate in the body of the host without the involvement of a nucleic acid (Griffith 1967). The so called "protein only hypothesis" was supported by Stanley B. Prusiner, who isolated a protein from the brains of scrapie-infected hamsters that corresponded to the properties described by Griffith, providing experimental evidence that the infectious agent causing prion diseases has a protein nature. The term "prion" was originally coined by Prusiner to indicate "proteinaceous and infectious particles" resistant to inactivation by most procedures aimed to destroy nucleic acids (Prusiner 1982).

Nowadays this definition has been modified and expanded into "proteins that acquire alternative conformations that becomes self-propagating" (Prusiner 2013).

1.4 Prion protein structure

Prion protein (PrP) can exist in two different conformations: the physiological cellular protein, PrP^{C}, ubiquitously expressed in most cell types in mammals, and the pathogenic isoform, called PrP^{Sc}, responsible for prion diseases. These two proteins share the same amino acid sequence, but they differ in the secondary structure and possess distinct biochemical properties (Legname 2017).

PrP is encoded by PRNP gene located on the short arm of chromosome 20 in humans and on a homologous region of chromosome 2 in mice. The gene contains two (in human) or three (in mouse) exons, with the coding region entirely present within the last exon (Puckett, Concannon et al. 1991, Colby and Prusiner 2011, Legname 2017). In the case of the 16 kb long human PRNP gene, the first exon acts as a transcriptional initiation site, whereas the second exon contains the PrP coding sequence (Bernardi and Bruni 2019).

In human, the precursor PrP^{C} protein, of approximately 253 amino acid residues, is synthesized in the endoplasmic reticulum, where the protein undergoes several post-translational modifications, in particular the cleavage of the C-terminal signal peptide and the subsequent attachment of a glycosylphosphatidylinositol (GPI)-anchor (Stahl, Borchelt et al. 1987), the formation of a disulfide bond between Cys179 and Cys214 (Maiti and Surewicz 2001) and the N-linked glycosylations at Asn181 and Asn1978 (Lawson, Collins et al. 2005).

In the Golgi network, the high mannose glycans attached to the asparagine are modified to produce complex-type chains with sialic acids (Caughey, Race et al. 1989). Distinct glycosylation pattern of the two asparagine residues determines four different isoforms of the protein: un-glycosylated, two different mono-glycosylated forms, represented by the glycosylation of either of the two asparagine, and the di-glycosylated form where both asparagine are occupied by glycans (Legname 2017).

GPI-anchored PrP protein, constituted by 208 amino acids, is generally located on the outer leaflet of the cell membrane and associated with caveola-like domains (Ying, Anderson et al. 1992). Mature PrP^{C} is characterized by a flexible N-terminal disordered “tail” and a well-structured C-terminal globular domain. The unstructured N-terminal domain is composed of a hydrophobic region and four octa-repeats containing histidine residues known to bind monovalent and divalent cations, such as Cu^{+} and Cu^{2+}, and zinc (Walter, Stevens et al. 2007). C-terminal domain consists of three α-helices (α1, α2, α3), with the disulphide bridge between α2 and α3 (Zahn, Liu et al. 2000), a three stranded antiparallel β-sheet (β0, β1, β2), two of which flank the first α-helix (Abskharon, Giachin et al. 2014), and a signal sequence for membrane attachment through the GPI anchor. (**Figure 1.2**).

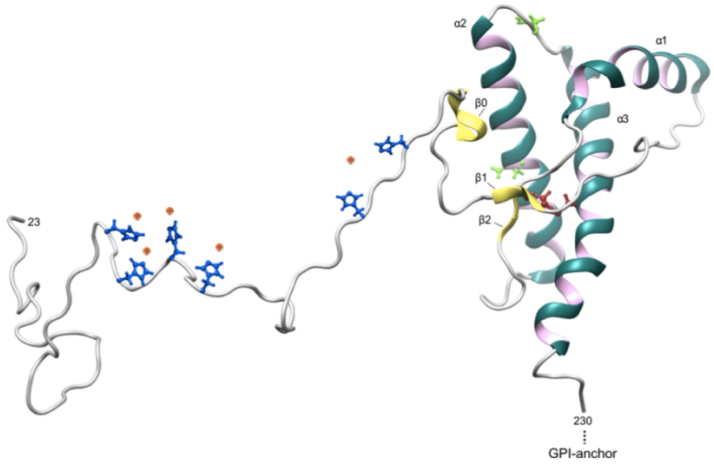

Figure 1.2 Schematic representation of cellular prion protein. The GPI-anchored 23-230 PrP^C is composed of two domains. The unstructured N-terminal domain of PrP^C possesses octapeptide repeats which contain histidine residues (in blue) able to bind monovalent and divalent cations, such as copper ions Cu^+ and Cu^{2+}(orange dots). The C-terminus contains a single disulfide bridge (in red) and asparagine glycosylation sites (in green). The overall structure of the C-terminus is composed of three short antiparallel beta sheet strands, namely β0, β1 and β2 (in yellow) and three alpha helices, indicated as α1, α2, and α3 (Legname 2017).

1.5 PrP cleavage

PrP^C undergoes post-translational endoproteolytic processing known to regulate PrP physiological functions and influence prion disease progression (Linsenmeier, Altmeppen et al. 2017).

α-cleavage takes place during the vesicular trafficking of PrP^C along the secretory pathway (Walmsley, Watt et al. 2009) at position 111/112 of the human sequence, producing the N-terminal N1 soluble fragment (11kDa) and the GPI- anchored C-terminal C1 fragment (16 kDa) (Chen, Teplow et al. 1995). Although some disintegrin and metalloproteinase (ADAM) family members have been proposed as suitable proteases implicated in the constitutive α-cleavage (Vincent, Paitel et al. 2001, McDonald, Dibble et al. 2014), the identity of the putative enzyme involved in this process remains unsolved (Linsenmeier, Altmeppen et al. 2017). α-cleavage may hinder the misfolding event (Altmeppen, Puig et al. 2012) since, on one side, C1 fragment cannot be converted into PrP^{Sc} and act as a dominant negative inhibitor of the PrP^C pathological conversion (Hölscher, Delius et al. 1998, Westergard, Turnbaugh et al. 2011) and, on the other, N1 fragment shows neuroprotective properties against PrP^{Sc} toxic effect (Resenberger, Harmeier et al. 2011).

N-terminal to the α-cleavage region, β-cleavage (occurring at residues 90–91 of human protein) produces a N2 (~ 9 kDa) and a C2 fragment (18–20 kDa, depending on the glycosylation status) which remains bound to the cellular membrane (Chen, Teplow et al. 1995). β-cleaved PrP^C may influence

the disease development, given the high levels of C2 found in both post-mortem brain samples from CJD patients (Jiménez-Huete, Lievens et al. 1998) and in prion-infected cells (Caughey, Raymond et al. 1991). Interestingly, given the similar molecular weight, resistance to protease and detergent insolubility, C2 fragment can be considered as the "*in vivo* homologue" of the protease-resistant core of PrP^{Sc} (Altmeppen, Puig et al. 2012). The enzymatic nature of β-processing has been demonstrated via pharmacological inhibition of calpains or by the overexpression of its endogenous inhibitor, calpastatin, in prion-infected cell cultures (Yadavalli et al., 2004; Hachiya et al., 2011). However, a reactive oxygen species-dependent cleavage (McMahon, Mangé et al. 2001) was also reported.

Shedding is another type of physiological PrP^{C} cleavage which occurs in close proximity to the GPI-anchor and results in the release of an almost full-length (shed-PrP) protein from the plasma membrane (Borchelt, Rogers et al. 1993). Both *in vitro* and *in vivo* studies confirm ADAM10-dependent murine PrP shedding (Taylor, Parkin et al. 2009, Altmeppen, Prox et al. 2011). A physiological role of shed PrP is supported by its presence in cerebrospinal fluid (CSF) (Tagliavini, Prelli et al. 1992) and blood (Perini, Vidal et al. 1996). Similarly to N1 fragment, shed-PrP could potentially bind β-sheet-rich oligomers thereby blocking their deleterious effects. Furthermore, PrP shedding could reduce the membrane-dependent neurotoxic action of PrP^{Sc} (Altmeppen, Puig et al. 2012).

Recently identified γ-cleavage event results in the formation of the N-terminal N3 fragment (~ 20 kDa) and a small GPI-anchored C3 fragment (~ 5 kDa), suggesting that the involved region ranges between 170 and 200 aa, N-terminal to the first N-glycosylation site (Lewis, Johanssen et al. 2016). The enzymatic nature of γ-cleavage seems to be mediated by matrix metalloproteases present in Golgi and trans-Golgi network. Although its role is not clear, high levels of C3 found in prion-affected diseases brain imply the involvement of the γ-cleavage in the pathology (Lewis, Johanssen et al. 2016, Linsenmeier, Altmeppen et al. 2017).

1.6 PrP^{C} expression and functions

PrP^{C} expression starts during embryogenesis and it peaks in adulthood, especially in CNS. Other tissues expressing PrP are lymphoid organs, heart, skeletal muscle, lung, intestinal tract, spleen, testis and ovary (Bendheim, Brown et al. 1992, Halliez, Passet et al. 2014). However, since most mouse models knockout (KO) for PrP do not show gross abnormalities, PrP^{C} may be considered dispensable for embryonic development and adulthood (Legname 2017).

PrP KO animals allowed to disentangle putative cellular events in which PrP^C can be implied. One of the first well defined phenotype of Prnp ablated mice was their resistance to scrapie infection (Bueler, Aguzzi et al. 1993), supporting a PrP^C role in prion disease development. Further studies on PrP KO models revealed its involvement in circadian rhythms (Tobler, Gaus et al. 1996), neurogenesis and neuronal differentiation in CNS (Steele, Emsley et al. 2006), synaptic machinery of olfactory bulb (Le Pichon, Valley et al. 2009), myelin formation and maintenance in the peripheral nervous system (Bremer, Baumann et al. 2010), hippocampal synaptic plasticity (Caiati, Safiulina et al. 2013) and N-Methyl-D-Aspartate receptors (NMDARs) regulation (Gasperini, Meneghetti et al. 2015).

Extracellular localization of PrP^C allows partnering with other transmembrane proteins modulating several components of signaling pathways implicated in proliferation, cell adhesion, transmembrane signaling, differentiation and trafficking (Atkinson, Zhang et al. 2016, Legname 2017). In particular, it was found that the caveolin-1-dependent coupling of PrP^C to the proto-oncogene tyrosine-protein kinase Fyn plays a role in the maturation of neuronal progenitor mouse cell line (Mouillet-Richard, Ermonval et al. 2000). PrP^C promotes neuritogenesis via the tyrosine kinase Fyn through a physical interaction with neural cell adhesion molecule (NCAM) (Schmitt-Ulms, Legname et al. 2001, Kanaani, Prusiner et al. 2005, Santuccione, Sytnyk et al. 2005, Slapšak, Salzano et al. 2016).

Other membrane proteins described as PrP^C interactors, include the above-mentioned NMDA receptor (Gasperini, Meneghetti et al. 2015), the laminin precursor receptor (LPR) (Rieger, Edenhofer et al. 1997), the α7 nicotinic acetylcholine receptor (Beraldo, Arantes et al. 2010) and the metabotropic glutamate receptor, mGluR1 (Beraldo, Arantes et al. 2011).

High levels of PrP^C expression in cells of hematopoietic origin (e.g., myeloid dendritic cells, and T cells) (Burthem, Urban et al. 2001) suggest its biological functions in the immunological system (Manni, Lewis et al. 2020).

Besides the above mentioned putative physiological functions, PrP^C has been proposed as the cellular mediator of PrP^{Sc} neurotoxic effects, since the latter instigate cellular prion protein to convey neuronal cell death signal (Brandner, Isenmann et al. 1996). Similarly, PrP^C was found to be involved in mediating the toxic effects exerted by Aβ (Laurén, Gimbel et al. 2009, Fluharty, Biasini et al. 2013), suggesting its function in other non-prion neurodegenerative diseases.

1.7 PrP^{C} to PrP^{Sc} conversion

According to the "protein only" hypothesis, the triggering event occurring in prion diseases is the conversion of PrP^{C} to PrP^{Sc}, followed by the accumulation of the pathological form of the protein (Walker and Jucker 2015). This structural transition occurs through a process where a portion of α-helices and coil structure of PrP^{C} is aberrantly folded into β-sheet, resulting in a protein with high content of β-sheet structures (43%) with respect to α-helices (30%). Conversely, the physiological prion protein shows 42% of α-helices and only 3% of β-sheets (Pan, Baldwin et al. 1993). Together with the structural transformation, a change in physical-chemical properties of PrP^{C} can be observed. Particularly, the newly formed PrP^{Sc} is characterized by proteinase K (PK)-resistant β-sheet enriched C-terminal fragment and insolubility in non-denaturing detergents, whereas PrP^{C} is soluble and can be entirely degraded upon PK digestion (Prusiner 1982).

Specific resistance to PK digestion, visualized by Western Blot (WB) analysis, is commonly used to discriminate PrP^{Sc} from PrP^{C}. While signal coming from PK-treated PrP^{C} is undetectable at WB, PK treatment of PrP^{Sc} has a lower molecular weight than PrP^{C}, maintaining the characteristic three glycosylated bands (i.e. with two, one or without glycosylation).

Two models were proposed to explain the conformational conversion of PrP^{C} into PrP^{Sc} (**Figure 1.3**). The "template-assisted" (or refolding) model predicts the interaction between an exogenous PrP^{Sc} and the endogenous PrP^{C}, leading to its conversion into a new PrP^{Sc} molecule. The rate-limiting state of this model is represented by the dimerization between PrP^{C} and PrP^{Sc} monomers. The "seeding" or "nucleation-polymerization" model proposes that PrP^{C} and PrP^{Sc} are in a reversible thermodynamic equilibrium and only when several PrP^{Sc} molecules form a highly-ordered seed, further monomeric PrP^{Sc} molecules can be recruited and eventually aggregate into an amyloid. According to this model, the apparent replication of the infectious agent, identified as the seed, is ensured by the fragmentation of PrP^{Sc} aggregates and the consequent recruitment of other PrP^{Sc} molecules (Aguzzi and Calella 2009).

Unfortunately, structural and molecular mechanisms leading to PrP^{Sc} conversion are still unknown. However, these two models are not mutually exclusive and might represent different stages of PrP^{Sc} formation. The initial seed could be produced by the nucleation-polymerization process while the template assisted model might be involved in the elongation of the fibrils.

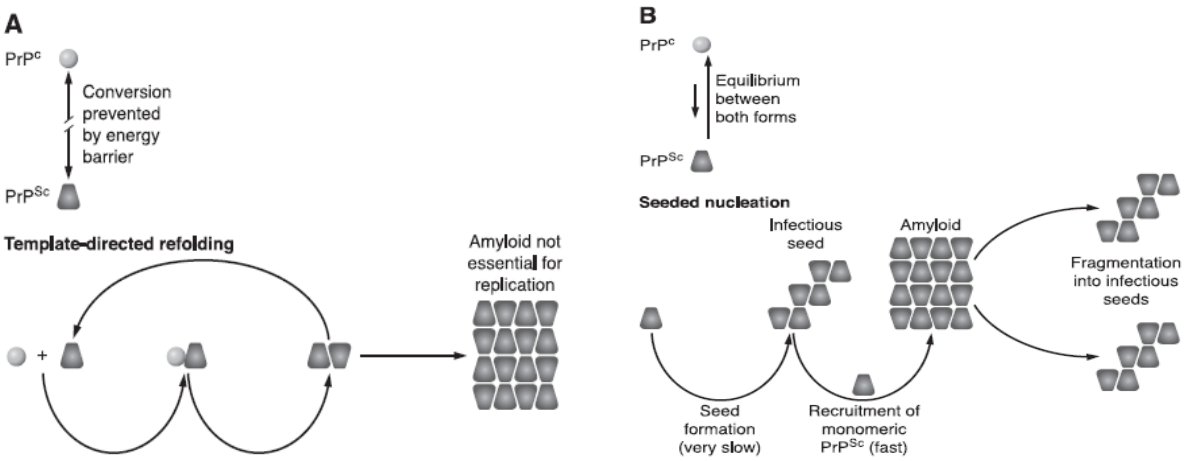

Figure 1.3. Models for PrP^{C}-to-PrP^{Sc} conformational conversion. A Template assistance (or refolding) model: interaction between exogenous PrP^{Sc} and endogenous PrP^{C}, which is induced to transform into PrP^{Sc}. A high energy barrier may prevent spontaneous conversion. **B** Nucleation-polymerization (or seeding) model: PrP^{C} and PrP^{Sc} are in a reversible thermodynamic equilibrium. Only if enough monomeric PrP^{Sc} molecules are mounted into a highly ordered seed, further PrP^{Sc} can be recruited into amyloid. Fragmentation of PrP^{Sc} aggregates produces higher number of nuclei, increasing the number of PrP^{Sc} which can be recruited (modified from Aguzzi and Calella, 2009).

1.8 PrP^{Sc} structure

The infectious misfolded PrP^{Sc} tends to polymerize and form “amyloid plaques” which can be detected in brain sections of prion-affected individuals with specific amyloid dyes like Congo-red (Merz, Somerville et al. 1983, Prusiner, McKinley et al. 1983).

Notably, infectivity and converting activity reside in PrP^{Sc} containing particles of 300–600kDa, whereas these activities are weaker in large PrP amyloid fibrils, suggesting that non-fibrillar particles with masses equivalent to 14-28 PrP molecules can be considered the most efficient initiators of prion diseases (Silveira, Raymond et al. 2005). Intrinsic characteristic of PrP^{Sc} (e.g. insolubility and propensity to aggregate) limited the determination of its 3D structure. Low resolution cryogenic electron microscopy (cryo-EM) analysis indicated that infectious GPI-anchorless mouse PrP^{Sc} fibrils are defined by the presence of two distinct protofilaments formed by 4-rung β solenoid (4RβS) monomers (Vázquez-Fernández, Vos et al. 2016). A recent molecular dynamics model, based on the 4RβS architecture, allowed the first simulation of the sequence of events underlying autocatalytic mechanism for propagation giving rise to the alternative conformation of PrP^{Sc} (Spagnolli, Rigoli et al. 2019). However, a very recent 3.1 A resolution cryo-EM structure of highly infectious 263K hamster brain-derived PrP^{Sc} fibrils, with GPI-anchor and the N-linked glycans revealed amyloid fibrils

comprised of monomers assembled with parallel in-register intermolecular β sheets (PIRIBS) with no evidence of either β-solenoids or independent protofilaments. They also proposed a model of seeding surfaces for incoming monomers. According to their hypothesis, these surfaces are proposed to be perpendicular to cellular membrane (Kraus, Hoyt et al. 2021). The asymmetric 263K PIRIBS-based core architecture resembles the synthetic amyloid fibrils of full-length or N- and/or C-terminally truncated bacterially-derived recombinant PrP (Glynn, Sawaya et al. 2020, Wang, Zhao et al. 2020).

1.9 Prion strains

Prions may exist in different strains defined by alternate conformational arrangements of PrP^{Sc} (Morales, Abid et al. 2007).

Traditionally, in infectious diseases, the term strain referred to a polymorphism or a mutation in the nucleic acid of the infectious agent. Since prions are not composed of nucleic acid, the term strain refers to infectious isolates responsible for the unique prion-disease phenotypes of affected animal and human hosts (Bartz 2016).

Prion strains are mainly enciphered by distinct conformations and aggregation states of PrP^{Sc} which are usually maintained upon serial transmission to the host (Aguzzi, Heikenwalder et al. 2007, Castilla, Morales et al. 2008).

Strains are characterized by different biochemical properties, such as electrophoretic mobility, glycosylation profile, proteolytic and chaotropic agent-dependent denaturation resistance. *In vivo,* prion strains can be identified according to their biological features, the time between the inoculation and the manifestation of the pathological symptoms (incubation time) and the time between the inoculation and the terminal stage of the disease (survival time), clinical signs, PrP^{Sc} deposition pattern and degree of spongiform alterations in specific brain areas (Morales 2017).

1.10 Species barrier

Prions are characterized by their ability to infect only a limited number of species. This phenomenon, called “species barrier”, is based on the fact that the experimental transmission of spongiform encephalopathy within a species is more efficient than a transmission between different species. Probably, this partially hampered infection between hosts resides in the different PrP^{C} amino acidic sequences (Moore, Vorberg et al. 2005). Because of this barrier, prions isolated from

one species result to be less infectious to other species (Aguzzi, Heikenwalder et al. 2007). However, rare cases of transmission between different hosts were reported, as the consumption of Bovine Spongiform Encephalopathy (BSE) infected-meat responsible for the human variant Creutzfeldt-Jakob disease (vCJD) (Bruce, Will et al. 1997).

Factors which may influence cross-species transmission include the nature of the prion strain, compatibility between the primary amino acid sequence of donor and host PrP, and the dose/ exposure route in the recipient host (Houston and Andréoletti 2018).

In other cases, inoculation of prions into a new host species produces a low or inconsistent disease incidence, and prolonged incubation periods or subclinical infection. After one or more sub-passages in the same host, called adaptation period, clinical incidence rate increases, incubation periods become shorter and very predictable for a defined dose and route of infection (Béringue, Vilotte et al. 2008).

1.11 Animal prion diseases

Animal prion disorders include scrapie that affects sheep and goats, BSE (or mad cow disease) in cattle, Chronic Wasting Disease (CWD) in moose, elk and deer, Transmissible Mink Encephalopathy in mink, Feline Spongiform Encephalopathy in cats, and Exotic Ungulate Spongiform Encephalopathy of antelopes, transmissible spongiform encephalopathy in non-human primates and a recently discovered prion disease in camels (Babelhadj, Di Bari et al. 2018).

Although, the majority of animal TSEs are acquired by infection with prions from affected cattle or sheep, some atypical TSEs forms, such as H- and L- type of BSE (categorized on the basis of low and high apparent molecular masses of unglycosylated protease-resistant PrP on WB) have an idiopathic etiology (Imran and Mahmood 2011, Head and Ironside 2012).

The epidemic-like outbreak of BSE in Great Britain, started in 1986 and reached its peak with 3500 new cases per month in 1992 and 1993 (Anderson, Donnelly et al. 1996). The BSE epidemic, often referred to as "mad cow disease", has taken the attention of the public health authorities and the scientific community since it was shown to cause a new variant form of Creutzfeldt-Jakob disease (vCJD) in humans (Bruce, Will et al. 1997). An increase in BSE cases was assumed to be caused by feeding animal with meat and bone meal (MBM) coming from scrapie-containing sheep carcasses and cattle carcasses containing BSE (Wilesmith, Ryan et al. 1991). Since the MBM usage ban in the ruminants feed, classical BSE cases have been declining progressively (Ducrot, Arnold et al. 2008).

Since its first report in UK, scrapie spread to different countries in the world through the export of living animals, and it is still endemic in most of these regions (Detwiler and Baylis 2003). Interestingly, in 1998, a new form of sheep prion disease, with epidemiological features and biochemical properties of PrP^{Sc} different from classical scrapie, was identified in Norway and named "atypical" (Benestad, Arsac et al. 2008). It has been known for several centuries that scrapie is endemic in sheep used for human food production (Detwiler and Baylis 2003), however, in spite of the likely exposure of certain individuals to infected sheep, no link has been established between scrapie and human TSEs occurrence (van Duijn, Delasnerie-Lauprêtre et al. 1998). Interestingly, a recent study reported the transmission of classical scrapie isolates to cynomolgus macaques, after a 10-year silent incubation period, with features similar to those reported for human cases of sporadic CJD (Comoy, Mikol et al. 2015).

CWD was first recognized as a disease of captive mule deer in Colorado (USA) during the 1960s, and confirmed to be a prion disease some years later (Williams and Young 1980). It has been confirmed in at least 26 U.S. states, three Canadian provinces, South Korea, Finland, Norway, and Sweden (Osterholm, Anderson et al. 2019). There is evidence that a human species barrier exists, as transgenic mice expressing human PrP were not susceptible to CWD by intracerebral inoculation (Tamgüney, Giles et al. 2006). However, brain homogenate from CWD infected cervids was able to convert human PrP^{C}, indicating that the species barrier between human PrP^{C} and cervids PrP^{Sc} is not absolute (Barria, Balachandran et al. 2014). A 2018 study found no evidence of CWD transmission in macaque monkeys inoculated with CWD prions (Race, Williams et al. 2018), even if the debate on CWD transmissibility to humans still exists (Nemani, Myskiw et al. 2020).

1.12 Human prion diseases

The annual incidence of human prion diseases is estimated to be around 1 to 1.5 per million population worldwide and it seems to have increased over the past two decades, likely owing to improved diagnostic methods and the expanding aging population (Tee, Longoria Ibarrola et al. 2018).

Human prion diseases can be subdivided in three major categories: sporadic, which accounts for 85 % of all cases, genetic (10-15%), while less than 1% are acquired (Geschwind 2015).

Regardless of the etiology, it seems that *PRNP* gene has an influence on prion infection susceptibility (Gambetti, Kong et al. 2003). Indeed, the common genetic polymorphism at codon 129, where

either methionine (M) or valine (V) may be encoded, dictate a strong disease susceptibility and phenotype modifying effect. The most dramatic example of this single nucleotide polymorphism (SNP) is that all vCJD patients, except one recent case (Mok, Jaunmuktane et al. 2017), are homozygous for methionine (Manix, Kalakoti et al. 2015). Similarly, a susceptibility effect at codon 129 for sporadic CJD (sCJD) was shown, in particular, individuals homozygous for codon 129M or 129V are more prone to develop the disease (Mead 2006).

Another polymorphism at codon 219, between glutamine and lysine (E219K, c.655G4A), was shown to have a profound effect on susceptibility to prion diseases. In particular, it seems to confer resistance against sCJD, but not entirely against the acquired or genetic form of prion diseases (Kobayashi, Teruya et al. 2015).

1.12.1 Sporadic prion diseases

The precise cause of sCJD and variably protease-sensitive prionopathy (VPSPr), which composed the group of idiopathic prion disease, is unknown. It has been hypothesized that sporadic forms of prion diseases could arise from spontaneous conversion of PrP^{C} into PrP^{Sc} or by somatic mutations in the *PRNP* gene, which render it more prone to undergo misfolding (Prusiner 1998).

1.12.1.1 Sporadic CJD

sCJD patients are generally characterized by cognitive decline (memory loss, aphasia, visual impairment), ataxia and myoclonus (Kovacs and Budka 2009, Manix, Kalakoti et al. 2015). The peak age of onset is in the 60s and the mean survival time is about six months (Tee, Longoria Ibarrola et al. 2018).

The heterogeneity of sCJD cases, highlighted by the number of variants described by different authors, is partially explained by classification based on polymorphism at codon 129 of *PRNP* gene and physiochemical characteristics of disease-associated PrP^{Sc} (Gambetti, Kong et al. 2003).

Two PrP^{Sc} subtypes have been identified from patients with sCJD: when PrP^{Sc} is partially digested by proteinase K, it shows two major patterns of electrophoretic mobility, with the molecular mass of the unglycosylated band being approximately either 21 kDa (type 1) or 19 kDa (type 2). These two types have been associated with distinct phenotypes suggesting that two major prion strains are linked to sCJD (Gambetti, Cali et al. 2011).

Furthermore, it has been suggested that the methionine to valine polymorphism, responsible for the aforementioned disease phenotypic influence on sCJD, could affect also the PrP^{Sc} type. Indeed,

more than 90% of sCJD patients MM homozygous at codon 129 have type 1 PrP^{Sc}, whereas more than 80% of sCJD cases homo- or heterozygous for valine, have PrP^{Sc} type 2 (Parchi, Giese et al. 1999, Puoti, Bizzi et al. 2012). These findings have led to the theory that the 129 genotype favors the formation of particular PrP^{Sc} conformers, which then affects the disease phenotype (Gambetti, Cali et al. 2011).

The three different genotypes at codon 129 (MM, MV, VV) and the two PrP^{Sc} types (1, 2) result in six different combinations, and based on clinical and neuropathological features, the six original "molecular" subtypes of sCJD proposed by Parchi and colleagues in 1999, were subdivided as following (Gambetti, Kong et al. 2003):

- sCJDMM1 and sCJDMV1 are phenotypically almost identical and represent about 50% of all sCJD cases (Geschwind 2015). In this subgroup, MM1 is the most prevalent molecular type, while MV1 cases are rare. MM1/MV1 subtype corresponds to the classical or myoclonic sCJD and the Hendianian variant. The clinical phenotype is characterized by a rapidly progressive cognitive impairment (observed in 70 % of cases) and ataxia, while mental and visual signs are the next common features. Post-mortem brains analysis reveals diffuse fine spongiform degeneration, astrogliosis and neuronal loss with severe lesions in occipital lobe and entorhinal cortex. Immunohistochemistry for PrP^{Sc} shows a "synaptic" pattern of staining.
- sCJDVV2 phenotype represents about 15% of the cases (Geschwind 2015) and corresponds to the previously described ataxic variant. It is characterized by a rapidly progressive ataxia from the onset while dementia, myoclonus and pyramidal signs appear during the course of the disease. In contrast to MM1/MV1 subtype, the frontal cortex is the most severely affected brain region and also the cerebellar neocortex shows atrophy. Immunopathological signs are the presence of focal PrP^{Sc} plaque-like aggregates particularly in the cerebellum, while uniform amounts of PrP^{Sc} are found in almost all grey matter brain regions, and not exclusively located in cerebral cortex as in MV1 and MM1 subjects.
- sCJDMV2 matches the previously described ataxic or cerebellar variant. It shows longer mean disease duration of around sixteen months if compared to the aforementioned subtypes, but it is phenotypically similar to VV2 (Geschwind 2015). Its diagnostic signature is seen in the presence of amyloid kuru plaques in cerebellum, where there is no significant sign of cortical atrophy as found in VV2 subjects.
- sCJDMM2 subtype has a frequency from 2 to 8 % and it refers to the cortical variant (MM2-C) identified by Parchi in 1999. Cognitive impairment is the most common clinical presentation and,

from a histopathological point of view, patients present spongiform degeneration with large vacuoles, identified as coarse spongiosis, in all cortical layers, often accompanied by intense astrogliosis.

- sCJDVV1 is the rarest type, representing 1% of all sCJD cases. The clinical presentation is frontotemporal dementia and eventually myoclonus with pyramidal signs. It is characterized by severe fine spongiosis and a faint synaptic-like PrP^{Sc} immunostaining.

- sporadic fatal insomnia (sFI) corresponds to the previously annotated MM2-thalamic variant, introduced in 1999 by Parchi. This very rare subtype is not strictly related to CJD phenotypes, even if it is correlated to the MM2 subtype. Its clinical phenotype is indistinguishable from that of the familial form of the disease (fatal familial insomnia, FFI), indeed together with ataxia, visual signs and cognitive impairment, patients eventually suffer from insomnia. The thalamus of sFI patients is the most affected brain region showing severe astrogliosis and neuronal loss. As in FFI, the amount of PrP^{Sc} is lower if compared to MM1 subtype, but the glycoform ratio is more similar to the one of sCJD subtypes allowing the distinction of the sporadic from the genetic one with immunoblot (Puoti, Bizzi et al. 2012).

These observations suggest that the phenotypic distinction from sCJDMM2 subtype could be explained by the different glycans carried on PrP^{Sc} species, leading to hypothesize a possible role of post-translational modifications in the phenotypic determination of a unique PrP^{Sc} type (MM2 in this case) (Parchi, Giese et al. 1999).

This classification has been challenged because types 1 and 2 PrP^{Sc} co-exist in some cases (Parchi, Giese et al. 1999, Puoti, Bizzi et al. 2012, Tee, Longoria Ibarrola et al. 2018). The co-existence of the two types appears to be related to the genotype at codon 129: type 1 is better represented than type 2 in sCJD subjects homozygous for M, while in sCJD patients homozygous for V, type 2 seems to be more prevalent. As a result, clinicopathological presentation and the PrP^{Sc} deposition depend on the amount of the two prion types (Gambetti, Kong et al. 2003).

1.12.1.2 Variably Protease-Sensitive Prionopathy (VPSPr)

VPSPr is a very rare sporadic prion disease which may account for almost 2% of all sporadic prion diseases (Notari, Appleby et al. 2018). Contrary to sCJD, the majority of VPSPr cases are homozygous for valine at codon 129 (65%), and the minority are homozygous for methionine (11%) (Notari, Appleby et al. 2018).

This disease is estimated to affect two-three people per one hundred million per year (Bonda, Manjila et al. 2016), but this might be an underestimation since many cases of VPSPr could be classified as atypical dementias and not further investigated (Puoti, Bizzi et al. 2012).

The difficulty in VPSPr diagnosis could be due to the peculiar pattern of PK-resistance in WB analysis. In particular, the disease-associated abnormal PrP isoform is characterized by high sensitivity to protease K digestion and a ladder-like electrophoretic profile, never associated to any case of sCJD (Gambetti, Dong et al. 2008). Another distinctive feature is the presence of very small prion plaques in the molecular layer of the cerebellum. Furthermore, data from experimental transmission indicate that, compared to most subtypes of sCJD, PrP^{Sc} propagation is slow and very limited (Notari, Appleby et al. 2018).

1.12.2 Genetic prion disease

To date, more than sixty different mutations in PRNP that may result in diverse clinicopathological phenotypes have been documented, most of them are 100% penetrant, although some have very low penetrance (<1%) and might just be risk factors (Schmitz, Dittmar et al. 2016, Kim, Takada et al. 2018). A large study in 2005 revealed that almost one-half of the cases, found to be genetic through European CJD Surveillance programs, had no family history of prion diseases or other neurologic syndromes (Kovács, Puopolo et al. 2005). Although the majority are missense mutations, several insertions, a few non-sense mutations and at least one deletion have also been identified (Takada, Kim et al. 2018). Most insertions are octapeptide repeat insertions (OPRIs) in the *PRNP* region corresponding to the copper-binding domain of PrP (Brown and Mastrianni 2010).

Some genetic prion diseases are known to be transmissible by direct inoculation into animals (Baker, Duchen et al. 1990, Collinge, Palmer et al. 1995), however, human-to-human transmission of genetic forms has not been reported.

Even for genetic forms of prion diseases, the methionine/valine (M/V) polymorphism at codon 129 of *PRNP* seems to influence the clinical-pathological phenotype of genetic prion diseases as in the case of sCJD. In particular, when it is present on the same allele harboring a mutation it confers a phenotypic susceptibility, while on the normal allele it may influence the age of onset and the disease duration (Gambetti, Kong et al. 2003). For examples, in D178N mutation, the codon 129 polymorphism may even determine two completely distinct phenotypes: when it is in association with methionine at codon 129 it causes FFI, while coupling with valine is responsible for genetic CJD (gCJD) phenotype.

Although the majority of PRNP mutations are related to a prion disease, certain mutations in this gene have also been described in non-prion disease patients. For example, an octa repeat deletion around the codon 82 has been linked to a phenotype which is similar to Alzheimer's disease and a 288 base pair insertion, consisting of twelve octa-peptide repeats, has been reported in a family exhibiting clinical-behavior changes and neuroimaging features of atypical FTD cases (Schmitz, Dittmar et al. 2016).

Even if data regarding the large populations of South and East Asia are not yet reported, the most common worldwide PRNP mutations are E200K, D178N, P102L, and OPRI (Mead 2006) (**Figure 1.4**). The historical classification in gCJD, FFI and Gerstmann–Sträussler–Scheinker Syndrome (GSS) occurred before the identification of PRNP and many nonsense mutations and OPRIs and an octapeptide repeat deletion (OPRD) do not fit completely into one of these three clinicopathological categories. Thus, genetic prion diseases have been recently subdivided into fast and slow types, according to the speed of cognitive decline and the total disease duration. gCJD, FFI, a few OPRIs (usually those with four or fewer octapeptide repeats) and the single OPRD are considered as fast types, and almost all GSS, most OPRIs (some five to seven OPRI and most octapeptide repeats greater than eight), and all nonsense mutations as slow (Kim, Takada et al. 2018).

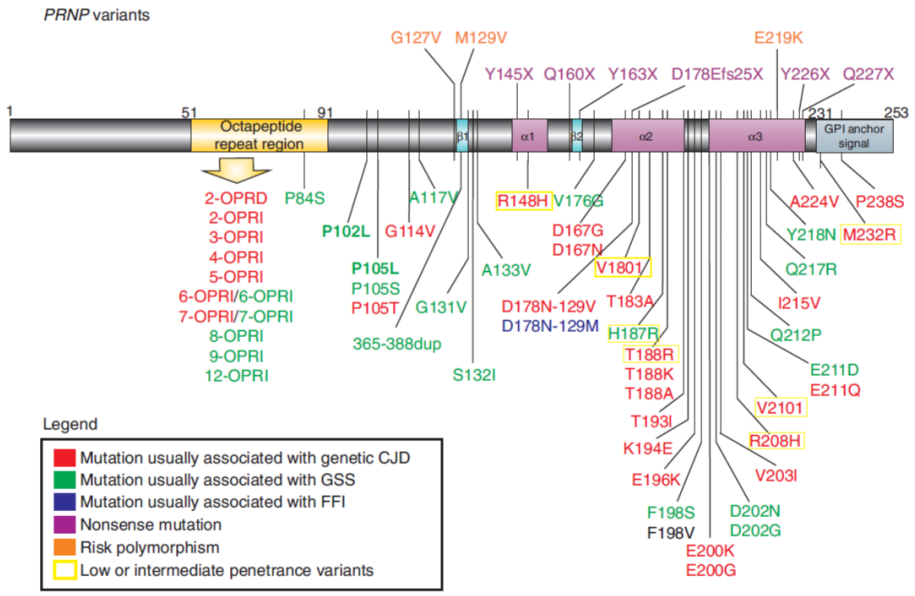

Figure 1.4. Representation of PRNP pathogenic variants. Mutations are color-coded on the basis of the associated disease or nonsense mutations. The vast majority of mutations are indicated below; nonsense mutations and polymorphisms are shown above. Most likely benign variants are not included. (from Kim et al., 2019)

1.12.2.1 Genetic CJD

Since more than 50 % of "familial" CJD cases have been reported without a family history, the term "genetic" CJD (gCJD) is now becoming established (Imran and Mahmood 2011).

The first report of kindred with gCJD dates back to 1930. However, only many decades later, affected family descendants were shown to carry the D178N PRNP mutation linked to 129V (Kretzschmar, Neumann et al. 1995).

To date twenty-three missense variants in PRNP have been reported to cause gCJD, but some of are low-penetrance mutations or risk factors for prion disease (Minikel, Vallabh et al. 2016, Kim, Takada et al. 2018).

E200K is the most common gCJD mutation and the most frequent PRNP mutation in general (Kovács, Puopolo et al. 2005, Minikel, Vallabh et al. 2016). Other known mutations are V180I and M232R, common in Japan and V210I, common in Italy (Minikel, Vallabh et al. 2016, Kim, Takada et al. 2018).

For gCJD, the frequency of 1 and 2 PrP^{Sc} subtypes is associated with the allele harboring the M/V polymorphism at the codon 129. In particular, PrP^{Sc} type 1 is typically associated with gCJD E200K and V210I (especially in patients homozygous for M at codon 129), while PrP^{Sc} type 2 is associated with gCJD E200K codon 129 VV (Schmitz, Dittmar et al. 2016) .

The most common form is the CJD with the E200K-129M haplotype (Capellari, Strammiello et al. 2011), whit a median age of onset of sixty and a disease duration around six months (Kovács, Puopolo et al. 2005, Takada, Kim et al. 2018). Phenotypically, it is similar to sCJDMM1, with cognitive and mental abnormalities at clinical onset and rapid progressive dementia, myoclonus and cerebellar signs (such as ataxia) during the course of the disease (Gambetti, Kong et al. 2003, Kim, Takada et al. 2018). Spongiform degeneration, astrogliosis and neuronal loss are present as in sCJD even if more severe and widespread in the cerebral cortex, basal ganglia, and thalami (Kovacs, Seguin et al. 2011, Kim, Takada et al. 2018). PrP^{Sc} immunohistochemical synaptic pattern is positive throughout the brain accordingly to the lesions, while a peculiar stripe-like PrP deposit has been described in cerebellar molecular layer of E200K patients homozygous for M at codon 129 (Gambetti, Kong et al. 2003). In E200K mutation carriers, the diglycosylated form of PrP^{Sc} appears to be overrepresented compared to the unglycosylated one (Kovacs, Seguin et al. 2011).

The gCJD cases associated with D178N mutation in patients carrying the codon 129V of the PRNP gene at the same allele, initially present cognitive impairment followed by depression and irritability, ataxia, speech impairment, tremor, and myoclonus (Brown, Goldfarb et al. 1992). The mean disease duration of gCJD cases caused by D178N-129V mutation is two years, which is longer compared to sCJD, however, the neuropathological findings of D178N- 129V cases are similar to

those reported in sCJD VV1 (Brown, Goldfarb et al. 1992, Kim, Takada et al. 2018). In particular, subjects display widespread spongiosis and neuronal loss in cerebral cortex, while thalamus, cerebellum and brainstem are less affected. They show a more abundant PK-resistant PrP^{Sc} banding pattern and an enrichment of PrP^{Sc} in parietal and frontal cortex if compared to FFI patients (Gambetti, Kong et al. 2003). Furthermore, CJD with D178N-129V haplotype shows an under-representation of type 1 PrP^{Sc} isoform that is derived exclusively from the mutant PrP, suggesting no direct participation of PrP^{C} expressed by the normal allele (Gambetti, Kong et al. 2003, Schmitz, Dittmar et al. 2016).

1.12.2.2 Fatal Familial Insomnia (FFI)

The term "FFI" was coined in 1986 by Lugaresi and colleagues who reported an Italian family with progressive insomnia, dysautonomia, motor dysfunction, and degeneration of the thalamus (Lugaresi, Medori et al. 1986).

However, the D178N mutation responsible for FFI was first described in a Finnish family in 1991 (Monari, Chen et al. 1994). One year later, Goldfarb and colleagues established the aforementioned haplotypic relationship between the polymorphism at codon 129 and the associated disease mutation: when it is present as 129M it leads to FFI, while 129V leads to gCJD (Goldfarb, Petersen et al. 1992).

Although no differences regarding median age of onset, which is around fifty (Mead 2006), were observed between 129MM and 129MV patients, the disease duration was shown to depend on polymorphism at codon 129: among MM patients, the average disease duration is around eleven months, while in MV patients, the disease lasts for around two years (Gambetti, Kong et al. 2003).

The initial clinical features of FFI consist of profound disruption of the normal sleep–wake cycle, leading to progressive insomnia, and dysautonomia, reflecting damage to the mediodorsal thalamic nuclear group and its connections to the hypothalamus and other central (cortical and subcortical) autonomic control areas. Cognitive impairment (seen as markedly impaired attention, confusion, disorientation) and motor deficits develop later during the disease progression (Collins, McLean et al. 2001, Gambetti, Kong et al. 2003, Geschwind 2015).

Neuropathologically, FFI patients show neuronal loss and astrogliosis in anterior ventral and mediodorsal pulvinar nuclei. The severity of the histopathological features in the cerebral cortex increases with the disease duration, often with spongiosis and astrogliosis in the entorhinal cortex and the piriform and para-olfactory cortices (Gambetti, Kong et al. 2003, Schmitz, Dittmar et al.

2016). PrP^{Sc} deposits are usually absent, but sometimes they may be detected in cerebellum, as a strip-like pattern, or as a sparse vacuolation in the midbrain and hypothalamic gray matter (Parchi, Castellani et al. 1995, Gambetti, Kong et al. 2003). WB analysis shows very low amounts of PrP^{Sc} type 2 with a marked underrepresentation of the unglycosylated form (Monari, Chen et al. 1994).

1.12.2.3 Gerstmann–Sträussler–Scheinker Syndrome (GSS)

The first known GSS family was an Austrian kindred described in 1936, whose affected members presented slowly progressive cerebellar ataxia and dementia in the late stage of the disease. Decades later, the P102L mutation within PRNP was identified in the same family (Hainfellner, Brantner-Inthaler et al. 1995).

GSS was later described also in association with at least fifteen other missense mutations and OPRI mutations, particularly with longer insertions (Mead 2006, Takada, Kim et al. 2018). The age of onset ranges from twenty-five to sixty years, with a mean illness duration of around sixty months (Kovács, Puopolo et al. 2005).

The clinical presentation is a slowly progressive cerebellar ataxia, with parkinsonism and dementia occurring later during the course of the disease (especially in patients carrying P102L). Interestingly, cognitive impairment is a common early or main clinical presentation in A117V carriers, but ataxia is less common. Patients having a shorter disease course, usually present symptoms more typical of sCJD (Mastrianni, Curtis et al. 1995, Mead 2006, Kim, Takada et al. 2018).

The neuropathological feature of all GSS patients is the appearance of widespread multicentric PrP-amyloid plaques in the cerebellum and cortex (Gambetti, Kong et al. 2003). WB analysis typically presents an additional 7-10 kDa PK-resistant fragment, resembling a ladder-like PrP^{Sc} electrophoretic pattern (Schmitz, Dittmar et al. 2016).

1.12.2.4 Octapeptide Repeat Insertions (OPRI)

Insertions and the deletion in PRNP octapeptide repeat region are thought to occur by replication slippage or recombination between identical 24 base pair repeats (Beck, Mead et al. 2001, Chen, Chuzhanova et al. 2005).

OPRIs have been subdivided according to the repeat insertion size into distinct clinicopathological groups (Kim, Takada et al. 2018). Patients carrying two- to four-OPRIs usually share phenotypic similarities to sCJD subjects, have later age at onset, and shorter clinical duration. Subjects with five-

to seven-OPRIs present a prolonged clinical course in early adulthood, and a variable clinical presentation including cognitive, psychiatric, motor dysfunction and seizures. Eight-OPRIs or more are more frequently reported in association with subjects harboring the GSS phenotype and in patients with a much earlier disease onset (Gambetti, Kong et al. 2003, Mead 2006).

1.12.3 Acquired prion diseases

A defining feature of prions is their infectivity, which consists in their ability to cause the disease when transmitted from an affected individual to a healthy one. Among humans, the transmission of prion disease is very rare and involves only particular routes of infection, such as contamination of food supplies, iatrogenic transmission associated to medical and surgical procedures, or ritual cannibalism (Tee, Longoria Ibarrola et al. 2018).

The BSE epidemic in UK and other European countries, emerged between 1980s and 90s, and the subsequent demonstration of its transmission to human beings as a new phenotype of acquired prion disease, vCJD, provoked enormous public and scientific concern about prion diseases (Will 2003).

Acquired prion diseases are known to have long silent incubation times, therefore, uncertainties remain about the eventual size of vCJD outbreak (Mead 2006).

1.12.3.1 Iatrogenic CJD (iCJD)

iCJD is a form of acquired prion disease caused by accidental human-to-human transmission of prions via parenteral route, due to surgical or medical procedures (Will 2003, Brown, Brandel et al. 2012). Almost five-hundred iCJD cases have been reported worldwide (Tee, Longoria Ibarrola et al. 2018).

The first case of iatrogenic transmission of CJD reported in literature dates back to 1974, when a patient developed a prion disease eighteen months after the transplantation of cadaveric corneal tissue from a donor with pathologically confirmed CJD (Duffy, Wolf et al. 1974)

Transplantation of dura mater was also shown to cause patient-to-patient CJD transmission, with more than two-hundred cases worldwide. Most dura mater–transmitted iCJD cases received grafts manufactured by the German company B. Braun Melsungen AG. They had been distributed worldwide and most widely used in Japan, where roughly 60% of the cases have been reported (Bonda, Manjila et al. 2016).

Other mechanisms of transmission related to surgical procedures include contaminated neurosurgical instruments and stereotactic electroencephalography (EEG) recordings, previously used on CJD patients (Brown, Brandel et al. 2012, Bonda, Manjila et al. 2016).

Among iCJD linked to medical procedures, over two-hundred cases were associated with the injection of human pituitary-derived growth hormones (hGH) used to treat pathological short stature in children (Bonda, Manjila et al. 2016). In almost all cases hGH was supplied by the US National Hormone and Pituitary Program prior to 1977, when highly selective column chromatography step was included in the purification protocol (Abrams, Schonberger et al. 2011). Given that hGH required the collection of thousands of cadaveric pituitary glands, it is believed that the contamination arose due to the inclusion of material from patients who died from, or were incubating CJD (Will 2003). Regarding the usage of cadaver-derived hormone, some Australian cases of iCJD have been reported also among women treated for infertility with human pituitary gonadotrophin (Brown, Brandel et al. 2012). Many individuals were potentially exposed to cadaver-derived prion-contaminated pituitary hormones worldwide and it remains uncertain if they will ever develop iCJD or end up as carriers (Tee, Longoria Ibarrola et al. 2018).

Another way of iCJD transmission includes blood transfusion, even if these cases are related to the aforementioned vCJD pathology (Wroe, Pal et al. 2006).

The inoculation route of the infectious agent seems to influence the incubation period and the clinical presentation. iCJD cases associated to peripheral route of transmission, have long incubation time and they are predominantly characterized by cerebellar symptoms (Tee, Longoria Ibarrola et al. 2018). On the contrary, patients infected through brain inoculation (either via neurosurgical or EEG electrodes) presented shorter incubation period and dementia as initial symptoms, similar to sCJD subjects (Will 2003, Xiao, Yuan et al. 2014).

The clinicopathological features of CJD linked to treatment with hGH resemble the cerebellar symptoms of Kuru, while the iCJD cases linked to grafting of dura mater or the use of neurosurgical instruments resemble those of sCJD (Imran and Mahmood 2011). Although safety procedures were put in place decades ago, due to long iCJD incubation period, ranging from five to forty-two years for hGH-associated cases and from sixteen months to thirty years for dura mater-associated ones, new cases continue to be identified (Geschwind 2015).

1.12.3.2 Variant CJD (vCJD)

vCJD represents the only example of a prion disease transmission to humans from another species, which occurred through the inadvertent consumption of BSE-contaminated meat products (Bruce, Will et al. 1997, Hill, Desbruslais et al. 1997). The high public and scientific profile was raised with the occurrence of vCJD and the potential transmissibility from peripheral tissues, threatening both the bovine-derived meat consumption and the worldwide safety concerning blood transfusions, respectively.

The incidence of vCJD peaked in 2000, about eight years after the peak of the BSE epidemic in 1992 (Pattison 1998) and it has declined dramatically since then. As of 2017, 231 worldwide deaths from vCJD have been reported, the majority of which had been UK residents during the high-risk period 1980-1996 of BSE supporting the temporal relationship between the two diseases (Mackay, Knight et al. 2011, Tee, Longoria Ibarrola et al. 2018).

The decreased incidences of BSE and vCJD are believed to be due to the strong implementation of import control policies and ban-feed regulations (Pattison 1998).

The first two cases dated back to 1995 and were initially associated to sporadic CJD pathology (Bateman, Hilton et al. 1995, Britton, al-Sarraj et al. 1995). A year later, other eight cases of patients who died relatively young (average age of 29 years) if compared with the majority of sCJD patients, were reported (Will, Ironside et al. 1996). Furthermore, when compared to from sCJD cases, vCJD patients showed longer disease incubation periods and longer disease duration (Will 2003).

Under a clinical point of view, vCJD patients presented initial psychiatric symptoms, such as withdrawal, anxiety, irritability, anhedonia and insomnia. These are often followed by neurological symptoms, including dystonia, chorea, myoclonus and gait disturbance (Spencer, Knight et al. 2002).

Variant CJD differs pathologically from the previously observed CJD cases in the occurrence of florid plaques in brain tissue, consisting of dense core prion amyloid deposits surrounded by vacuoles which gives them a flower-like appearance (Will, Ironside et al. 1996), very similar to those of Kuru patients and BSE-infected monkeys (Lasmézas, Deslys et al. 1996).

Given the oral route of infection for contaminated BSE-affected bovine meat, highly specific feature of vCJD appears to be the gut accumulation of PrP^{Sc} in the lymphoreticular system, confirmed by WB and immunohistochemical analysis of the spleen, lymph nodes, appendix and tonsils (Hilton and Ironside 2003). This allowed tonsil biopsy to be included in diagnostic criteria for probable vCJD (Frosh, Smith et al. 2004). Interestingly, a large series of appendix specimens indicate a 1/2000 rate of infection in UK population, suggesting a high prevalence of asymptomatic carriers (Gill, Spencer et al. 2013).

Detection of the peripheral PrP^{Sc} infection among asymptomatic subjects raises concern about the risk of disease transmission through blood transfusion. Indeed, three clinical vCJD cases and two additional cases of asymptomatic infection in the UK were likely acquired through blood product transfusion (Knight 2010).

Since the majority of vCJD cases are younger than forty years of age, the young age seems to be a risk factor. It is hypothesized that, as part of the development of the human immune system, there is a greater volume of gut-associated lymphoid leading to larger surfaces of the available tissue ready to absorb the infected material and allow for a more efficient infection (Mackay, Knight et al. 2011).

All but one vCJD cases presented methionine homozygosity at codon 129 of *PRNP* (Mok, Jaunmuktane et al. 2017), suggesting that individuals with the codon 129 MV polymorphism (possibly VV as well) are less likely to develop clinical vCJD, being carriers of the disease with a significant transmission risk, or they might just have longer incubation periods than patients who are MM at codon 129 (Tee, Longoria Ibarrola et al. 2018).

1.12.3.3 Kuru

Kuru has been a devastating prion disease epidemic, known since 1941, when it was recognized to be endemic amongst the Fore linguistic and cultural group resident in the Eastern Highlands of New Guinea. In the Fore language Kuru means ‘to shiver’ (or ‘to be afraid’) which, along with cerebellar ataxia, constitutes one of the salient clinical hallmarks of the disorder (Collins, McLean et al. 2001). It was initially associated to a TSE disease because of clinical and neuropathological similarities to scrapie, even if it was confirmed to be caused by a transmissible agent in 1966, thanks to Gajdusek experiments on Kuru-inoculated chimpanzee (Gajdusek, Gibbs et al. 1966).

At its peak in the 1950s, Kuru was the leading cause of death in young women in the South Fore (Mead 2006). Indeed, among Kuru victims over three-quarters were adult women, then children of either sex constituted the next major subgroup, while adult males only rarely developed the disease (Collins, McLean et al. 2001).

The collection of scientific and epidemiological data culminated in the theory for which Kuru had been transmitted by cannibalistic rituals typical of the deceased relatives' funerals of those populations. At these ceremonies, women and children ate the internal organs (including the highly infectious central nervous system) while adult males took the "noble" and relatively non-infectious

limbs, such as skeletal muscles (Collins, McLean et al. 2001). Since the cessation of cannibalism in the mid 50's, the occurrence of Kuru showed a gradual and steady decline.

The overall clinical picture is extremely uniform, predominantly manifesting as a progressive cerebellar ataxia with tremors. In later stages of the disease communication is impaired because of severe dysarthria but, in the majority of patients, dementia was absent (Collins, McLean et al. 2001, Will 2003).

While incubation period ranges from four to forty years, illness duration can range from four to twenty-four months, even if methionine homozygosity at codon 129 is associated with shorter disease duration. Furthermore, homozygous individuals present a mean onset of the disease in early adulthood, whereas heterozygous individuals show a delayed middle-age onset (Collins, McLean et al. 2001, Will 2003). In 2009, Mead and colleagues identified a novel PRNP point mutation - G127V - located in a highly conserved and structured region of PrP. Heterozygosity at codon 127 was shown to provide strong, and possibly complete, resistance to Kuru (Mead, Whitfield et al. 2009). Unrevealing the molecular mechanism which allows this polymorphism to prevent PrP^{C} from misfolding into PrP^{Sc} could be useful for the development of treatments for human prion diseases (Tee, Longoria Ibarrola et al. 2018).

Kuru is characterized by a distinctive spongiform degeneration pattern, a widespread micro-vacuolation in cerebral cortex and glial proliferation, which tend to mirror the anatomical pattern of neuronal degeneration. Amyloid-Kuru plaques are not constantly found but are seen in approximately 50–75% of cases especially in the granular layer of cerebellum, however the accumulation of PrP^{Sc} is pronounced also in deep layers of cerebral cortex (Collins, McLean et al. 2001).

1.12.4 Diagnosis

Currently, a definitive diagnosis of TSEs relies on postmortem identification of pathognomonic histological features (e.g. vacuolation, astrogliosis), or immunohistochemical/immunoblotting detection of PK-resistant PrP, in brain tissue samples (Ascari, Rocha et al. 2020).

In case of genetic prion diseases, detection of a pathogenic PRNP mutation can be helpful when a family history is present. Unfortunately, in more than 60% of genetic patients there was not any known history of prion diseases (Geschwind 2015).

Given the high risk of human-to-human transmission of acquired forms, especially vCJD and iCJD, their diagnosis is of particular relevance. iCJD cases are generally diagnosed postmortem, analyzing

the patient's medical record: in particular, the main indication of iCJD comes from the report on the use of tissues from afterwards diagnosed CJD patients.

Generally, sCJD diagnosis is extremely difficult because of the involvement of many brain areas and also because of different clinical presentations of the disease, especially at early stages, similar to many others neurologic or psychiatric conditions (Geschwind 2015).

The first biomarkers used for sCJD diagnosis were periodic short-wave complexes (PSWCs) of EEG, which have been incorporated into probable sCJD diagnostic criteria by the World Health Organization (Geschwind 2015, Manix, Kalakoti et al. 2015). However, PSWCs have also been reported in patients with Alzheimer's disease, vascular dementia, Lewy body disease (Wieser, Schindler et al. 2006, Tee, Longoria Ibarrola et al. 2018).

The first reports on brain magnetic resonance imaging (MRI) of sCJD were increased signal in deep nuclei, primarily striatum, on T2-weighted images (Urbach, Klisch et al. 1998). Nowadays, sCJD diagnostic criteria by bioimaging include the presence of hyperintensity on diffusion-weighted imaging in caudate and putamen and/or in a gyral pattern of the cortex (Zerr, Kallenberg et al. 2009, Figgie and Appleby 2021). However, MRI findings also vary within different molecular subtypes and are difficult to interpret (Tee, Longoria Ibarrola et al. 2018).

Interestingly, brain MRI of vCJD patients usually shows the characteristic "pulvinar sign", a highly specific hyper intense signal in the posterior thalamus of affected individuals on T2-weighted sequences (Manix, Kalakoti et al. 2015).

Among the surrogate biomarkers exploited for TSE diagnosis, CSF 14-3-3 is considered in current guidelines, even if found to be elevated in many conditions characterized by rapid neuronal injury (Tee, Longoria Ibarrola et al. 2018). Other CSF biomarkers that have been proposed for prion diseases include total tau, phosphorylated tau, neurofilament light chain, neuron-specific enolase, alpha-synuclein, S100B and thymosin B4 (Figgie and Appleby 2021).

The reason at the basis of this lack of homogeneous results resides in features of these proteins, which are considered as general markers for neuronal injury, not specific for prion disorders (Geschwind 2015). Given the low specificity of these biomarkers, they should only be used to give confidence in the sCJD diagnosis with the right clinical picture, and never used to rule out the disease (Manix, Kalakoti et al. 2015).

Novel diagnostic tests, however, are helping with earlier and more accurate diagnosis of CJD, allowing also pre-mortem, minimally-invasive collection of peripheral tissues (Tee, Longoria Ibarrola et al. 2018).

Originally developed by Claudio Soto in 2001 the Protein Misfolding Cyclic Amplification (PMCA) is an ultrasensitive technique able to sustain the phenomenon of PrP^{Sc} amplification by mimicking *in vitro* the pathogenic replication observed *in vivo* (Saborio, Permanne et al. 2001). PMCA consists of repeated cycles ("rounds") of incubation and sonication of samples containing PrP^{Sc} in presence of an excess of PrP^{C} from the brain homogenates of healthy animals. During the incubation phase, PrP^{Sc} induces the conversion and aggregation of PrP^{C} substrate. In the sonication phase, PrP^{Sc} aggregates are fragmented in smaller "seeds" able to further convert new PrP^{C} molecules. Therefore, after several rounds, the amount of PrP^{Sc} increases exponentially to reach the level detectable with PK-digestion and WB analysis (Bieschke, Weber et al. 2004). Diagnostic assays based on PMCA are able to detect PrP^{Sc} in vCJD urine, providing a sensitivity of 93% (Moda, Gambetti et al. 2014) and blood, with almost 100% of specificity and sensitivity (Bougard, Brandel et al. 2016, Concha-Marambio, Pritzkow et al. 2016). Interestingly, the PMCA-based diagnostic method was also able to detect prions at a pre-clinical stage supporting its potential for detecting presymptomatic vCJD patients (Bougard, Brandel et al. 2016).

Real-time Quaking Induced Conversion (RT-QuIC) technique was originally developed in 2008 (Atarashi, Wilham et al. 2008) and further combined with the amyloid seeding assay (Colby, Zhang et al. 2007) read-out method using the amyloid binding dye thioflavin-T (ThT) (Wilham, Orrú et al. 2010). Differently from PMCA, it is based on cycles of incubation and shaking. During incubation period, PrP^{Sc}, contained in the tested sample, induces the conformational change of soluble recombinant prion protein, used as substrate, that aggregates forming large amyloid fibrils. The aggregated structures can be detected with fluorescence plate readers, using ThT. The shaking phase promotes the fragmentation of the amyloid fibrils, forming more seeds able to recruit further recombinant PrP substrates and resulting in an exponential increase of amyloid formation (Wilham, Orrú et al. 2010). RT-QuIC is a very promising ante-mortem diagnostic test, given that it permits the detection of trace-amount PrP^{Sc} in biological samples from different sources achieving high sensitivity and specificity. This technique was optimized for the detection of PrP^{Sc} in CSF and in olfactory mucosa brushings from patients with sCJD (Orrú, Bongianni et al. 2014), and even in skin biopsy (Orrú, Yuan et al. 2017, Mammana, Baiardi et al. 2020). Currently, RT-QuIC, in combination with other techniques, characterizes TSE diagnosis only as probable, not definitive (Tee, Longoria Ibarrola et al. 2018).

1.12.5 Therapy

Currently, no cures for human prion disease are available and only some of the symptoms can be temporarily treated or controlled (Colini Baldeschi, Vanni et al. 2020).

The targets toward which anti-prion therapeutic strategies have been focused on are mainly PrP^{Sc} and PrP^{C}, since according to the two models proposed for conformational conversion, the accumulation of latter one is dependent on the presence of the former one, which it is used as substrate to be corrupted (Aguzzi and Calella 2009). However, recent approaches have focused on different molecules thought to be involved in prion pathogenesis mechanism (Zattoni and Legname 2021).

A plethora of small molecules demonstrated an anti-prion activity in cell culture and prion-infected animals models, but, unfortunately, only few of them reaches clinical trials. Quinacrine and doxycycline did not demonstrate any ability to affect the course of the diseases (Barret, Tagliavini et al. 2003, Haik, Marcon et al. 2014).

Interestingly, a preventive clinical trial with doxycycline treatment has been recently designed, including individuals at genetic risk of developing FFI, with the aim to compare the incidence of the disease among those treated asymptomatic carriers to that of an historical dataset (Forloni, Tettamanti et al. 2015).

However, recent developments in the *in silico* screening approach for the selection of molecules able to bind PrP^{C}, preventing its abnormal conformational changes, will pave the way for a new era of PrP^{C}-directed anti-prion therapeutic strategy. One of the first compound selected for its ability to bind PrP folding intermediates was GN8420, which required very low concentrations to clear prion *in vitro* (Kuwata, Nishida et al. 2007). Recently, the molecular chaperone N,N'-([cyclohexylmethylene]di-4,1-phenylene)bis(2-[1-pyrrolidinyl]acetamide) was found to slow the disease progression in mice and macaques models of prion disease (Yamaguchi, Kamatari et al. 2019).

Not-PrP directed strategies have been pursued to find alternative ways aimed to fight prion diseases. Indeed, many genes, and related proteins, have been scrutinized as putative players in the PrP^{C} to PrP^{Sc} conversion. For examples, a clear anti-prion effect *in vivo* has been demonstrated for the antiretroviral drug Efavirenz which, probably via a cholesterol reduction in neuronal membranes, is able to hamper PrP^{Sc} replication (Ali, Hannaoui et al. 2021).

RNA interference-mediated knockdown of PrP^{C}, leading to less substrate available for conversion into PrP^{Sc}, has recently been proposed as innovative PrP^{C}-directed anti-prion therapeutic strategy.

In particular, anti-sense oligonucleotide designed to bind PrP transcript led to prolonged survival time in prion-infected animals (Raymond, Zhao et al. 2019).

Since prion diseases are characterised by the deposition of amyloid aggregates in the CNS, antibodies may opsonise pathological misfolded proteins, or mediate their degradation through means of phagocytic cells (Senatore et al., 2020). Currently, a major advancement in anti-PrP antibody therapy approach is represented by PRN100, a humanised anti-PrP^C monoclonal antibody ICSM18 (Beringue, Vilette et al. 2004), which reached clinical trials a few years ago (Dyer 2018).

1.13 *In vitro* and *in vivo* models for prion diseases

To mimic TSEs and to study their molecular features, prion-infected immortalized cell lines are widely used as *in vitro* models of the disease. Although only *in vivo* models accurately recapitulate all the neuropathological aspects, low cost and easy manipulation make cell lines a good model to study prion diseases. In addition, infected cell cultures might provide a substrate on which infectivity can be titrated and PrP^{Sc}-cell interaction unveiled (Race et al., 1987).

Nowadays, several immortalized mouse cell lines supporting prion infection can be used for research purposes. However, since no naturally occurring prion diseases in mice exist, it was necessary to "adapt" prions to murine PrP^C sequence by repeated passaging of sheep scrapie prions in mice. The resulting mouse-adapted scrapie strain enabled the infection of mouse PrP^C-expressing cells (Chandler, 1961). The first example was the Chandler strain, which was used to generate a cell line able to reproduce a stable prion infection, called scrapie brain model (Clarke & Heig, 1970; Chandler, 1961).

Since the infection susceptibility is almost exclusively limited to mouse-adapted strains, only a small number of cell lines were found to support prions propagation (Lawson 2008). The majority of prion susceptible cells derived from mouse neural tissue, such as neuroblastoma-derived (N2a) (Butler, Scott et al. 1988) and hypothalamic gonadotropin-releasing hormone immortalized neuronal (GT1) cells (Schätzl, Laszlo et al. 1997), with the only exception of an epithelial rabbit cell line, in which the expression of the ovine PrP^C renders them permissible to sheep scrapie agent infection (Vilette 2008).

Prion-infected mouse neuroblastoma cells (ScN2a) represent the most widely used paradigm for studying prion propagation in cultured cells. Indeed, N2a cells are susceptible to certain strains of mouse prions, such as the RML strain (ScN2a RML) (Nishida, Harris et al. 2000), as evidenced by the

presence PrP^{Sc}strain-related infectivity even after multiple passages (Enari et al., 2001; Klöhn et al., 2003). For this reason, ScN2a cells can be considered as a valuable tool for dissecting the molecular events that characterize prion diseases pathogenesis.

Recently, prion infection has been found to be sustained in an immortalized murine astrocytic-derived cell line (Tahir, Abdulrahman et al. 2020). Moreover, another recent work highlighted the possibility to stably infect an immortalized human cell line (SH-SY5Y) with prions. Replacement of the human PRNP gene with its ovine counterpart minimized the risk of laboratory-acquired human prion infection (Avar, Heinzer et al. 2020).

Immortalized cell-lines are a simplified model to study prion disorders lacking the contribution of diverse cell populations in the CNS. Therefore, prion-infected primary cells, organotypic slices and neurospheres have been proposed as more reliable models for prion diseases (Cronier, Laude et al. 2004, Giri, Young et al. 2006, Falsig, Julius et al. 2008, Victoria, Arkhipenko et al. 2016). Few years ago, human cerebral organoids have been successfully infected with a sCJD strain (Groveman, Foliaki et al. 2019), paving the way for their establishment as viable models for drug screening (Groveman, Ferreira et al. 2021).

However, in prion disease field, animal models remain the most reliable tool allowing a complete and extensive overview of the clinical and neuropathological phenotypes, transmission barriers, and roles of pathogenic mutations. Interestingly, compared to AD and PD, where clinical–pathological correlation between the animal model and a human disease is often difficult, prion diseases are characterized by an *in vivo* model of the diseases which allows for more precise conclusions on the efficacy of the tested treatment (Brandner and Jaunmuktane 2017).

Hamster have been originally used to understand prion spreading and CNS distribution after peripheral challenge (Kimberlin and Walker 1986, Jendroska, Heinzel et al. 1991). Bank voles have been discovered to maintain neuropathological and biochemical strain properties (Nonno, Di Bari et al. 2006) and, more importantly, to be susceptible to prions originating from multiple different species (Watts, Giles et al. 2014).

Primates, especially Cynomolgus macaque monkey, infected with different prion strains, represent a high relevant model of prion diseases because of their genetic and physiology proximity to humans (Gibbs, Gajdusek et al. 1968, Barbisin, Vanni et al. 2014).

Nowadays transgenic mouse models expressing human or other animal PrP, carrying a desired mutation and or polymorphism, are commonly used to have a better insight on pathogenesis of prion disorders (Brandner and Jaunmuktane 2017).

1.14 Transcriptomic approach in prion diseases

Transcriptome analysis in prion and neurodegenerative diseases, in general, represents a powerful tool that may contribute to reveal the molecular mechanism at the basis of these disorders and to identify potential targets for novel therapeutic approaches.

Large-scale gene expression profiling of prion disease and healthy individuals may help in identifying novel genes and pathways that are switched on or off in prion disease pathogenesis (Benetti, Gustincich et al. 2012, Vanni 2017). These analyses identified molecular pathways altered upon prion infection, including cholesterol synthesis, apoptosis, lysosomal pathway, immune and inflammation response (Vanni 2017).

The majority of studies carried out in order to investigate gene expression alterations during the course of prion infection, have involved animal models such as mice (Booth, Bowman et al. 2004, Riemer, Neidhold et al. 2004, Xiang, Windl et al. 2004, Hwang, Lee et al. 2009), sheep (Filali, Martin-Burriel et al. 2012, Filali, Vidal et al. 2013, Gossner and Hopkins 2014) and cattle (Tang, Xiang et al. 2010, Almeida, Basu et al. 2011, Xerxa, Barbisin et al. 2016).

In 2014, a microarray-based gene expression study of brains from BSE-infected cynomolgus macaques revealed altered expression levels in genes belonging to oxygen homeostasis, lipid metabolism and inflammation response pathways. Further validation of differentially expressed transcripts, using reverse transcription quantitative polymerase chain reaction (RT-qPCR), confirmed the upregulation of *SERPINA3* transcript encoding for a member of the serine protease inhibitor family of acute phase proteins (Barbisin, Vanni et al. 2014).

1.15 Serpins

Serpins represent the largest and most widely distributed superfamily of protease inhibitors (Irving, Pike et al. 2000), which accounts for about 1500 members (Gettins 2002, Law, Zhang et al. 2006, Whisstock, Silverman et al. 2010).

The term “serpin” (*ser*ine *p*roteases *in*hibitors), was originally coined in 1985 by Carrell and Travis because the first serpins identified inhibited chymotrypsin-like serine proteases (Gettins and Olson 2016). However, serpin family members exert inhibitory function toward other protease classes (i.e. caspases and papain –like cysteine proteases), and some of them perform diverse non-inhibitory functions, as hormone transport, molecular chaperons and protein storage (Irving, Pike et al. 2000,

Law, Zhang et al. 2006). Eukaryotic serpins have been divided into 16 clades, classified from A to P, according to their sequence similarity (Silverman, Bird et al. 2001, Olson and Gettins 2011). Each clade consists of a variety of members and, according to the current nomenclature, each serpin is named SerpinXy, where X indicates the clade and y the number within each clade. However, many serpins possess alternative names derived from previous nomenclatures. At present, there are some serpins that are classified as "orphans", since they do not belong to any other clade, but they will probably form other clades once new serpins are identified (Law, Zhang et al. 2006, Heit, Jackson et al. 2013).

Despite the great variety of processes in which they are involved, serpins are unique under the evolutionary perspective. Sequence homology analysis revealed that members of serpin family are phylogenetically grouped by species and not by function, suggesting that the evolution of serpins happened by speciation to fulfill their role in different biological processes rather than in parallel with serine proteases (Krem and Di Cera 2003).

1.15.1 Serpins structure and conformations

Primary structure od serpins consists of ~380 up to 500 amino acid residues that fold into an N-terminal helical domain and a C-terminal β-barrel domain (Huntington 2011, Heit, Jackson et al. 2013). Inhibitory serpins are mainly characterized by a highly conserved core, thought to be instrumental in determining their peculiar conformational flexibility (Irving, Pike et al. 2000). Serpins secondary structure consists of three β-sheets (A, B and C), and eight or nine α-helices (hA-hI) that are mostly packed on one side of the β-sheet A. Crucial for their protease inhibitory function, serpins possess an exposed and flexible loop, named the reactive centre loop (RCL) that is connected to strand 5 of β-sheet A on the N-terminal end and to strand 1 of β-sheet C on the C-terminal (Silverman, Bird et al. 2001, Gettins and Olson 2016). RCL of serpins is typically 20-24 residues long and, in the classic orientation, it is on top of serpin facing the sheet A (Huntington 2011). The interaction of RCL with the active site of a protease leads to the inhibition of its proteolytic activity (Heit, Jackson et al. 2013).

Besides RCL, other two structural regions are necessary to accomplish the inhibitory conformational change typical of serpins: the conserved "breach" region, located at the top of the β-sheet A is crucial for initial RCL insertion inside serpins structure, the "shutter" region is thought to control the β-sheet A opening during the inhibitory activity (Huntington 2011, Sarkar and Wintrode 2011). The

most extensively investigated inhibitory serpin, in terms of structural studies, is α_1-antitrypsin (SERPINA1), depicted in **Figure 1.5** to indicate serpin basic fold.

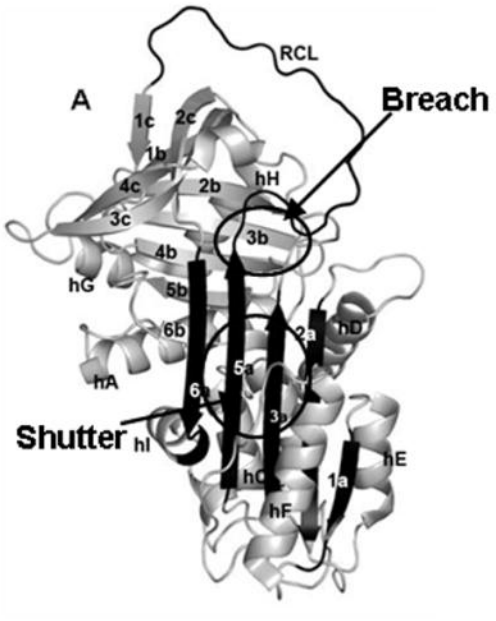

Figure 1.5. Overall native structure of α_1- antitrypsin (SERPINA1). Native SERPINA1 with the relative structural elements: the nomenclature of the α-helices and strands of β-sheet are shown, as well as the positions of the shutter and breach regions (from Sarkar & Wintrode, 2011).

Serpins spontaneously fold into an active metastable state, energetically far from its most stable conformation (Huntington 2011, Gettins and Olson 2016). This metastable state, in which native serpins are trapped (**Figure 1.6A**) represents a rare exception of Anfinsen's conjecture, according to which protein sequence folds to a single structure that represents the lowest free energy state (Law, Zhang et al. 2006). In the native state the exposed RCL loop is accessible for interaction with protease. According to RCL moiety location, serpins can exist also in other forms (Irving, Pike et al. 2000, Huntington 2011).

The most stable serpin conformation is the so called "cleaved form" (**Figure 1.6B**), which is acquired upon RCL interaction with the protease and subsequent cleavage of the RCL towards its C-terminus, where the protease recognition sequence lies. Following proteolysis, the fourth strand of β-sheet A is enabled to insert into serpin structure to give again a six-stranded antiparallel β-sheet, without strand 1 displacement from β-sheet C (Gettins & Olson, 2016). This thermodynamically driven process of native to cleaved change is called "stressed to relaxed" (S to R) transition and it is essential for serpin inhibitory activity (Irving, Pike et al. 2000, Whisstock, Pike et al. 2000, Gettins 2002).

Another alternative stable serpin conformation is the not-cleaved "latent" conformation (**Figure 1.6C**), in which the intact RCL is inserted into the β-sheet A, as in the cleaved form, to give an alternative R conformation (Whisstock, Pike et al. 2000). The RCL insertion into the centre of β-sheet A occurs together with strand 4, thereby expanding β-sheet A to six strands of antiparallel β-sheet (Gettins and Olson 2016). The structure of the latent form was first described in plasminogen activator inhibitor-1 (SERPINE1), which uniquely forms this latent state spontaneously under physiological conditions (Mottonen, Strand et al. 1992, Whisstock, Pike et al. 2000). This state is called "latent" because it can be converted back into the active form through denaturation and refolding. Transition from native to latent conformation provides a fine level of functional control which could be considered as a homeostatic mechanism of serpins activity regulation (Irving, Pike et al. 2000, Law, Zhang et al. 2006).

δ-state is an intermediate serpin conformation between latent and native state (**Figure 1.6D**). From a structural point of view, it is characterised by the RCL insertion into the β-sheet A and the unwinding of one of the helices that completes hydrogen bonding of the β-sheet. δ conformation functional role remains to be understood but it has been proposed to favour transition to latent or, as discussed later on, polymeric transition (Law, Zhang et al. 2006, Heit, Jackson et al. 2013).

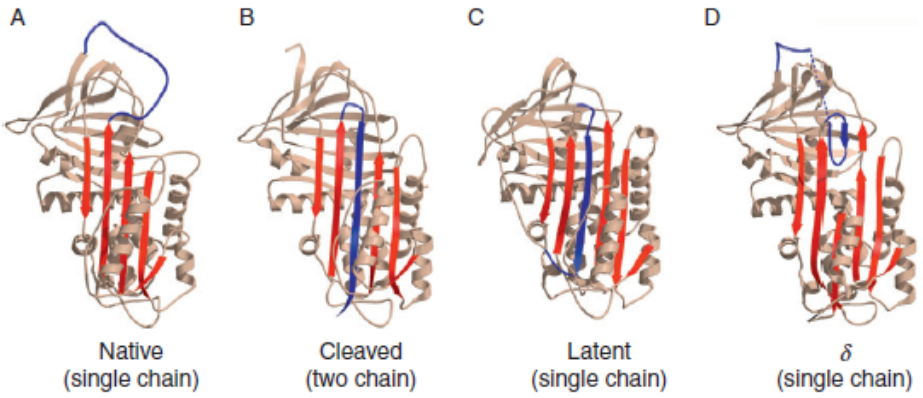

Figure 1.6. Serpins conformational states. Comparison of X-ray structures of the metastable native (**A**, SERPINA1), cleaved (**B**, SERPINA1) and latent (**C**, SERPINE1) serpin conformation, and δ-conformation of an SERPINA3 (**D**). All structures are shown in ribbon representation with the RCL colored blue, the A β-sheet red, and the remainder of the structure in gray (modified from Gettins 2002).

1.15.2 Serpins mechanism of action

The remarkable conformational change features of inhibitory serpins suggest a mechanism different from the well-known "lock-and-key" mechanism used by canonical protease inhibitors. Indeed, other families of serine protease inhibitors have a short and rigid RCL, responsible for a tight but

reversible protease docking, excluding conformational changes. In contrast, inhibitory serpins present a long and flexible RCL, fundamental element for the so-called "branched pathway suicide substrate mechanism" (Huntington, 2011).

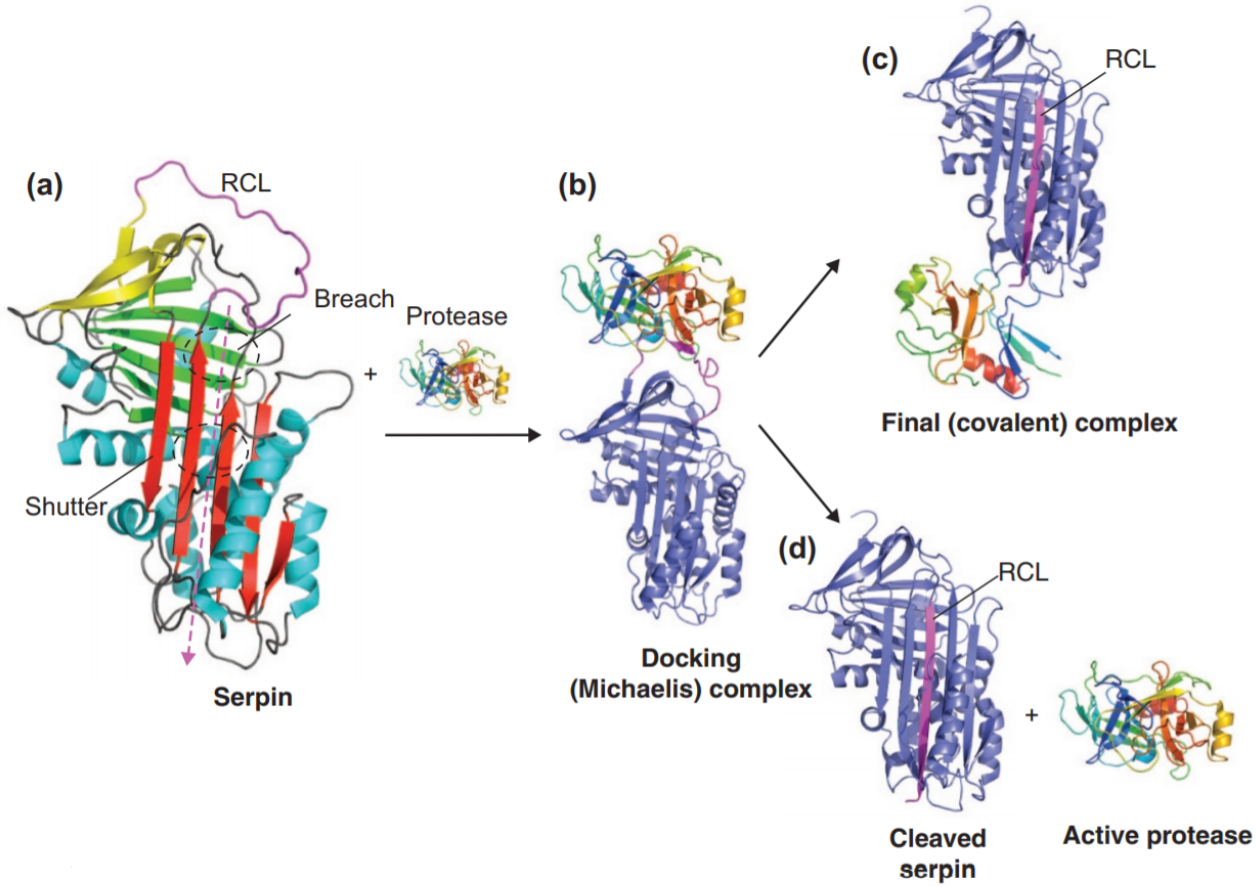

Figure 5. The structure and mechanism of inhibitory serpins. (a) The structure of native SERPINA1 highlighting the β-sheet A in red, the β-sheet B in green and the β-sheet C in yellow is depicted above. The RCL is located at the top of the molecule, in magenta. Breach and shutter locations are shown and the path of RCL insertion is indicated through the magenta dashed line. **(b)** Upon the active protease interaction with serpin, there is the formation of the Michaelis complex between SERPINA1 and inactive trypsin (multicolour) docked onto the RCL. Two distinct pathways are possible then. **(c)** The final covalent serpin-protease complex is ultimately formed, following the S to R serpin transition and the protease active site distortion. **(d)** The structure of cleaved SERPINA1 is indicated, with a magenta label on the RCL, which forms the fourth strand of β-sheet A. In this case, the protease maintains the activity because it has escaped serpin's conformational trap (modified from Law et al., 2006)**.**

Initially serpin and protease associate non-covalently to form a Michaelis complex, in which the protease active site recognizes and engages specific residues flanking the RCL scissile bond (P1-P1' residues). Subsequently, the protease-dependent RCL cleavage leads to the formation of an acyl-enzyme intermediate, in which the serine in the active site of the protease is covalently attached through an ester bond to the backbone carbonyl of the P1 residue (Gettins and Olson 2016). Such

RCL cleavage allows serpin S to R transition due to the energetically favourable insertion of the RCL into the centre of β-sheet A. Since the protease is still covalently attached to the C-terminal end of the cleaved RCL, during serpin conformational change it is transported to the distal end of serpin, with a 70 Å translocation (Stratikos and Gettins 1999). The protease active site undergoes distortion preventing any efficient hydrolysis of the acyl-intermediate and the subsequent release of the protease. Thus, in the final and irreversible inactive serpin-protease complex, the kinetically-trapped protease remains covalently attached to the serpin. The driving force for this conformational change is thought to derive from the dramatic increase in thermal stability associated with the serpin cleaved conformation (Law, Zhang et al. 2006, Gettins and Olson 2016).
Since the suicide substrate mechanism is a branched pathway, there is a competition between serpin conformational change responsible for the formation of the kinetic trapping of the acyl-enzyme intermediate and the normal deacetylation of the intermediate responsible to free cleaved serpin and to regenerates the active protease. This implies that the cleaved RCL, together with the tethered protease, needs to be inserted rapidly into β-sheet A, to induce the distortion of the protease active site, before deacetylation can occur (Gettins and Olson 2016).
The energy released by the conformational change of a serpin, from native metastable state to the stable cleaved one, already seems to be expended in the translocation of the protease into the β-sheet A. Therefore, the Michaelis complex transition to the kinetically trapped acyl-enzyme intermediate complex, leading to the distortion of protease active site, must require additional energy under a kinetic point of view. It has been observed that helix F, overlying β-sheet A, hampers the insertion of the RCL with the tethered protease. Hence, it is likely that the energy released by the serpin conformational change is partially stored by movement or unfolding of helix F. Upon full RCL insertion and protease translocation, this stored energy might then be recovered by the helix F return into its native state and coupled to conformationally distorting the protease (Gettins 2002).

1.15.3 Serpins polymerization and serpinopathies

The conformational flexibility of serpins renders them particularly susceptible to point mutations responsible for aberrant molecular linkage, polymer formation and subsequent deficiency and disease (Law, Zhang et al. 2006). Although, the mechanism responsible for serpin polymerization needs to be clarified, two hypothetical models have been proposed: the domain-swapping model postulates that serpin polymerization results from the unfolding of the native protein, whereas the

loop-sheet mechanism proposes that polymer formation takes place along with the serpin folding pathway (Huntington 2011, Gettins and Olson 2016).

Point mutations in the amino acidic sequence are responsible for distorting the RCL and β-sheet A relationship. The subsequent alteration in structure leads to the formation of an unstable intermediate, where RCL inserts into the β-sheet A of another serpin to form a dimer, which in turn extends to form long chains of polymers. The related diseases triggered by these ordered serpin polymers would be responsible for a clinical phenotype deriving from a toxic gain of function, caused by an intracellular serpin polymers accumulation, or a loss serpin inhibitory activity (Davies and Lomas 2008). The most extensively studied examples of mutant serpins causing a harmful gain of function are the Z variant allele of SERPINA1, accumulating in the endoplasmic reticulum of hepatocytes in association with liver disease, and mutants of neuroserpin (SERPINI1), eliciting the dementia familial encephalopathy with neuroserpin inclusion bodies (Lomas, Evans et al. 1992, Miranda, Romisch et al. 2004). Loss of function phenotypes such as angioedema, emphysema and thrombosis are due to polymerization of mutant C1-inhibitor (SERPING1), α_1-antichymotrypsin (SERPINA3) and antithrombin (SERPINC1), respectively. The common mechanism underlying these conditions allowed to group them all in one class of diseases, known as serpinopathies (Davies and Lomas 2008).

1.15.4 Serpins members

Serpins are ubiquitously expressed from higher eukaryotes to viruses. The human serpin superfamily accounts for thirty-six members and five pseudogenes represented by the first nine clades (from A to I) with the largest part of them playing mainly an inhibitory role (Heit, Jackson et al. 2013). Mouse serpins account for sixty functional genes, the majority of which are orthologous to human SERPINs gene while some have been expanded into multiple paralogue genes (Heit, Jackson et al. 2013, Aslam and Yuan 2019).

Clade A, which is the largest class, is composed by members classified as antitrypsin-like extracellular proteins. It includes eleven human genes (1,3-12) and two pseudogenes, localized on chromosome 1, 14 and X. SERPINAs members are involved in inflammatory response (SERPINA1/SERPINA3) or they act as non-inhibitory hormone transport molecules (SERPINA6/SERPINA7) (Law, Zhang et al. 2006, Heit, Jackson et al. 2013). Instead, concerning Clade A in mouse, the A1 is expanded into six members, a-f and the A3 into nine members, a-c and f-n. The other serpins composing clade A are orthologous to human gene (Heit, Jackson et al. 2013).

Clade B is composed of intracellular serpins, considered to be ancestors of the extracellular ones, representing an exception since most of the other serpins are mainly secreted by specific tissue (Irving, Pike et al. 2000, Olson and Gettins 2011). They have shorter N- and C-terminal and lack the secretory signal peptide (Silverman, Bird et al. 2001). In humans, on chromosomes 18 and 6, there are thirteen genes encoding for SERPINB and one pseudogene, which are mainly involved in inflammation and immune system function. In particular SERPINB1, B6, B7 and B9 play a role in neutrophil and megakaryocyte development and inhibition of cytotoxic granules proteases granzyme B and SERPINB3 inhibits papain-like enzyme (Law, Zhang et al. 2006, Heit, Jackson et al. 2013). SERPINB5, instead, doesn't have an inhibitory function, does not undergo classical conformational change and prevents metastasis in breast cancer (Zou, Anisowicz et al. 1994, Law, Zhang et al. 2006). On the other hand, in mouse, SerpinB1 is expanded in three members a-c, SerpinB3 and B6 include four members each and SerpinB9 is expanded to seven members and one pseudogene. SerpinB11 is active in mouse, while the human orthologue is inactive.

The Clade C is composed of only one member, antithrombin, as well as Clade D serpin, also known as heparin cofactor II, an inhibitor of thrombin. SERPINC1 and D1 have their orthologous in mice (Vicente, He et al. 2004, Rau, Deans et al. 2009, Heit, Jackson et al. 2013).

Clade E is characterized by three extracellular members (SERPINE1, 2 and 3) and also in this case the three mouse genes are orthologous to human ones. They are involved in coagulation and recovery of nerve structure and function (Lino, Atanasoski et al. 2007, Heit, Jackson et al. 2013).

Clade F is composed of two members, F1 and F2 having their own mouse orthologous respectively. They mainly play a role in angiogenetic regulation and fibrinolysis (Heit, Jackson et al. 2013). Interestingly, SERPINF1 seems to act as a neurotrophic factor (Irving, Pike et al. 2000).

Clade G includes only SERPING1, better known as C1 inhibitor.

Clade H consists of only one member - heat-shock protein 47 (HSP47) - which has its orthologue in mouse. HSP47 does not act as protease inhibitor, but as chaperon for collagen (Widmer, Gebauer et al. 2012). Interestingly, it has been found that deletion of HSP47 is lethal in mouse (Nagai, Hosokawa et al. 2000, Heit, Jackson et al. 2013).

Clade I is composed of two extracellular proteins, SERPINI1 also known as neuroserpin inhibitor and SERPINI2, known as pancipin.

The other eight clades of serpins superfamily, clades J-P, represents viral, nematode, horseshoe crab, blood fluke and plant serpins (Irving, Pike et al. 2000, Heit, Jackson et al. 2013).

1.16 SERPINA3/SerpinA3n

Human SERPINA3 (also known as α1-antichymotrypsin) is a glycoprotein of 423 amino acids including a 25-residue signal peptide at the N-terminal that is cleaved once the protein is mature (Baker, Belbin et al. 2007) (**Figure 1.7**). Due to heavy glycosylation, among which six N-glycosylation sites harbouring four oligosaccharide side-chains, it reaches 55-66 kDa (Hwang, Steineckert et al. 1999, Ianni, Manerba et al. 2010).

SERPINA3 gene located in a cluster on chromosome 14q32.1, which includes nine other serpins. As for the human gene, also murine clade A3 serpin is present in a cluster located on chromosome 12F1, including 14 genes (named SerpinA3a-n). Importantly, SerpinA3n shares 70% homology with the human gene (Forsyth, Horvath et al. 2003) therefore it has been considered as the functional orthologue of human SERPINA3 in the brain (Horvath, Forsyth et al. 2004).

The expansion of SerpinA3 gene is not restricted to mouse species, indeed in rat genome there are six antichymotrypsin-like serpins. Therefore, the presence of only one α_1-antichymotrypsin in human, differently from mouse and rat, seems to be an exception rather than a rule. This may be due to gene loss, even if further studies on the clade A cluster in other primates should be carried out to confirm this hypothesis (Forsyth, Horvath et al. 2003, Horvath, Forsyth et al. 2004).

SERPINA3 is primarily synthesized by hepatocytes, bronchial epithelial cells and monocytes, but it can be also expressed in other organs, such as kidney, brain and prostate (Papadimitriou, Stein et al. 1980, Kalsheker 1996). As the human SERPINA3, also its murine orthologue shows a wide tissue distribution, being expressed in the liver, brain, testis, lungs, thymus, spleen, and to a lesser extent in bone marrow, skeletal muscle, and kidney (Horvath, Irving et al. 2005).

In the CNS, the primary source of SERPINA3 are astrocytes (Gopalan, Kasza et al. 2005) where its expression is up-regulated by IL-1, TNF, oncostatin M, IL-6 soluble and IL-6 receptor complexes (Das and Potter 1995, Kordula, Rydel et al. 1998, Kordula, Bugno et al. 2000).

Functional STAT and NF-kB sites are located within the regulatory regions of the SERPINA3/SerpinA3n gene suggesting their cytokine-mediated activation to ensure SERPINA3/SerpinA3n expression (Kordula, Bugno et al. 2000, Baker, Belbin et al. 2007).

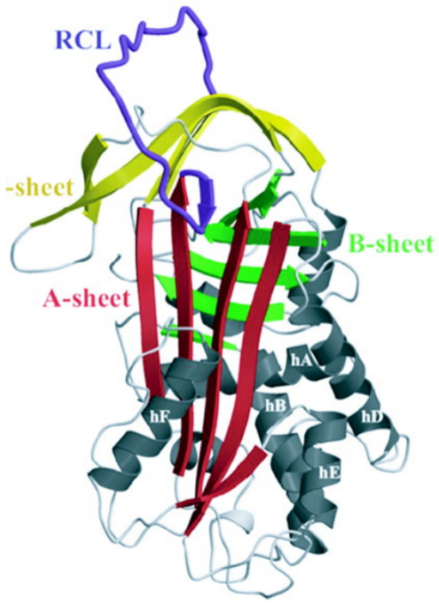

Figure 1.7. The structure of the murine α_1-antichymotrypsin. The structure of SerpinA3n, with β-sheet A in red, β-sheet B in green, β-sheet C in yellow, RCL in purple and helices in grey (Modified from Horvath et al., 2005)

1.16.1 SERPINA3 physiological and pathological functions

SERPINA3 is an acute phase plasma protein, whose blood concentration increases during the inflammatory process. Indeed, its physiological role involves the inhibition of serine proteases during inflammation to keep the activity of proteases under control, avoiding possible tissue damages (Baker et al., 2007). The inhibitory effect of SERPINA3 appears to be specific for neutrophil cathepsin G, mast cell chymase and pancreatic chymotrypsin. It has been shown that it inhibits purified DNA polymerase and DNA primase and that would be physiologically relevant since SERPINA3 contains a nuclear localization signal and nuclear distribution has been shown in some cells (Forsyth 2003).

Both SERPINA3/SerpinA3n are involved in the same physiological processes as complement cascade, apoptosis, wound healing, inflammation and extracellular matrix remodeling. Furthermore, together with their biological role, they also share other similarities such as the overexpression in some pathologies (Aslam and Yuan 2019).

Alteration of the serpin-protease equilibrium can lead to severe consequences. Regarding the SERPINA3, its dysregulation has been associated to different diseases such as obstructive pulmonary disease, AD, PD, stroke, cystic fibrosis, MSA, pancreas, stomach, breast, lymphatic and hepatic cancers (Aslam and Yuan 2019).

High SERPINA3 levels were detected in serum of people affected by malignant diseases (Matsuzaki, Iwamura et al. 1981, Bernacka, Kuryliszyn-Moskal et al. 1993), suggesting its use as a potential biomarker (Aslam and Yuan 2019). Indeed, SERPINA3 in complex with prostate specific antigen has been proposed as clinical marker for prostate cancer (Leinonen, Lovgren et al. 1993, Ishibashi 2006). Because of its ability to bind DNA polymerase and DNA primase, it may be involved in the protection against tumor progression by inhibiting DNA replication (Takada, Tsuda et al. 1988, Tachikawa, Tsuda et al. 2001).

Physiologically, basal level of the SERPINA3 expression in the brain is very low, but immunohistochemical analysis reveals the presence of SERPINA3 in activated astrocytes during aging, both in humans and monkeys (Abraham, Selkoe et al. 1988, Koo, Abraham et al. 1991). Upregulation of the SERPINA3 in the brain of non-demented people aged over sixty-five years compared to younger individuals was observed, further confirming a SERPINA3 involvement in aging process (Vanni, Colini Baldeschi et al. 2020).

1.16.2 SERPINA3 in neurodegeneration

SERPINA3 was firstly linked to AD when it was found to be a relevant component of amyloid brain deposit, being highly expressed in AD affected brain regions (Abraham, Selkoe et al. 1988).

SERPINA3 overexpression appears to be involved in the progression of AD (Kanemaru, Meckelein et al. 1996, Abraham 2001, Yamada 2002) and, in line with this hypothesis, upregulation of *SERPINA3* transcript in human frontal cortex samples of patients at early-stages of AD-related pathology has been observed (Vanni, Moda et al. 2017). Furthermore, high concentration of SERPINA3/SerpinA3n has been found both in the CSF and brain of AD affected subjects and disease animal models, respectively (Licastro, Campbell et al. 1999, Porcellini, Davis et al. 2008).

In situ hybridization studies on AD brains have shown that SERPINA3 is mainly produced by reactive astrocytes surrounding senile plaques. This is also confirmed by the high level of soluble protein and by RNA-sequence analysis of AD brains (Pasternack, Abraham et al. 1989, Zhou, Song et al. 2020). However, transcriptomic and immunofluorescence analyses of brains from mouse model of AD, undergoing Aβ accumulation, revealed the appearance of SerpinA3n positive oligodendrocytes cell populations, which provides some evidence for a difference in the cell type of origin between mice and humans (Zhou, Song et al. 2020).

Interestingly, a SERPINA3 signal peptide polymorphism at codon 17 (A/T), in combination with APOE4 allele, has been associated with an increased susceptibility to AD (Kamboh, Sanghera et al.

1995). Furthermore, the correlation between APOE4 and SERPINA3/SerpinA3n has been recently confirmed, observing that human APOE4-targeted replacement in mice leads to increased expression of Serpina3 family genes in their brains (Zhao, Ren et al. 2020). This finding was also supported by the co-localization of APOE and SERPINA3/SerpinA3n found in amyloid plaques (Licastro, Campbell et al. 1999).

Furthermore, a link between SERPINA3 and tau has been proposed. Indeed, SERPINA3 can influence tau phosphorylation, neurite degeneration and apoptosis in primary mouse and human neurons. For this reason, it was hypothesized that SERPINA3 does not only contribute to amyloid deposition, but also to tau hyperphosphorylation, tangle formation, thus enhancing neurodegeneration (Padmanabhan, Levy et al. 2006).

SERPINA3 was found to be significantly upregulated in the motor cortex of sporadic ALS patients (Sanfilippo, Longo et al. 2017) and in the frontal cortex of MSA-affected patients (Mills, Ward et al. 2016).

Nevertheless, polymorphism of SERPINA3 gene is also associated with an increased susceptibility to neurological illnesses and may be related to an early onset of PD and MSA (Yamamoto, Kondo et al. 1997, Furiya, Hirano et al. 2005), suggesting SERPINA3 involvement in other types of neurodegenerative diseases.

Despite these evidences, the role of SERPINA3/SerpinA3n in neurodegeneration remains speculative.

Concerning prion diseases, *SERPINA3* transcripts upregulation has been observed in brains from BSE-infected cynomolgus macaques (Barbisin, Vanni et al. 2014). WB and RT-qPCR analysis of human frontal cortex specimens from patients affected by other types of prion diseases confirmed elevated levels of SERPINA3 (Vanni, Moda et al. 2017). However, *SERPINA3* up-regulation was already observed in the CNS of sporadic Creutzfeldt-Jakob disease (sCJD) patients, while CSF and urine samples revealed high level of SERPINA3 protein (Miele, Seeger et al. 2008). Moreover, increased level of SerpinA3n mRNA has been found in different prion disease mouse models (Campbell, Eddleston et al. 1994, Dandoy-Dron, Benboudjema et al. 2000, Riemer, Neidhold et al. 2004, Xiang, Windl et al. 2004, Xiang, Hummel et al. 2007, Hwang, Lee et al. 2009), and its expression progressively increases during the course of the disease (Chen, Xu et al. 2017, Nuvolone, Schmid et al. 2017, Vanni, Moda et al. 2017, Smith, Freeman et al. 2020).

2. AIM

SERPINA3/SerpinA3n is a member of the huge superfamily of serine protease inhibitors, found to be upregulated in patients affected by prion diseases. The aim of this project was focused on the identification of the role played by SERPINA3/SerpinA3n in prion diseases.

To confirm the peculiar SERPINA3/SerpinA3n-prion relation, other members of the serpin superfamily were tested for their putative differential expression in the frontal cortex of patients affected by sporadic form of prion disease compared to non-neurodegeneration affected controls.

Considering the SerpinA3n upregulation observed in animal model of prion disease, the levels of other mouse serpins were analyzed even in RML-infected mice.

SerpinA3n expression levels were then evaluated in cell lines infected with prions. Subsequently, through conditioned medium of SerpinA3n expressing cells and recombinant SerpinA3n treatment, prion accumulation changes were evaluated in ScN2a RML cells. Similarly, SerpinA3n transcriptional inhibition was performed in prion-infected cells to evaluate PrP^{Sc} variations.

A mouse-line knockout for SerpinA3n was characterized under molecular point of view and its resistance to prion infection was assessed by challenging it with three different prion strains.

3. MATERIAL AND METHODS

3.1 Patient samples

A total of thirty frontal cortex tissue samples from prion-affected patients and control subjects were collected. The study was performed on samples coming from sCJD type 1 cases (n=15). Age-matched subjects died from unrelated conditions, lacking any neurological sign or pathological lesions in brain were included as controls (n=15). sCJD cases were all confirmed by means of neuropathological analysis and the detection of PrP^{Sc} by WB. Samples and associated data were provided by the MRC Edinburgh Brain Bank (UK), the Carlo Besta Neurological Institute (Milan, Italy) and the University hospital of Verona (Italy). The full list of samples and patient details is reported in **Table 1**.

Sample	Sex	Age	Sample	Sex	Age	Codon 129
Ctrl 15221	M	53	**sCJD 1508**	F	53	M/M
Ctrl 3783	M	56	**sCJD 1722**	M	59	nd
Ctrl 24781	M	57	**sCJD 1679**	M	60	M/M
Ctrl 24780	F	57	**sCJD 1728**	F	61	nd
Ctrl 18391	M	58	**sCJD 1620**	F	63	nd
Ctrl 7628	M	60	**sCJD 1368**	M	64	M/M
Ctrl 22612	M	61	**sCJD 1675**	M	64	M/V
Ctrl 18407	M	62	**sCJD 1548**	M	65	M/M
Ctrl 20121	M	63	**sCJD 9214**	M	71	M/M
Ctrl 13410	M	68	**sCJD 1669**	M	72	M/M
Ctrl 14395	F	71	**sCJD 9230**	M	77	M/M
Ctrl 9508	M	76	**sCJD 1524**	F	78	M/V
Ctrl 1656	F	62	**sCJD 1407**	F	79	nd
Ctrl 1682	F	59	**sCJD 9001**	M	83	M/M
Ctrl 1714	M	76	**sCJD 1723**	F	86	M/M

Table 1. Human brain samples for RT-qPCR analysis. The table lists sex and age of non-neurodegeneration affected controls (CTRL) and sporadic Creutfeldt-Jakob (sCJD) included in the present study. F female, M male, MM methionine/methionine, MV methionine/valine, VV valine/valine.

3.2 Mouse samples

Prion-infected and age- and sex-matched CD1 mice brain samples were kindly provided by Dr. Moda (Fondazione IRCCS Istituto Neurologico Carlo Besta, via Celoria 11, Milan, Italy) (Vanni et al., 2017). SerpinA3n knockout (C57BL/6N-Serpina3n$^{em1(IMPC)J}$) mice were obtained from The Jackson Laboratory. RNA guides (CTCAGAAGCGGTGTTAACTG, AGTGCCCATGATGAGCATGG and CCTGTTCTGTCCTCAGCCTA) and Cas9 were microinjected into C57BL/N6 zygotes. Brains from

SerpinA3n KO (SerpinA3n$^{-/-}$, n=4), heterozygous (SerpinA3n$^{+/-}$, n=4) and wild-type mice (SerpinA3n$^{+/+}$, n=4), sacrificed at six months of age using CO_2, were used to confirm SerpinA3n transcript and protein ablation.

3.3 SerpinA3n$^{-/-}$ mice genotyping

DNA was extracted from 0.2-0.5 cm tail or ear biopsies. Tail snips were digested in 250 μl tail buffer (100mM Tris pH8.5, 5mM EDTA pH 8.0, 125mM NaCl, 0.2% SDS) and 100 μg/ml Proteinase K (#EMR022001, Euroclone), and then placed in shaker at 55 °C at 500 rpm overnight. The samples were centrifuged for 5 min at room temperature at maximum speed. The supernatant was collected and 300 μL of EtOH 100% were added. The samples were centrifuged for 5 min at room temperature at maximum speed and supernatant was discarded. 600 μL of EtOH 70% were added to the pellet and were centrifuged at maximum speed for 5 min. The supernatant was removed and the step was repeated. The pellet was let dry and 100 μL of TE Buffer were added. The samples were put in shaker for 30 min at 56 °C and then vortexed. For HotSHOT DNA purification protocol (Truett et al., 2000) performed on ear biopsies, 75 μL of 15 mM NaOH, 0.2 mM disodium EDTA pH 12.0 were added to the samples. They were then placed in Veriti™ 96-well Thermo Cycler (Applied Biosystems) at 98 °C for 1 hour. 75 μL of Tris HCl pH 5.5, were then added, and the samples were centrifuged at 800 g for 5 min.

1:10 dilution of stock sample was used as template for subsequent PCR reactions, carried out in 12 μL on 96-well plates using KAPA2G Fast HotStart PCR Kit (#KK5510, Sigma-Aldrich). Primers were designed by The Jackson Laboratory as follows in **Table 2**.

Name	**Primer sequence 5'→3'**
Common	AAC CAA GCC TGG AGA CAA TG
Wild-type reverse	CGT GTC AAG AGG GTC AAA GG
Mutant reverse	TTA AGT CAG AGC CTG GCA CA

Table 2. Primer sequences for PCR of mouse samples.

PCR cycling program on a Veriti™ 96-well Thermo Cycler (Applied Biosystems) was the following: 94 °C for 2 min; 94 °C for 20 sec, 65 °C for 15 sec, 68 °C for 10 sec for 10 cycles; 94 °C for 15 sec; 60 °C

for 15 sec; 72 °C for 10 sec for 28 cycles; 72 °C for 2 min; 10 °C. PCR products were load on 2% agarose gel in TBE 0.5X, to which Midori Green Advance (# MG04, NIPPON Genetics) (1:15000) was added, at a fixed voltage (90-110 V) and then visualised at transilluminator.

3.4 Data Source

Selection of serpin genes for transcriptomic analysis was performed using different databases. To evaluate the level of expression of *SERPINs* genes in human brain tissue, Consensus Normalized eXpression (NX) dataset, which combines data from the three transcriptomics datasets (HPA, GTEx and FANTOM5) was used (https://www.proteinatlas.org/).

For mouse serpins genes, two different databases were used. Data were analyzed from Mouse ENCODE transcriptome (https://www.ncbi.nlm.nih.gov/bioproject/PRJNA66167/) and Allen brain Atlas (https://mouse.brain-map.org/).

For human genes a threshold value of Transcripts Per Kilobase Million (TPM) ≥ 2 (Wagner, Kin et al. 2012) was set, while a cut-off value of Reads Per Kilobase Million (RPKM) ≥ 1 was used for mouse genes (Hebenstreit, Fang et al. 2011). Following this analysis, twelve and seventeen serpin transcripts were chosen for human and mouse, respectively.

3.5 RNA Extraction

Total RNA from human samples and CD1 mouse brains was isolated as already described in Vanni et al 2017. For SerpinA3n$^{-/-}$, SerpinA3n$^{+/-}$ and SerpinA3n$^{+/+}$ mice, one brain hemisphere was homogenized using T 10 basic ULTRA-TURRAX® homogenizer (# 0003737000, IKA Dispersers) in 1ml TRIzol™ Reagent (# 15596026, Invitrogen). For cell, 1mL of TRIzol reagent were used to homogenize pelleted cells after 5 min centrifugation at 0.4 g. RNA was extracted with PureLink® RNA Mini Kit (#12183020, Life Technologies) and on-column DNA digestion was performed using PureLink® DNase Set (# 12185010 Life Technologies). RNA was checked for concentration and purity on DS-11 Spectrophotometer (DeNovix). RNA integrity was analyzed using 2100 Bioanalyzer (# G2939BA, Agilent Technologies) with an RNA Integrity Number (RIN) ≥ 8, or determined by gel analysis, presenting sharp 28S and 18S rRNA bands.

3.6 RT-qPCR

For human frontal cortex, mouse brain and immortalized cells, cDNA was obtained starting from 3 µg of total RNA with 50 µM Oligo(dT)20 (#AM5730G, Invitrogen), 10mM ea dNTP mix (#18427013, Invitrogen), 40 U RNaseOUT™ Recombinant Ribonuclease Inhibitor (#10777019, Invitrogen), 5X First Strand Buffer, 0.1M DTT and 200 U SuperScript® III Reverse Transcriptase (#18080093, Invitrogen). A negative control was performed for each sample by omitting the reverse transcriptase.

qPCR primers were designed using the outline tool Primer-Blast provided by NCBI, setting the PCR product size between 70-150 nt, possibly spanning an exon-exon junction or flanking intron sequence/s, to prevent amplification of genomic DNA. Primers were validated using the online tool OligoCalc (http://biotools.nubic.northwestern.edu/OligoCalc.html), to exclude possible self-dimerization, hairpin formation, and self-annealing of 3' and 5' ends. Alternatively, qPCR human primer for *SERPINB6* was taken from (Heutinck, Kassies et al. 2012); *SERPINB9* from (Muthukumar, Ding et al. 2003); *SERPINF1* from (Dadras, Lin et al. 2015); *SERPING1* from (Pappalardo, Zingale et al. 2004) and *SERPINH1* from (Reis, Waldron et al. 2011) (**Table 3**). For what concerns qPCR mouse primer, *SerpinD1* and *SerpinF2* were taken from (Safdar, Cheung et al. 2012); *SerpinE2* from (Charles, Coury et al. 2012) and *SerpinI1* from (Lebeurrier, Launay et al. 2008) (**Table 4**).

Gene expression assays were performed using iQ™ SYBR® Green Supermix 2x (170-8882, Bio-Rad Laboratories), 400nM final concentration of the corresponding forward and reverse primer (Sigma-Aldrich) and 10 ng/µL final concentration of cDNA samples. CFX96 Real-Time System C1000 Touch™ Thermal Cycler (Bio-Rad Laboratories) was used to perform amplification and cycling conditions included an initial denaturation of 3 min at 95°C the 45 cycles at 95°C for 10 sec and 60° for 1 min. qPCR reaction was performed in 96-well plates, performing duplicates for each primer pair and sample. No reverse transcriptase control for each primer pair was analyzed to evaluate possible genomic DNA contamination and no template control was added in each plate to exclude the presence of contaminating DNA in the qPCR reaction mix. Melting curve analysis of each amplicon was performed for each primer pair to verify that artificial products or primer dimers were not responsible for the fluorescence signal obtained. Moreover, because of the high amplicon-specificity of the characteristic melting curve temperatures, specific for each primer pair, the melt temperature was used to identify transcript expression among different samples.

Gene	Forward primer sequence 5'→3'	Reverse primer sequence 5'→3'
GAPDH	CCTGCACCACCAACTGCTTA	TCTTCTGGGTGGCAGTGATG
B2M	AGATGAGTATGCCTGCCGTG	TCATCCAATCCAAATGCGGC
RPL19	CTAGTGTCCTCCGCTGTGG	AAGGTGTTTTTCCGGCATC
ACTB	AGAGCTACGAGCTGCCTGAC	AGCACTGTGTTGGCGTACAG
SERPINA3	TGCCAGCGCACTCTTCATC	TGTCGTTCAGGTTATAGTCCCTC
SERPINA8	CCAGCCTCACTATGCCTCTG	GTGGATGGTCCGGGGAGATA
SERPINB1	GGCGGCCTGTCGGTTTT	AGCCGGATTGTTCTCACTCA
SERPINB6	CCCTCCCGCGGTTTAAACTA	CCTCCGTGCCTTCCTCAT
SERPINB8	CGGATGAGGTACACACCCAG	TCCATCACTCTTTCACGGCG
SERPINB9	TCAACACCTGGGTCTCAAAAAA	CAGCCTGGTTTCTGCATCAA
SERPINE1	GCAACGTGGTTTTCTCACCC	GGCCATGCCCTTGTCATCAA
SERPINE2	CGAGCGCGGTCGTCCT	CCCGTGTTGGAGCCTAGTTC
SERPINF1	CCCGTGTTGGAGCCTAGTTC	AACTTTGTTACCCACTGCCCC
SERPING1	CCCATGATGAATAGCAAGAAGTACC	CTGCCCCACCTTGGCTT
SERPINH1	CCGTGGCTTCATGGTGACTCGG	AGTAGTTGTAGAGGCCTGTCCGGT
SERPINI1	AGAGACGAAAGCAGGAACGA	TGTAACAGTTTCAAGCCTCCCA

Table 3. Primer sequences for RT-qPCR of human samples

Gene	Forward primer sequence 5'→3'	Reverse primer sequence 5'→3'
Gapdh	TTCACCACCATGGAGAAGGC	GGCATGGACTGTGGTCATGA
Tubb3	CGCCTTTGGACACCTATTC	TACTCCTCACGCACCTTG
ActB	CACACCCGCCACCAGTTC	CACACCCGCCACCAGTTC
SerpinA3n	ACCCTGAGGAAGTGGAAGAA	CCTGATGCCCAGCTTTGAAA
SerpinA6	GCTGGCAGATGTGGGCATTA	TGGCCTTGTGGAGTACCGTT
SerpinA8	TGTCTAGGTTGGCGCTGAAG	GATGTATACGCGGTCCCCAG
SerpinB1a	GTTTTCCTCCTCGGCTTTTGC	AGTTTGAGGATGGAGTCGTCC
SerpinB1b	GTGCTTGCCAGTAAGACACTC	ATGGTGAAGGCTCCTCTGTAG
SerpinB6a	TTCCTGCACCCTTCTGTGTC	TGAAGCCGCCTAGATTCTCC
SerpinB8	TCGTGTGATTTCCTTTCGACCT	TTCCTGCACCCTTCTGTGTC
SerpinB9d	AAAGAACCCATGGAACGGGA	TCCTGAGCCTGAGAGCTTAC
SerpinD1	GAATGGCAATATGTCAGGCATCT	CACTGTGATGGTACTTTGGTGCTT
SerpinE1	TCCACAAGTCTGATGGCAGC	GGGGTGGTGAACTCAGTGTA
SerpinE2	CACATGGGATCGCGTCCATC	CAGCACTTTACCAACTCCGTTTA
SerpinE3	TGGAGCTTTCAGAGGAGGGTA	TACTGAAGACAAACCCTGTGCT
SerpinF1	ACGATCTGTACCGCCTGAGA	TTCGATGTTCAGCTCCCAGAG
SerpinF2	TTCTCCTCAACGCCATCCA	GGTGAGGCTCGGGTCAAAC
SerpinG1	GAACTTGGACCAGGACGCAG	GCTGGTAGCTTCGGGATCTG
SerpinH1	CCGGCCCAGAATGAAAAAGGC	TAAGGTGCCCAGAAGGAGAGA
SerpinI1	CGCCATTCAATGGGATATG	CAAAGAGCGAATTGGCAAG

Table 4. Primer sequences for RT-qPCR of murine samples

3.6.1 RT-qPCR data analysis

Differential expression of target human genes was normalized to three different reference genes (*ACTB, GAPDH* and *B2M*) expression. The expression stability of these three housekeeping genes was previously assessed in both disease and control patients and they effectively showed

comparable expression levels among the different groups (Vanni, Zattoni et al. 2018). For mouse samples, *Actb, Gapdh* and *Tubb3,* were used as reference genes for normalization.

The absolute expression value (C_T) of each serpin gene was addressed in human/mouse brain pool to select genes having a $C_T \leq 35$ (Vanni, Moda et al. 2017). RT-qPCR analysis for selected serpins mRNA was performed in the frontal cortex of 30 human brains and whole brain of 14 CD1 mice. The relative expression ratio (fold change) was calculated using $2^{-\Delta\Delta CT}$ method (Livak and Schmittgen 2001) as reported in (Vanni, Zattoni et al. 2018).

ΔC_T were calculated subtracting the C_T of the housekeeping gene to the C_T of the target one, both for "test" (sCJD affected patient/prion-infected mouse/heterozygous or knock-out mouse) and "calibrator" (control). Then, $\Delta\Delta C_T$ were obtained with the ΔC_T of each sample (both of calibrator and test) minus the mean ΔC_T of the population of calibrator samples (fifteen samples for human analysis, three and four samples for the pre and symptomatic stages of prion-infected mice analysis, respectively, and four samples for SerpinA3n$^{-/-}$ analysis). Fold change values smaller than 1 were converted using the equation -1/FC, for representation.

3.8 Cell culture

Non-infected and chronically infected with RML or with 22L prion strain (ScN2a RML and ScN2a 22L, respectively) N2a were grown in Minimal Essential Medium (MEM)-1X, GlutaMAX^{TM} supplement (#32561037, Gibco, Thermo Fisher Scientific) supplemented with 10% fetal bovine serum (FBS), 1% non-essential amino acids, and 1% penicillin-streptomycin. GT1-1 (hereafter called "GT1") and chronically infected with both RML and 22L prion strains (ScGT1 RML and ScGT1 22L, respectively), were grown in Dulbecco's modified Eagle's medium (DMEM)-1X, GlutaMAX^{TM} supplement (#10569010, Gibco, Thermo Fisher Scientific) supplemented with 10% FBS and 1% penicillin-streptomycin. All cell lines were cultivated in 10 cm^2 or 6 cm^2 Petri dishes (Falcon) at 37 °C under 5% CO_2.

3.9 N2a overexpressing SerpinA3n

Serpina3n coding sequences was amplified from mouse cDNA using the following primers: 5'-GGATATCTGCAGAATTCATCATGGCCTTCATTGCAGCTCTGGGG-3', 5'-GCTTGGTACCGAGCTCGGATCCTCATTTGGGGTTGGCTATCTTGGC-3'. Then the resulting amplicon was

cloned to pcDNA3.1 vector by restriction-free cloning. QIAprep® Spin Miniprep Kit (#27106, Qiagen) was used to purify the plasmid after transformation in *E. Coli* DH5α.

Cell transfections were performed using Effectene Transfection Reagent (Qiagen) according to the manufacturer guidelines. Plating of the cells has been performed in a volume of 10 mL Opti-MEM (#11058021, Gibco, Thermo Fisher Scientific) without FBS in a 10 cm^2 Petri dishes 24 hours before transfection (corresponding to 30 – 40 % confluency). Cells were incubated overnight. On the day of transfection, 0.4 µg DNA were diluted with Buffer EC, to a total volume of 100 µl. 3.2 µl Enhancer were added and mixed by vortexing for 1 s. Following a 5 min incubation at room temperature (RT), 10 µl Effectene Transfection Reagent (#301425, Qiagen) were added to the DNA-Enhancer mixture and incubated for a further 10 min at RT. DNA transfection mixture was added to the cells in a dropwise manner. Cells were incubated with DNA transfection mixture for 18 hours at 37 °C, following which FBS-supplemented OPTI-MEM medium was replaced. 48 hours after transfection cells were splitted into fresh medium containing 1mg/mL Geneticin (#10131027, Gibco). The selective medium was changed every 3–4 days until Geneticin-resistant foci could be identified. After that, the stable cell lines were maintained in medium contains 400 µg/mL Geneticin.

Transfection with empty pcDNA 3.1 plasmid (empty vector, EV) was performed in N2a as control (N2a-EV).

DNA was extracted using GenElute™ Mammalian Genomic DNA Miniprep Kit (#G1N70, Sigma-Aldrich), according to the manufacturer guidelines, from N2a clone overexpressing the highest level of SerpinA3n (Clone 2 here after, N2a-SerpinA3n) and PCR was performed to distinguish genomic SerpinA3n sequence from SerpinA3n sequence carried by pcDNA 3.1 using the primers present in **Table 5.**

Name	**Primer sequence 5'→3'**
SerpinA3n-FW	TTCAGACTGCAGAACACAGAAG
SerpinA3n-REV	ATCCATTCCCAACGTGCCAT
T7 Promoter Primer	TAATACGACTCACTATAGGG

Table 5 Primer sequences for PCR of N2a-SerpinA3n cells

3.10 Recombinant SerpinA3n production

SerpinA3n recombinant protein was produced as described in (Horvath, Irving et al. 2005) and (Visentin, Broggini et al. 2020) with some modifications.

A pET(11a) expression vector containing a C-terminal (6x)His-tagged murine SerpinA3n (Genetech) was used to transform *E. Coli* BL21 (DE3) pLysS cells. Cells were grown in Luria-Bertani medium at 25 °C in presence of ampicillin (100 µg/mL) until OD_{600} = 1, when protein production was induced with 0.1 mM isopropyl 1-thio-D-galactopyranoside the growth temperature was lowered to 15°C. After 21 hours of induction, bacteria were pelleted through centrifugation (9000 g for 10 minutes at 4°C) and the supernatant was discarded. The pellet was washed in physiological solution (0.9%), and collected after centrifugation (9000 g for 10 minutes at 4°C). Around 12 grams of pellet was then kept at -80 °C until purification was carried out. The frozen pellet was resuspended in 25 ml (per cell paste) of buffer A (50 mM Tris-HCl, pH 8.0, 300 mM NaCl, 20 mM Imidazole) to which 1 tab of cOmplete™ Protease Inhibitor Cocktail (#11697498001, Roche), 250 µL of 50 mM PMSF and 125 µL of 25 µg/mL DNase were added (homogenization buffer). Bacterial cell lysis was performed by sonication using 5 cycles of 60 seconds on and 60 seconds of rest in ice. Cell debris was discarded after 1 hour of centrifuge (12000 g at 4°C) and the supernatant was resuspended in 25 mL of homogenization buffer. Crude extract was loaded onto HisTrap™ Fast Flow Crude column (#GE17-5286-01, GE Healthcare). The purification was performed with ÄKTA pure chromatography keeping the system at 4°C. After a washing step in 100% buffer A (50 mM Tris-HCl, pH 8.0, 300 mM NaCl, 20 mM imidazole, 50 mM PMSF) to elute all proteins that do not bind to the column, the protein was eluted applying a linear imidazole gradient from up to 500 mM imidazole.

Protein expression and purity of eluted fractions were checked with SDS-PAGE followed by Coomassie brilliant blue staining. Following centrifugation for 5 minutes at 16000 g, the bacterial cells were resuspended in 12 µL of lysis buffer, 4X SDS-PAGE loading buffer was added in a 1:4 ratio and boiled at 100°C for 10 minutes. Samples of the eluted fractions were precipitated adding methanol, chloroform and $_{dd}H_2O$ in a 4:1, 1:1 and 3:1 ratio, respectively. Samples were vigorously vortexed after each addition step and centrifuged at 16000 g for 10 minutes to isolate the proteins at the interface of two layers. The first layer was then carefully removed, and methanol was added in a 4:1 ratio. After vortexing, samples were centrifuge at 16000 g for 10 minutes. The air-dried pellet was mixed with 1X SDS-PAGE loading buffer in a 1:1 ratio and boiled at 100°C for 10 minutes.

The fractions containing the higher amount of purified SerpinA3n were pooled together, dialyzed in buffer 10 mM Tris-HCl, 50 mM KCl pH 8.0 and concentrated using Amicon® Ultra-15 Centrifugal Filters 30 kDa cutoff (#UFC903024, Merk Millipore) to a final concentration of 8 μM.

3.11 Complex formation assay

The ability of SerpinA3n to inhibit the serine protease α-chymotrypsin (#MERC1.02307.0001, Merk) was observed following (Horvath, Irving et al. 2005) protocol. 1 or 5 μM of SerpinA3n was incubated with 1 μM of chymotrypsin in 10 mM Tris-HCl, 50 mM KCl, pH 8.0. Similarly, conditioned medium (CM) from N2a-SerpinA3n was concentrated 20X using Amicon® Ultra-15 Centrifugal Filters 30 kDa cutoff (#UFC903024, Merk Millipore) and 10 μl were incubated with 100 ng chymotrypsin in PBS 1X. Reactions were incubated at 37 °C for 30 min, then 5X SDS-PAGE loading buffer was added to the samples in a 1:5 ratio. Samples were denatured at 100 °C for 10 min and stored at -20°C until further processing or analysis.

3.12 Conditioned medium and recombinant SerpinA3n treatment

N2a-SerpinA3n, N2a-EV and N2a cells at 90% confluency were wash with PBS 1X and fresh, FBS-depleted, Opti-MEM was added. 24 hours later, CM were collected and cells were counted. 1 x 10^5 ScN2a RML cells were plated in a volume of 3 mL MEM in a 6 cm^2 plate (Falcon) 24 hours before treatment. The following day, CM medium from 1 x 10^6 N2a-SerpinA3n, N2a-EV and N2a cells were added to the cells and Opti-MEM was added to reach a final volume of 3mL. For recombinant SerpinA3n treatment, 0.5 μM and 1 μM has been selected as suitable concentration. Vehicle treated cells has been treated with 10mM Tris-HCl, 50 mM KCl pH 8.0. 72 hours after treatment cell lysate was collected.

3.13 siRNA transfection

MISSION® esiRNAs targeting SerpinA3n and EGFP (#EMU072851 and #EHUEGFP, Sigma Aldrich) were transfected on ScN2a RML. Transfection was performed using Lipofectamine 3000 (#L3000008, Invitrogen) according to the manufacturer guidelines. Briefly, 1.5 x 10^5 cells (corresponding to 30-40 % confluency) were plated in a volume of 3 mL Opti-MEM in a 6 cm^2 plate

24 hours before transfection. On the day of transfection, 3.5 μL Lipofectamine 3000 and 121.5 μL of FBS-depleted Opti-MEM were vortex for 5 seconds. Then, 112.5 μL FBS-depleted Opti-Mem and 12.5 μL of siRNA (2.5 μg) were added to diluted Lipofectamine 3000 and incubate for 15 minutes at room temperature. Transfection mixture was added to the cells in a dropwise manner. 72 hours later cell lysate and medium were collected.

3.14 shRNA production and transfection

The selected SerpinA3n (RefSeq NM_009252.1) target sequence for shRNA construction was selected from position 508 to 529 (ACGGGTAGTGCCCTGTTTATT). The oligos, designed for cloning by annealing to create a synthetic DNA duplex with overhang of EcoRI and BamHI, were the following: sh850n-F: GATCCCCGGACGGGTAGTGCCCTGTTTATTCTCGAGAATAAACAGGGCACTACCCGTTTTTTTGAATG and Sh850n-R: AATTCATTCAAAAAAACGGGTAGTGCCCTGTTTATTCTCGAGAATAAACAGGGCACTACCCGTCCGGG, giving rise to the following hairpin sequence: 5'-CCGG-ACGGGTAGTGCCCTGTTTATT-CTCGAG-AATAAACAGGGCACTACCCGT-TTTTTTGAAT-3'. The complementary oligos sh850n-F and sh850n-R were annealed. Then, pU6-Luc-Zgreen plasmid was digested with EcoRI and BamHI and further purified. Ligation of digested plasmid with the synthetic DNA duplex was performed using T4 DNA ligase. QIAprep® Spin Miniprep Kit (#27106, Qiagen) was used to purify the plasmid after transformation in *E. Coli* DH5α. ScN2a RML cells transfection were performed using Effectene Transfection Reagent according to the manufacturer guidelines. 2.5 x 10^5 cells (corresponding to 50 % confluency) were plated in a volume of 3 mL Opti-MEM in a 6 cm^2 plate 24 hours before transfection. On the day of transfection, 1 μg of DNA plasmids (shCTRL and shSerpinA3n) was diluted with Buffer EC, to a total volume of 150 μl. 8 μl Enhancer were added and mixed by vortexing for 5 seconds. Following a 5 min incubation at room temperature, 20 μl Effectene Transfection Reagent were added to the DNA-Enhancer mixture, mixed it gently by pipetting 5 times, and incubated for a further 10 min. 1 ml of Opti-MEM was added to the DNA transfection mixture and then added to each plate in dropwise manner. Cells were incubated with DNA transfection mixture for 18 hours at 37 °C, following which fresh Opti-MEM was added in replacement. 72 hours after transfection cell lysate and medium were collected.

3.15 Intracerebral injection of RML, ME7 and 139A brain homogenates

Ten percent (weight/volume (*w*/*v*)) RML, ME7 and 139A brain homogenates were prepared in sterile PBS and diluted at 10^{-3} (volume/volume (*v*/*v*)) in the same buffer. Six-week-old SerpinA3n$^{-/-}$ and SerpinA3n$^{+/+}$ mice (35–40 g) were anesthetized with tribromoethanol (100 µL/10 g) and stereotaxically injected in the hippocampus (1.8 caudal; + 0.5 lateral; 1.8 depth) with 2 µL of RML (*n* = 5 for SerpinA3n$^{-/-}$ and n=5 for SerpinA3n$^{+/+}$), ME7 (*n* = 5 for SerpinA3n$^{-/-}$ and n=5 for SerpinA3n$^{+/+}$) or 139A (*n* = 5 for SerpinA3n$^{-/-}$ and n=5 for SerpinA3n$^{+/+}$) brain homogenates. All surgical procedures were performed under sterile conditions, at Carlo Besta Institute, Milan.

3.16 Incubation and Survival Time

The incubation time (IT) was calculated considering the time between RML, ME7 and 139A injection and symptoms onset, including ataxia (uncoordinated movement), tail rigidity, and kyphosis (hunched back). Survival time (ST) was calculated as the time between RML, ME7 and 139A injection and the killing of animals. Brains were then harvested and divided in two hemispheres. The left hemisphere was used for biochemical analysis.

3.17 Mouse brain samples

One brain hemisphere from SerpinA3n$^{-/-}$, SerpinA3n$^{+/-}$ and SerpinA3n$^{+/+}$ mice were homogenized at 10% weight/volume in lysis buffer (10 mM Tris–HCl pH 8.0, 150 mM NaCl, 0.5% NP40, 0.5% deoxycholic acid sodium salt). Samples were centrifuged for 1 minute at 4 °C, at 800 g. Protein concentration of cleared homogenates was determined by Bicinchoninic Acid (BCA) method using the bicinchoninic acid solution (#B9643, , Sigma-Aldrich) and Copper(II) sulphate solution (#C2284, Sigma-Aldrich) in 1:50 dilution, and Protein standard (#P0834, Sigma-Aldrich) to build the standard curve. After 30 min at 37°C the reaction was visualized on Enspire Multimode Plate Reader (PerkinElmer).

The left hemispheres of the prion-injected mouse brain were homogenized at 10% (*w*/*v*) in lysis buffer (100 mM NaCl, 10 mM EDTA, 0.5% NP40, 0.5% Na-deoxycholate, 10 mM Tris-HCl pH 7.4) and centrifuged 800 *g* for 1 min. Ten microliters of cleared brain homogenates was treated with 50 µg/mL of PK (Invitrogen) under shaking (1 h, 37 °C, 550 rpm). Enzymatic digestion was stopped

by boiling (100 °C, 10 min) the samples supplemented with loading buffer (sample buffer 4× and reducing agent 10×, Thermo Scientific).

3.19 Cell lysate and conditioned medium samples

For secreted SerpinA3n analysis, CM of un-infected and prion-infected N2a and GT1 cell lines were collected, cleared and concentrated following Gueugneau, d'Hose et al. 2018 protocol. Briefly, after 24 h incubation in serum-free medium, the CM was cleared by centrifugation (10 min at 300 g followed by 20 min at 2000 g) to discard cell debris. Cleared CM were subsequently concentrated 10X using Amicon® Ultra-15 Centrifugal Filters 30 kDa cutoff. Then acetone precipitation was performed adding 4 volume of 100% acetone were added to 10X concentrated CM and vortex 5 seconds. After 1 hour at -20°C, samples were centrifuge at 12000 g at 4°C for 10 minutes. The resulting pellet were air dried and 100 uL of ddH2O was used to dissolved it.

For intracellular protein detection, after removing the medium, cells were washed with PBS 1X and lysed on ice in lysis buffer (10 mM Tris–HCl pH 8.0, 150 mM NaCl, 0.5% nonidet P-40, 0.5% deoxycholic acid sodium salt). Nuclei and large debris were removed with a centrifugation at 2000 g for 10 min at 4 °C.

Protein concentration of cleared cell lysate and CM was determined using the BCA method as previously described.

For intracellular and secreted SerpinA3n detection, 100µg of cell lysate and 50µg of CM, respectively, were added into 5X SDS-PAGE loading buffer in a 1:5 ratio. 6 h PNGaseF (#P0704S, New England Biolabs) treatment of CM was performed starting from 50 µg of CM proteins, following manufacturer's instruction in denaturing reaction condition.

For PrP detection, cell lysates were split into two parts. One part (125µg) was treated with 2.5µg of PK (#3115801001, Roche) at 37 °C for 1 h. The reaction was arrested with 2 mM of phenylmethylsulphonyl fluoride (PMSF, Sigma-Aldrich). The PK-digested samples were precipitated by centrifugation at 180000 g for 75 min at 4 °C in the OptimaTM MAX-XP Ultracentrifuge (Beckman Coulter) and the pellet was resuspended in 1X SDS- PAGE loading buffer. The non-PK-digested samples (15µg) were added into 2X SDS-PAGE loading buffer in a 1:1 ratio.

All samples were boiled for 10 min at 100 °C and stored at -20°C until further processing.

3.20 Western Blot

The desired amount of proteins was loaded onto 9% or 12% Acrylamide/Bis-acrylamide (#A7802 Sigma-Aldrich) gels, for SerpinA3n or PrP detection respectively, and separated by SDS-PAGE using SE 600 Ruby (GE Healthcare). Gels were then transferred to PVDF membrane (Millipore) using Criterion Blotter (Bio-Rad) for 2 hours at 4°C. Secreted SerpinA3n membranes were incubated for 2 minutes in shaking with Ponceau solution. After one washes of 5 minutes, Ponceau stained membrane has been developed as "preview" image on UVITEC (Cambridge). After 1h of blocking in 5% milk in TSB-T, membranes were incubated with polyclonal a mouse SerpinA3n antibody (0.4 μg/mL, R&D Systems), W226 (Petsch, Müller-Schiffmann et al. 2011) (2 ug/ml, kindly provided by Prof. Krammerer) or (6D11, 0.2 μg/mL, Covance) for PrP, overnight. The following day, after three washes in TSB-T, membranes were incubated for one hour with rabbit anti-goat HRP secondary antibody for SerpinA3n or goat anti-mouse HRP secondary antibody for W226 and 6D11 and, subsequently, monoclonal anti-β-actin−peroxidase antibody (1:10000, Sigma-Aldrich). After three membranes washes with TSB-T, the reactions were visualized by chemiluminescence on UVITEC (Cambridge) using Immobilon Classico Western HRP substrate (#WBLUC0500, Millipore), or G:BOX Chemi Syngene system for WB of prion-infected mouse brain tissue, using Amersham ECL Prime (GE Healthcare Life Sciences). Densitometric analysis was carried out using UVIBand software.

3.21 Statistical analysis

All data were processed using GraphPad Prism 6.0. Normal distribution of data was assessed by D'Agostino-Pearson normality test. Differences between the normalized Serpins transcript ΔC_{Ts} of disease-affected and age-matched control group human and mouse samples were assessed with Mann-Whitney test. SerpinA3n transcript and protein differences between prion-infected cells and uninfected ones were assessed using Kruskal-Wallis test and the level of significance was calculated using Dunn's multiple comparisons test. Differences between N2a CM, siRNA and shRNA treated and untreated cells has been evaluated with Wilcoxon-matched pairs signed rank test. Differences between recombinant SerpinA3n treated and untreated cells was calculated with Friedman test and level of significance was calculated using Dunn's multiple comparisons test. p values < 0.05 were considered as statistically significant. Log-rank test was used for the survival and incubation time analysis.

4. RESULTS

4.1 *SERPIN* gene expression analysis in human brain

Among 41 human SERPIN superfamily genes, twelve SERPIN transcripts (SERPINA3, SERPINA8, SERPINB1, SERPINB6, SERPINB8, SERPINB9, SERPINE1, SERPINE2, SERPINF1, SERPINH1, SERPING1, SERPINI1) met the established criteria of TPM ≥ 2 (Wagner, Kin et al. 2012), thus they were selected for the transcriptomic analysis.

However, SERPINB8, SERPINB9 and SERPINE1 were excluded from the analysis because their expression was not detected in the analyzed samples.

Among the nine transcripts, as for the marked upregulation of *SERPINA3* in sCJD patients (average FC=54) (Vanni, Moda et al. 2017), a significant up-regulation of *SERPINB1* (average FC=5.2) compared to controls was observed (**Figure 4.1**). *SERPINI1*, instead, was significantly downregulated in sCJD (average FC= -3.1) group compared to age-matched controls. Similarly, a mild, although statistically significant, downregulation of *SERPINE2* (average FC= -1.8) has been observed in prion affected patients.

SERPINB6, *SERPING1* and *SERPINH1* exhibited a significant upregulation in sCJD group (average FC=3; average FC= 3.2; average FC=6, respectively) compared to controls.

No significant differences were found in *SERPINA8* and *SERPINF1* gene expression analysis between prion affected and age-matched non-neurodegeneration affected controls, also when normalized to the other reference genes (**Figures 4.2-4.3**).

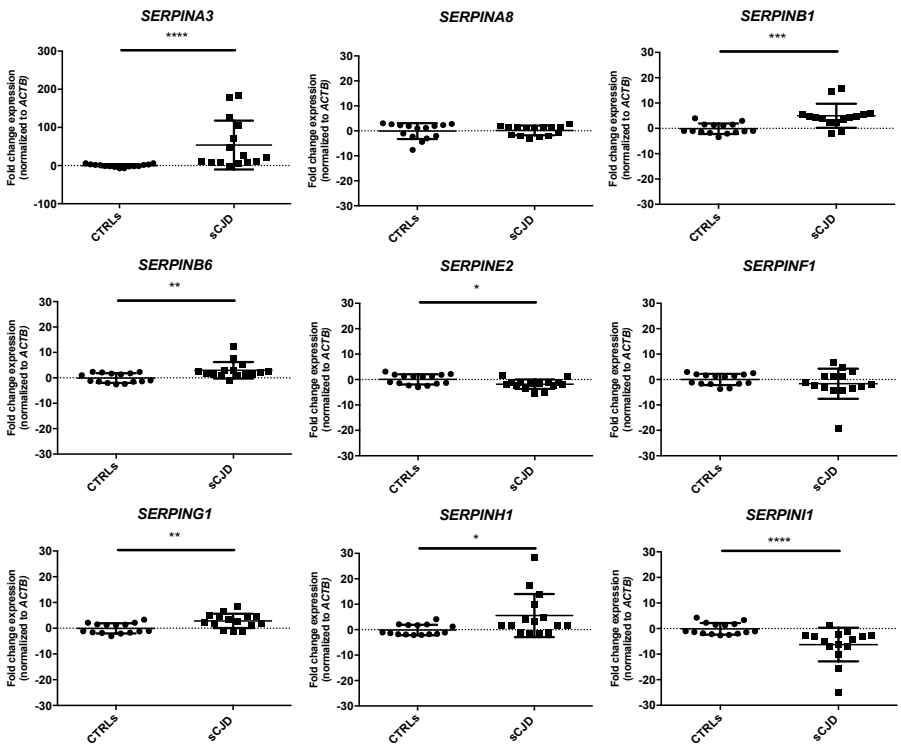

Figure 4.1. *SERPINs* expression level in sCJD human brain samples normalized on *ACTB*. RT-qPCR analysis for *SERPINs* mRNA expression in sCJD (n=15) and relative age-matched controls (CTRLs, n=15) frontal cortex samples normalized on *ACTB* as reference gene. Statistical analysis was performed with Mann-Whitney test. Adjusted *p* value *<0.05, **<0.01, ***<0.001, **** <0.0001. The relative expression ratio (fold change) was calculated using the $2^{-\Delta\Delta C}{}_T$ method. ΔC_T were calculated subtracting the C_T of the reference gene (*ACTB*) to the C_T of the target one (*SERPINs*). $\Delta\Delta C_T$ values were obtained with the ΔC_T of each sample (both of calibrator and test) minus the mean ΔC_T of the calibrator samples group.

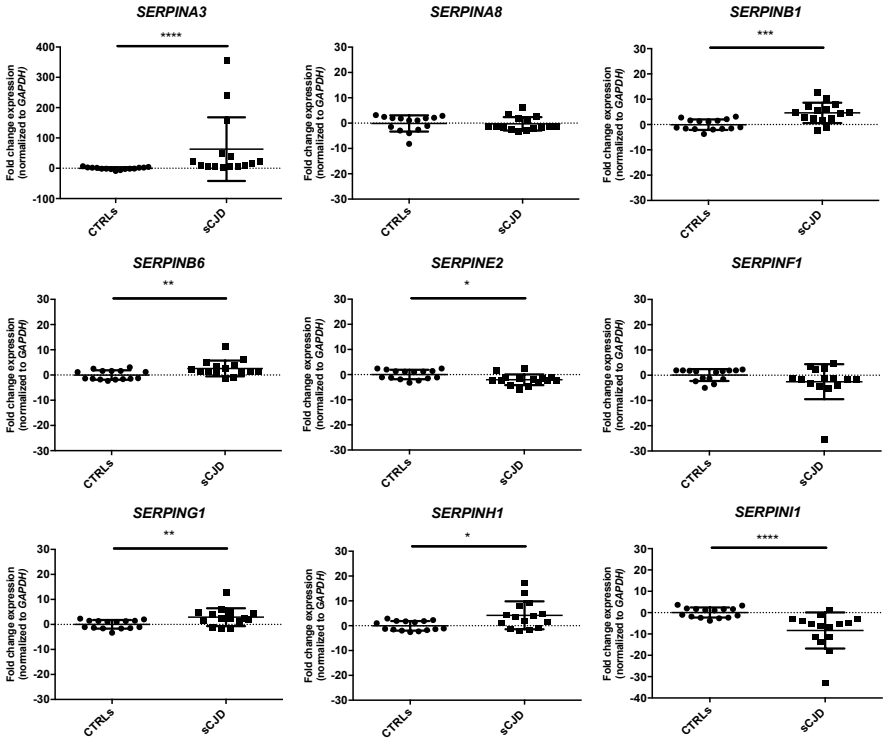

Figure 4.2. *SERPINs* expression level in sCJD human brain samples normalized on *GAPDH*. RT-qPCR analysis for *SERPINs* mRNA expression in sCJD (n=15) and relative age-matched controls (CTRLs, n=15) frontal cortex samples normalized on *GAPDH* as reference gene. Statistical analysis was performed with Mann-Whitney test for multiple comparisons. Adjusted *p* value *<0.05, **<0.01, ***<0.001, **** <0.0001. The relative expression ratio (fold change) was calculated using the $2^{-\Delta\Delta C_T}$ method. ΔC_T were calculated subtracting the C_T of the reference gene (*GAPDH*) to the C_T of the target one (*SERPINs*). $\Delta\Delta C_T$ values were obtained with the ΔC_T of each sample (both of calibrator and test) minus the mean ΔC_T of the calibrator samples group.

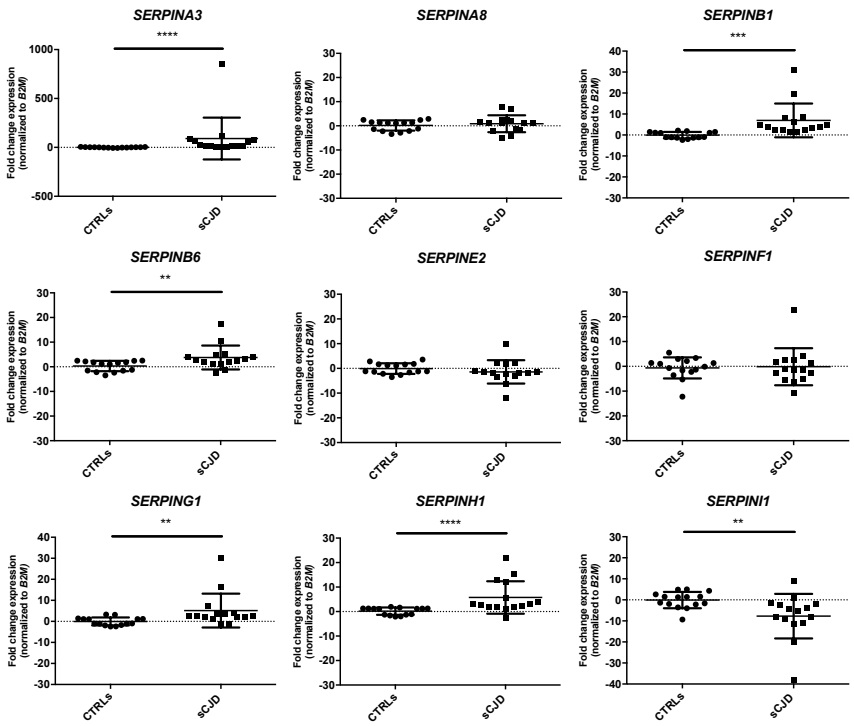

Figure 4.3. *SERPINs* expression level in sCJD human brain samples normalized on *B2M*. RT-qPCR analysis for *SERPINs* mRNA expression in sCJD (n=15) and relative age-matched controls (CTRLs, n=15) frontal cortex samples normalized on *B2M* as reference gene. Statistical analysis was performed with Mann-Whitney test for multiple comparisons. Adjusted *p* value *<0.05, **<0.01, ***<0.001, **** <0.0001. The relative expression ratio (fold change) was calculated using the $2^{-\Delta\Delta C}{}_T$ method. ΔC_T were calculated subtracting the C_T of the reference gene (*B2M*) to the C_T of the target one (*SERPINs*). $\Delta\Delta C_T$ values were obtained with the ΔC_T of each sample (both of calibrator and test) minus the mean ΔC_T of the calibrator samples group.

4.2 *Serpin* gene expression analysis in RML-infected CD1 mouse brain

A threshold value of RPKM ≥ 1 was set (Hebenstreit, Fang et al. 2011) to select mouse serpins gene for the transcriptomic analysis. Seventeen transcripts among seventy-one mouse Serpins: *SerpinA3n, SerpinA6, SerpinA8, SerpinB1a, SerpinB1b, SerpinB6a, SerpinB8, SerpinB9d, SerpinD1, SerpinE1, SerpinE2, SerpinE3, SerpinF1, SerpinF2, SerpinG1, SerpinH1, SerpinI1* were selected and then analyzed by RT-qPCR. However*, SerpinA6, SerpinB9d, SerpinE3* were not considered in the transcriptomic analysis because their expression level was not detectable.

Pre-symptomatic RML-infected CD1 mice (3 months post infection, 3mpi) did not show any significant variation in *Serpin* expression compared to age-matched controls (5 months, 5mo). However, a trend of upregulation was present both for *SerpinA3n* and *SerpinF2* in 3mpi mice (**Figure 4.4**). The results were coherent for all the three housekeeping genes used to normalize (**Figures 4.4**-**4.6**).

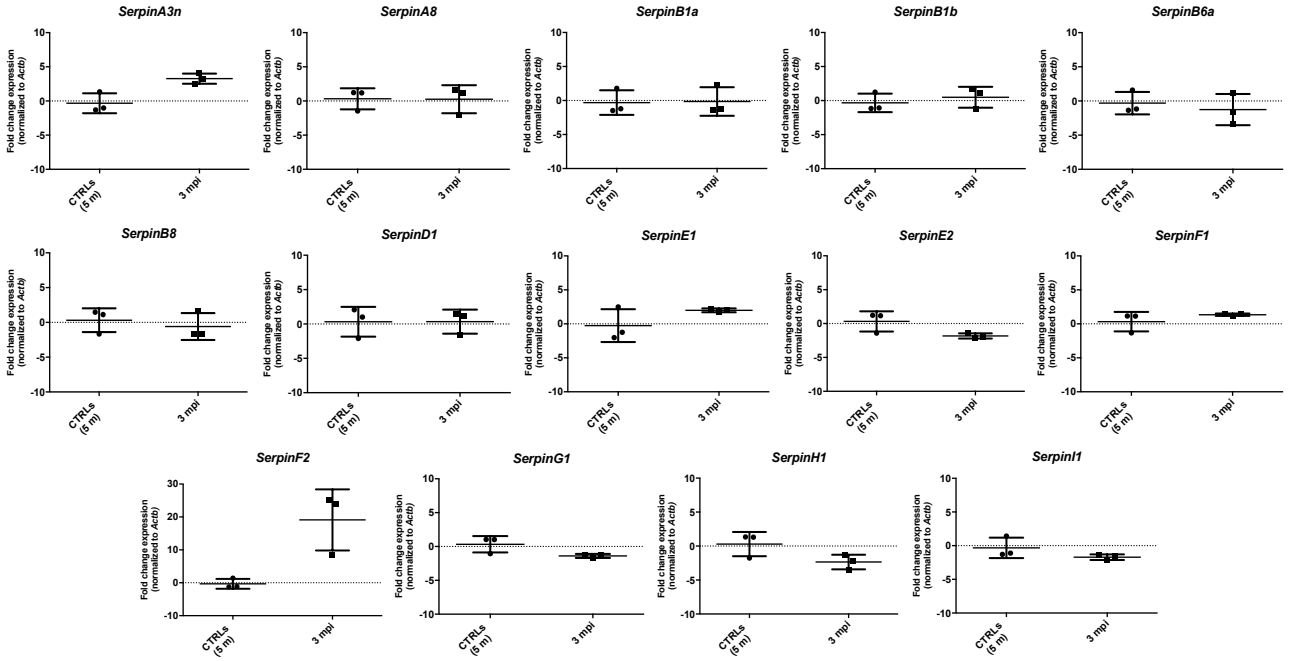

Figure 4.4. *Serpins* expression level in pre-symptomatic RML-infected CD1 mouse brain normalized on *Actb*. RT-qPCR analysis for *Serpins* mRNA expression in 3 months post infection (3mpi, n=3) and relative age-matched controls whole brain samples (5mo, n=3) normalized on *Actb* as reference gene. Statistical analysis was performed with Mann-Whitney test. The relative expression ratio (fold change) was calculated using the $2^{-\Delta\Delta CT}$ method. ΔC_T were calculated subtracting the C_T of the reference gene (*Actb*) to the C_T of the target one (*Serpins*). $\Delta\Delta C_T$ values were obtained with the ΔC_T of each sample, minus the mean ΔC_T of the population of calibrator samples.

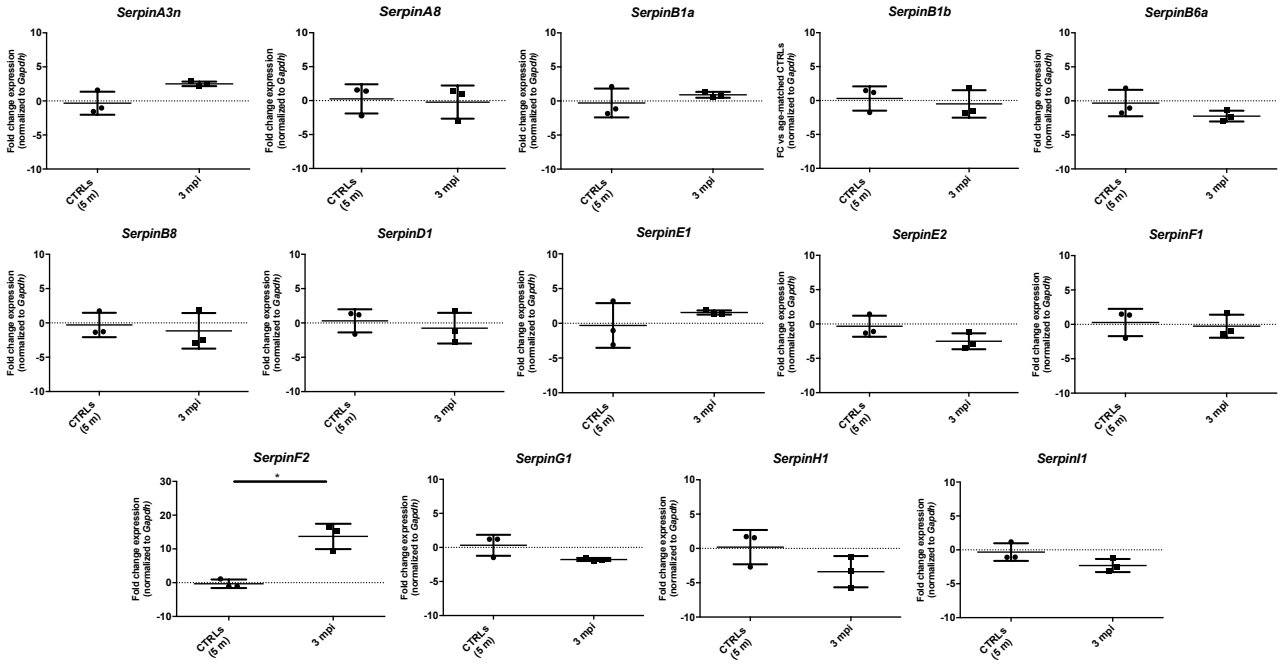

Figure 4.5. *Serpins* expression level in pre-symptomatic RML-infected CD1 mouse brain normalized on *Gapdh*. RT-qPCR analysis for *Serpins* mRNA expression in in 3 months post infection (3mpi, n=3) and relative age-matched controls whole brain samples (5mo, n=3) normalized on *Gapdh* as reference gene. Statistical analysis was performed with Mann-Whitney test. Adjusted *p* value * <0.05. The relative expression ratio (fold change) was calculated using the $2^{-\Delta\Delta CT}$ method. ΔC_T were calculated subtracting the C_T of the reference gene (*Gapdh*) to the C_T of the target one (*Serpins*). $\Delta\Delta C_T$ values were obtained with the ΔC_T of each sample, minus the mean ΔC_T of the population of calibrator samples.

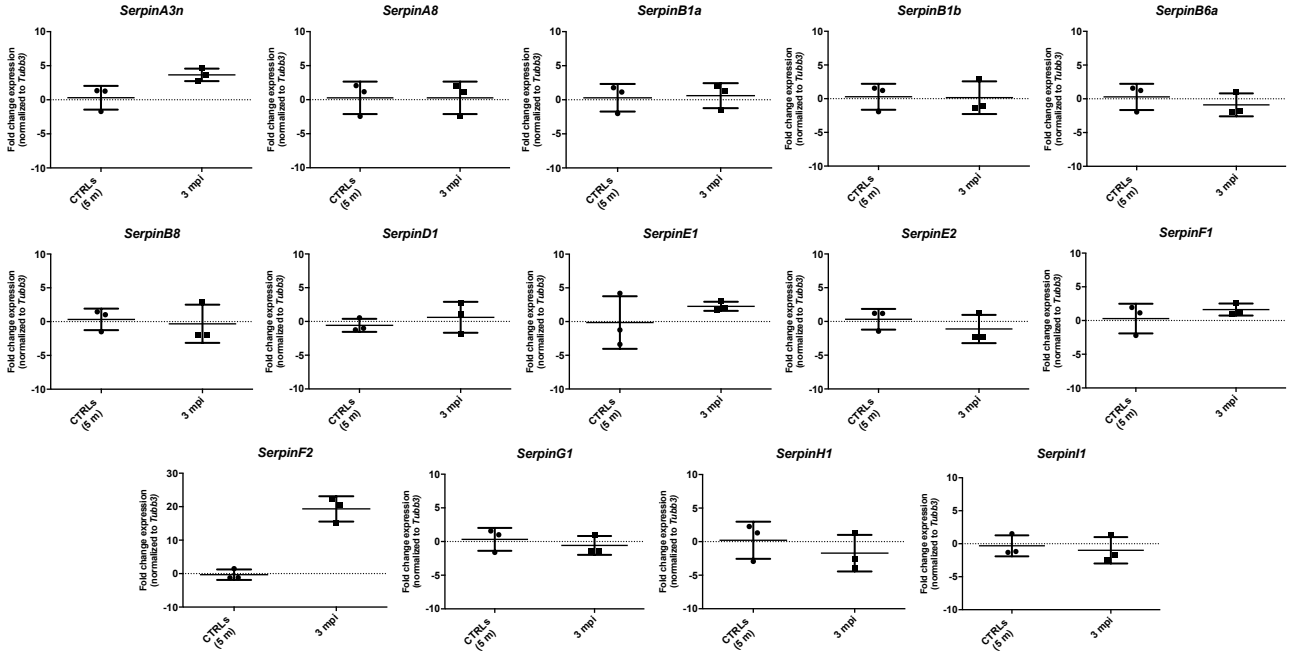

Figure 4.6. *Serpins* expression level in pre-symptomatic RML-infected CD1 mouse brain normalized on *Tubb3.* RT-qPCR analysis for *Serpins* mRNA expression in 3 months post infection (3mpi, n=3) and relative age-matched controls whole brain samples (5mo, n=3) normalized on *Tubb3* as reference gene. Statistical analysis was performed with Mann-Whitney test. The relative expression ratio (fold change) was calculated using the $2^{-\Delta\Delta CT}$ method. ΔC_T were calculated subtracting the C_T of the reference gene (*Tubb3*) to the C_T of the target one (*Serpins*). $\Delta\Delta C_T$ values were obtained with the ΔC_T of each sample, minus the mean ΔC_T of the population of calibrator samples.

The majority of analyzed serpins transcripts did not show significant variation in the expression between symptomatic RML-infected CD1 mice (5mpi) and relative controls (7mo) (**Figure 4.7**). However, together with *SerpinA3n* (average FC= 11) (Vanni, Moda et al. 2017), *SerpinF2* was significantly upregulated in prion-infected mice respect to control, with an average FC= 36. The results were shown using *Actb* as reference gene to normalize, but they were similar also with the other two reference genes. Nevertheless, a trend of downregulation for *SerpinI1* was reported against all three different reference genes (**Figures 4.7-4.9**).

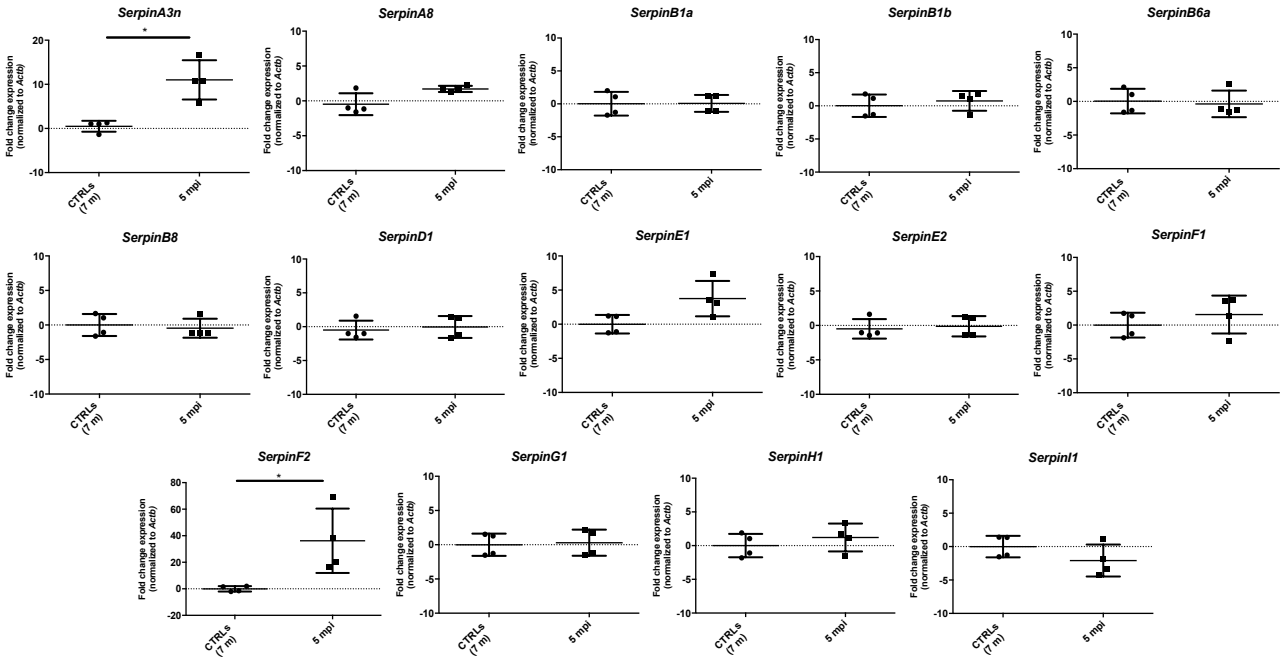

Figure 4.7. *Serpins* expression level in symptomatic RML-infected CD1 mouse brain normalized on *Actb*. RT-qPCR analysis for *Serpins* mRNA expression in 5 months post infection (5mpi, n=4) and relative age-matched controls whole brain samples (7mo, n=4) normalized on *Actb* as reference gene. Statistical analysis was performed with Mann-Whitney test. Adjusted *p* value * <0.05. The relative expression ratio (fold change, FC) was calculated using the $2^{-\Delta\Delta CT}$ method. ΔC_T were calculated subtracting the C_T of the reference gene (*Actb*) to the C_T of the target one (*Serpins*). $\Delta\Delta C_T$ values were obtained with the ΔC_T of each sample, minus the mean ΔC_T of the population of calibrator samples of calibrator samples.

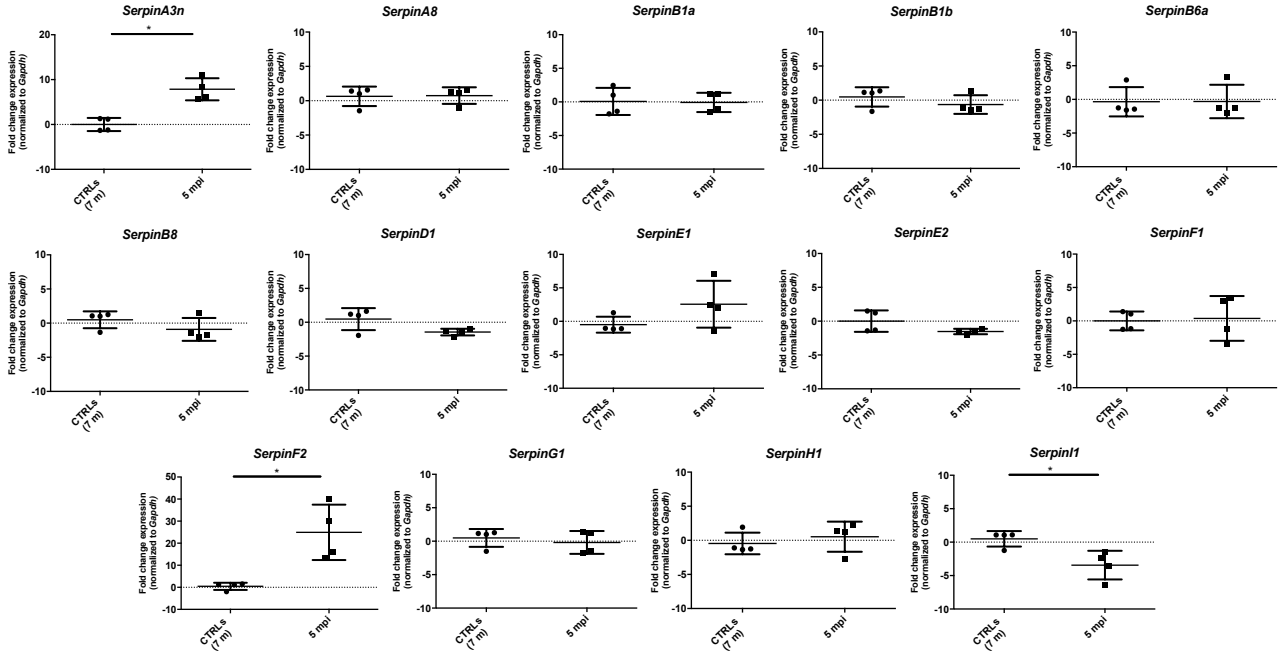

Figure 4.8. *Serpins* expression level in symptomatic RML-infected CD1 mouse brain normalized on *Gapdh*. RT-qPCR analysis for *Serpins* mRNA expression in 5 months post infection (5mpi, n=4) and relative age-matched controls whole brain samples (7mo, n=4) normalized on *Gapdh* as reference gene. Statistical analysis was performed with Mann-Whitney test. Adjusted *p* value * <0.05. The relative expression ratio (fold change, FC) was calculated using the $2^{-\Delta\Delta CT}$ method. ΔC_T were calculated subtracting the C_T of the reference gene (*Gapdh*) to the C_T of the target one (*Serpins*). $\Delta\Delta C_T$ values were obtained with the ΔC_T of each sample, minus the mean ΔC_T of the population of calibrator samples.

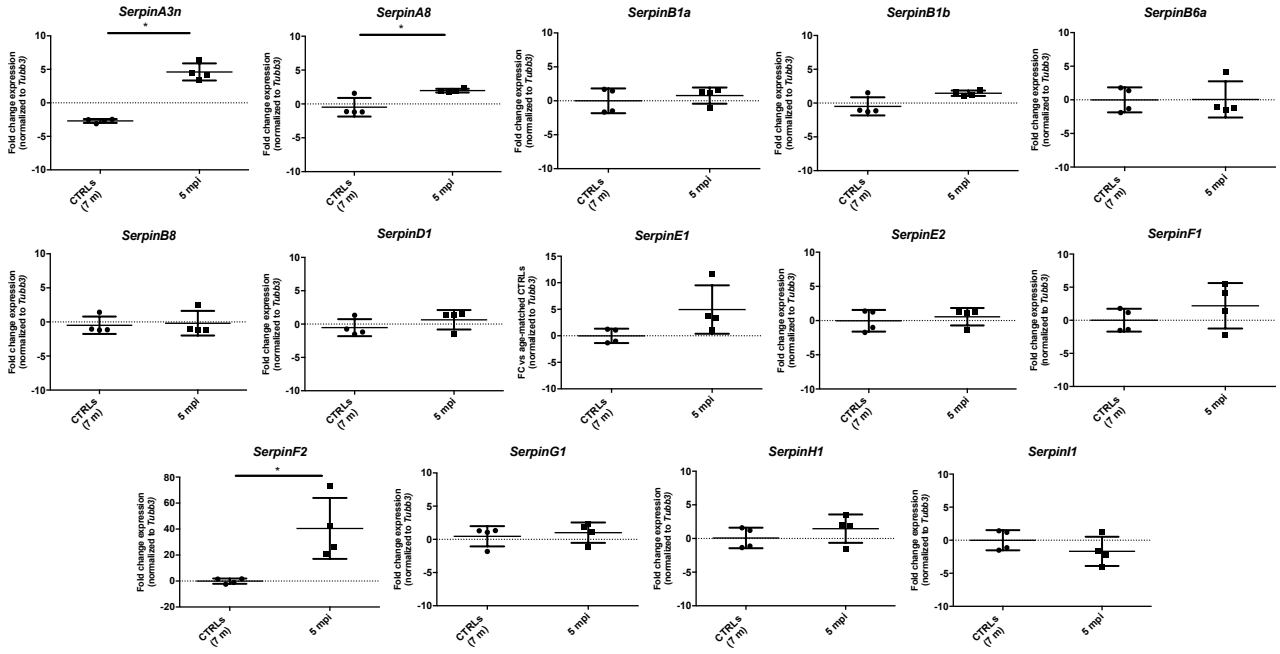

Figure 4.9. *Serpins* expression level in symptomatic RML-infected CD1 mouse brain normalized on *Tubb3*. RT-qPCR analysis for *Serpins* mRNA expression in 5 months post infection (5mpi, n=4) and relative age-matched controls whole brain samples (7mo, n=4) normalized on *Tubb3* as reference gene. Statistical analysis was performed with Mann-Whitney test. Adjusted *p* value * <0.05. The relative expression ratio (fold change, FC) was calculated using the $2^{-\Delta\Delta CT}$ method. ΔC_T were calculated subtracting the C_T of the reference gene (*Tubb3*) to the C_T of the target one (*Serpins*). $\Delta\Delta C_T$ values were obtained with the ΔC_T of each sample, minus the mean ΔC_T of the population calibrator samples.

4.4 SerpinA3n transcript and protein expression in prion-infected cells

SERPINA3/SerpinA3n transcript and protein level were fund upregulated in frontal cortex samples of prion-affected patients and in mouse model of the disease (Vanni, Moda et al. 2017). Thus, to investigate whether this increased expression was present in *in vitro* model of prion diseases, SerpinA3n expression has been investigated in GT1 and N2a prion-infected cells.

SerpinA3n mRNA was highly upregulated in both RML- and 22L- infected GT1 (**Figure 4.10A**-**C**) and N2a (**Figure 4.11A**-**C**) cells compared to uninfected ones.

SerpinA3n is a secreted protein (Gueugneau, d'Hose et al. 2018, Sergi, Campbell et al. 2018), therefore, WB analysis was performed either on cell lysate and on CM collected from both prion-infected and un-infected GT1 (**Figure 4.10D**) and N2a (**Figure 4.11D**) cell lines. A statistically significant increase of extracellular SerpinA3n in the medium of RML- and 22L-infected GT1 (**Figure 4.10E**) and N2a (**Figure 4.11E**) was observed. Nevertheless, increased levels of intracellular

SerpinA3n in both RML- and 22L-infected GT1 were observed (**Figure 4.10F**) and N2a (**Figure 4.11F**) compared to uninfected cells.

PNGase F treatment on CM of uninfected and prion-infected cells has been performed. The effective molecular weight of secreted SerpinA3n, without glycosylation, was shifted from over 55kDa to ≅ 47kDa, which corresponded to the molecular weight of recombinant *E. Coli*-produced SerpinA3n (**Figures 4.10G, 4.11G**).

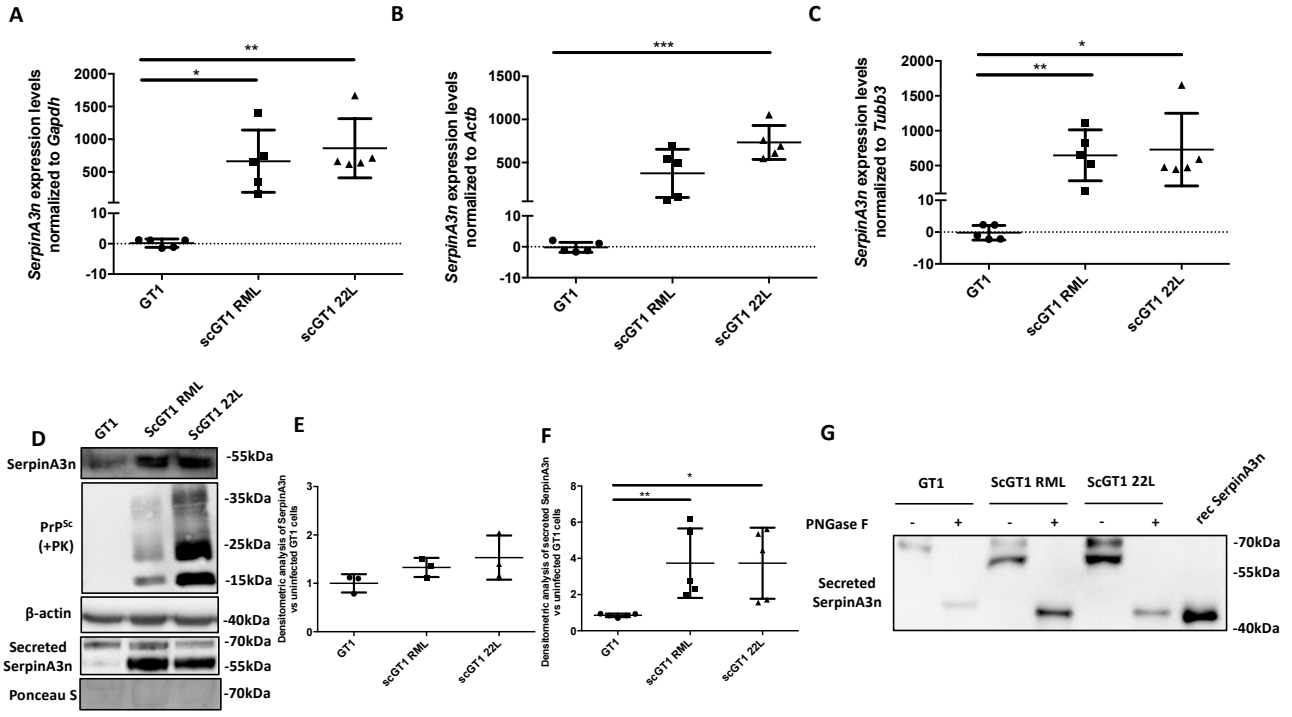

Figure 4.10. SerpinA3n expression in uninfected and prion-infected GT1 cell lines. A, **B**, **C**. Gene expression analysis of *SerpinA3n* in RML- (n=5) and 22L-infected GT1 cell lines (n=5) compared to uninfected cells (n=5), normalized on *Gapdh* (**A**) *Actb* (**B**) and *Tubb3* (**C**) as reference genes. The relative expression ratio (fold change, FC) was calculated using the $2^{-\Delta\Delta CT}$ method. ΔC_T were calculated subtracting the C_T of the reference genes (*Gapdh, Actb, Tubb3*) to the C_T of the target one (*SerpinA3n*). $\Delta\Delta C_T$ values were obtained with the ΔC_T of each sample from infected cell group (either with RML or 22L), minus the mean ΔC_T of the population of calibrator samples (uninfected cells). **D** Representative WB image of intracellular and secreted SerpinA3n on uninfected and RML- and 22L-infected GT1. Ponceau Staining of the membrane for Secreted SerpinA3n was used as proteins loading control. SerpinA3n and β-actin were developed on the same membrane, sequentially. PrP^{Sc} signal was developed on another membrane after PK-digestion of cell lysates. WB image has been cropped to improve clarity of the signal. Molecular weight was represented on the right (kDa). **E** Densitometric analysis of intracellular SerpinA3n levels normalized on β-actin WB signal between uninfected (n=3) and RML- (n=3) and 22L-infected GT1 cell lines (n=3) **F**. Densitometric analysis of Secreted SerpinA3n levels WB signal between uninfected (n=5) and RML- (n=5) and 22L-infected GT1 cell lines (n=5). Statistical significance was performed using Kruskal-Wallis test with Dunnett's multiple comparisons compared to un-infected cells. *p<0.05, ** p<0.01. **G** Representative WB image of secreted SerpinA3n with (+) or without (-) PNGase F treatment between uninfected and RML- and 22L-infected GT1. WB image has been cropped to improve clarity of the signal. Molecular weight was represented on the right (kDa).

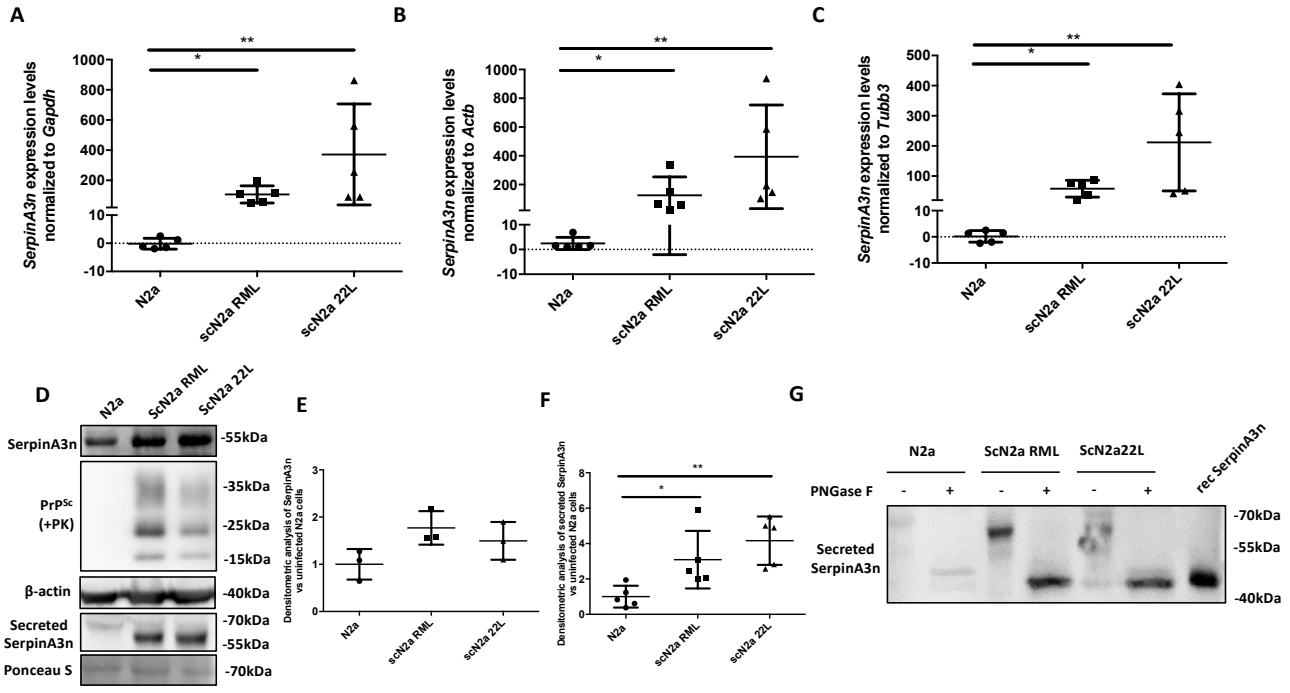

Figure 4.11. SerpinA3n expression in uninfected and prion-infected N2a cell lines. A, **B**, **C**. Gene expression analysis of *SerpinA3n* in RML- (n=5) and 22L-infected N2a cell lines (n=5) compared to uninfected cells (n=5), normalized on *Gapdh* (**A**) *Actb* (**B**) and *Tubb3* (**C**) as reference genes. The relative expression ratio (fold change, FC) was calculated using the $2^{-\Delta\Delta CT}$ method. ΔC_T were calculated subtracting the C_T of the reference genes (*Gapdh, Actb, Tubb3*) to the C_T of the target one (*SerpinA3n*). $\Delta\Delta C_T$ values were obtained with the ΔC_T of each sample from infected cell group (either with RML or 22L), minus the mean ΔC_T of the population of calibrator samples (uninfected cells). **D** Representative WB image of intracellular and secreted SerpinA3n on uninfected and RML- and 22L-infected N2a. Ponceau Staining of the membrane for Secreted SerpinA3n was used as proteins loading control. SerpinA3n and β-actin were developed on the same membrane, sequentially. PrP^{Sc} signal was develop on another membrane after PK-digestion of cell lysates. WB image has been cropped to improve clarity of the signal. Molecular weight was represented on the right (kDa). **E** Densitometric analysis of intracellular SerpinA3n levels normalized on β-actin WB signal between uninfected (n=3) and RML- (n=3) and 22L-infected N2a cell lines (n=3). **F** Densitometric analysis of Secreted SerpinA3n levels WB signal between uninfected (n=5) and RML- (n=5) and 22L-infected N2a cell lines (n=5). Statistical significance was performed using Kruskal-Wallis test with Dunnett's multiple comparisons compared to un-infected cells. *p<0.05, ** p<0.01. **G** Representative WB image of secreted SerpinA3n with (+) or without (-) PNGase F treatment between uninfected and RML- and 22L-infected N2a. WB image has been cropped to improve clarity of the signal. Molecular weight was represented on the right (kDa).

4.5 Recombinant and N2a produced SerpinA3n protease inhibitor activity

N2a cell line were transfected with pcDNA 3.1 encoding for SerpinA3n and an empty pcDNA3.1 ("Empty Vector", EV). To check SerpinA3n overexpression, RNA was extracted and RT-qPCR was performed. N2a Clone 2 was found to be the cell line expressing the highest level of *SerpinA3n* transcript (**Figure 4.12A**) and was named "N2a-SerpinA3n". The transfection of N2a-SerpinA3n was verified by PCR of N2a E.V. and N2a-SerpinA3n extracted DNA, using primers able to recognized the endogenous and the exogenous (plasmid derived) sequence of SerpinA3n (**Figure 4.12B**). Furthermore, WB analysis of N2a-SerpinA3n cell lysate and CM demonstrated the transfection efficacy (**Figure 4.12C**).

To test whether both recombinant and N2a produced SerpinA3n were able to act as protease inhibitor, complex formation assay was performed following (Horvath, Irving et al. 2005) protocol. Firstly, the activity of recombinantly produced in *E. Coli* cells SerpinA3n has been tested for its ability to form an SDS-stable and covalent complex together with chymotrypsin, one of its known target proteases (Horvath, Irving et al. 2005). 1:5 molar ratio of chymotrypsin:SerpinA3n revealed the appearance of a band around 70kDa corresponding to the sum of the molecular weight of recombinant SerpinA3n (≅ 47kDa) and chymotrypsin (25kDa) (**Figure 4.12D**). Similarly, the activity of N2a-SerpinA3n CM has been tested. Results demonstrated that secreted SerpinA3n was able to form a covalent and SDS-stable complex with chymotrypsin. The molecular weight of the final complex, around 90kDa, was relative to the sum of glycosylated SerpinA3n (≅ 55-60kDa) and chymotrypsin (25kDa) (**Figure 4.12E**).

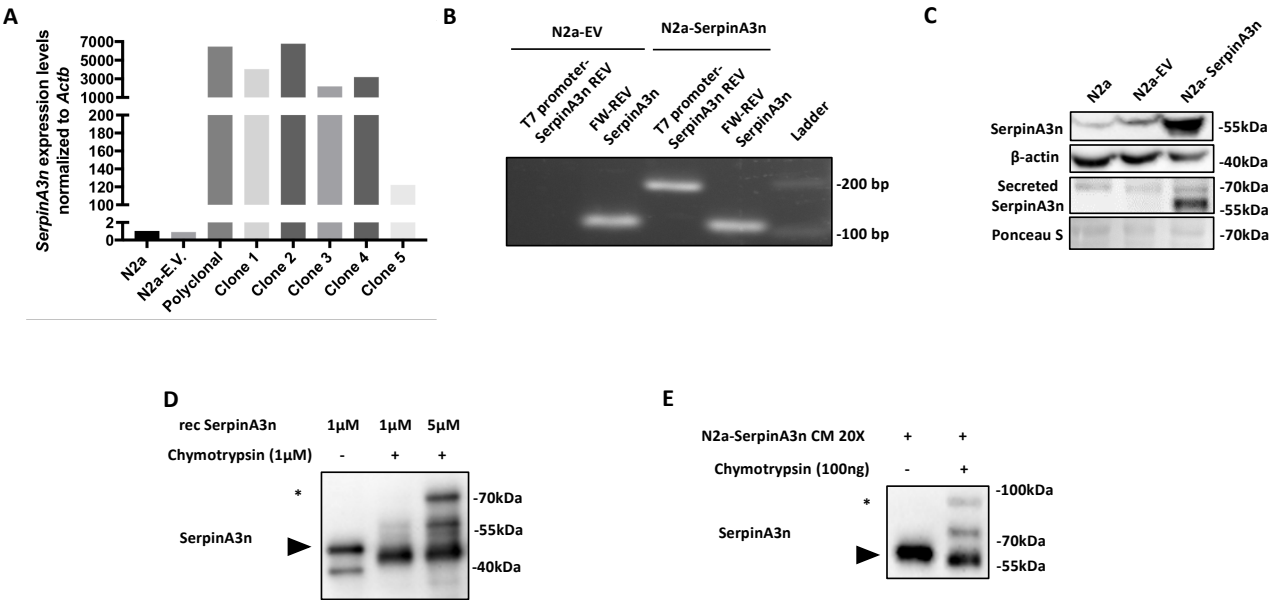

Figure 4.12. Biochemical characterization of recombinant and N2a secreted SerpinA3n. A Gene expression analysis of *SerpinA3n* N2a cells compared to not transfected N2a, normalized to *Actb* as reference gene. The relative expression ratio (fold change, FC) was calculated using the $2^{-\Delta\Delta CT}$ method. ΔC_T were calculated subtracting the C_T of the reference gene (*Actb*) to the C_T of the target one (*SerpinA3n*). $\Delta\Delta C_T$ values were obtained with the ΔC_T of each sample, minus the mean ΔC_T of the calibrator one (not transfected N2a). **B** Agarose gel image of PCR products from N2a-EV and N2a-SerpinA3n genomic DNA using three different primers T7 promoter, SerpinA3n FW and SerpinA3n REV. While the primer pair SerpinA3n FW - SerpinA3n REV amplified the genomic sequence of SerpinA3n, present in both N2a-EV and N2a-SerpinA3n, the pair T7 promoter-SerpinA3n REV recognized the plasmid-derived SerpinA3n sequence, present only in N2a-SerpinA3n. DNA base pair lengths was shown on the right (bp). **C** Representative WB image of intracellular and secreted SerpinA3n on transfected and control N2a cells. Ponceau Staining of the membrane for secreted SerpinA3n was used as proteins loading control. SerpinA3n and β-actin were developed on the same membrane, sequentially. WB image has been cropped to improve clarity of the signal. Molecular weight was represented on the right (kDa). **D** Representative WB image of 1μM α-chymotrypsin incubated with 1μM and 5μM recombinant SerpinA3n or 10 mM Tris-HCl, 50 mM KCl, pH 8.0. Triangle indicated recombinant SerpinA3n (≅ 47 kDa). The asterisk indicated a band at 70 kDa corresponding to the sum of the molecular weight of SerpinA3n (≅ 47 kDa) and the cognate protease (25 kDa). WB image has been cropped to improve clarity of the signal. Molecular weight was represented on the right (kDa). **E** Representative WB image of CM from N2a-SerpinA3n 20X concentrated incubated with 100 ng of chymotrypsin or MEM. Triangle indicated the secreted and glycosylated SerpinA3n (55-60kDa). The asterisk indicated a band around 90 kDa corresponding to the sum of the molecular weight of SerpinA3n (55-60kDa) and the cognate protease (25 kDa). WB image has been cropped to improve clarity of the signal. Molecular weight was represented on the right (kDa).

4.6 PrP^{Sc} changes upon SerpinA3n modulation

SerpinA3n-mediated modulation of prion accumulation has been tested by treating ScN2a RML cells with CM of N2a-SerpinA3n or N2a-EV and N2a cells as control. PK-digestion and WB analysis after 72-hour treatments of prion-infected cell lysates revealed an average 40% increased prion accumulation in cells treated with the conditioned medium of N2a-SerpinA3n compared to the ones that received N2a EV CM (**Figure 4.13A-B**).

To test whether the observed increased PrP^{Sc} signal was mediated even by a non-glycosylated form of SerpinA3n, ScN2a RML cells were treated with two different concentrations of recombinantly produced SerpinA3n. Either 0.5μM and 1μM were responsible for an increased prion accumulation (**Figure 4.13C**), however only 1μM SerpinA3n showed a statistically significant increase of PrP^{Sc} compared to vehicle treated cells (**Figure 4.13D**).

Since the upregulation of SerpinA3n seems to be associated to an increased prion accumulation, SerpinA3n inhibition has been evaluated to test whether it was able to exert any anti-prion effect.

SerpinA3n downregulation has been obtained either toward siRNA and shRNA techniques, leading to a substantial decrease of secreted SerpinA3n expression levels in transfected ScN2a RML cells (**Figure 4.13E**-**4.13G**). 72-hour treatments of RML-infected N2a cell, with either siRNA or shRNA designed for SerpinA3n led to a 20-30% reduction of PrP^{Sc} compared to cell transfected with the respective controls (**Figure 4.13F**-**4.13H**). However, only SerpinA3n targeting shRNA transfection led to a statistically significant reduction of prion load (**Figure 4.13H**).

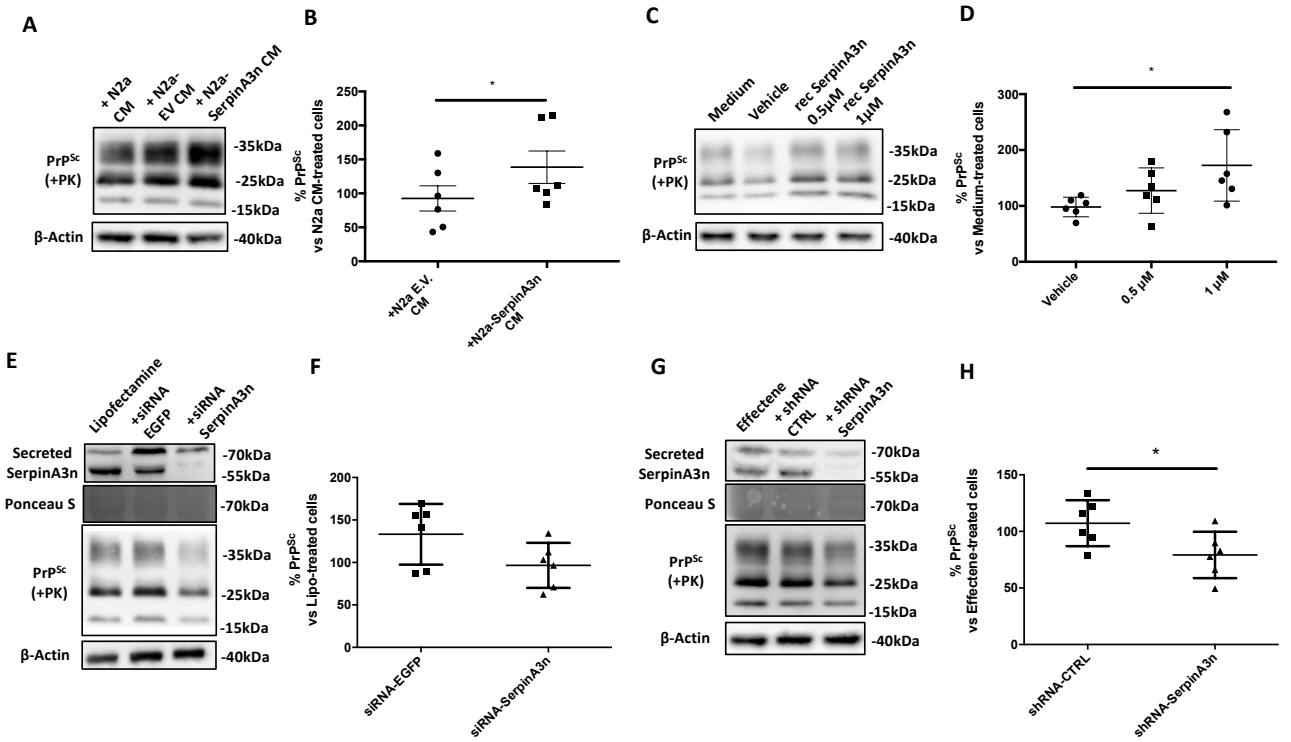

Figure 4.13 PrP^{Sc} changes after SerpinA3n modulation in ScN2a RML cells. A Representative WB image of PrP^{Sc} in lysates from ScN2a RML treated with CM from N2a, N2a-EV and N2a-SerpinA3n. β-actin was used as protein loading control. PrP^{Sc} signal was develop on another membrane after PK-digestion of cell lysates. WB image has been cropped to improve clarity of the signal. Molecular weight was represented on the right (kDa). **B** Densitometric analysis of β-actin-normalized PrP^{Sc} levels in N2a-EV and N2a-SerpinA3n CM-treated ScN2a RML relative to cell treated with CM from N2a (n=6). Statistical significance was performed by Wilcoxon matched pairs signed rank test, *p < 0.05. **C** Representative WB image of recombinant SerpinA3n (0.5μM and 1μM), vehicle (10 mM Tris-HCl, 50 mM KCl, pH 8.0) and medium-only treated cells. β-actin was used as protein loading control. PrP^{Sc} signal was develop on another membrane after PK-digestion of cell lysates. WB image has been cropped to improve clarity of the signal. Molecular weight was represented on the right (kDa). **D** Densitometric analysis of β-actin-normalized PrP^{Sc} levels in recombinant SerpinA3n and vehicle-treated N2a relative to cell treated with medium only (n=6). Statistical significance was performed by Friedman test with Dunn's multiple comparisons test, *p < 0.05. **E, G** Representative WB image of PrP^{Sc} in lysates from ScN2a RML transfected with siRNA (E) and shRNA (G) designed to target SerpinA3n. β-actin was used as protein loading control. PrP^{Sc} signal was develop on another membrane after PK-digestion of cell lysates. Ponceau Staining and secreted SerpinA3n signal development were performed on the same membrane. WB image has been cropped to improve clarity of the signal. Molecular weight was represented on the right (kDa). **F** Densitometric analysis of β-actin-normalized PrP^{Sc} levels in siRNA-EGFP and siRNA-SerpinA3n transfected cells relative to ScN2a RML cells transfected with Lipofectamine only (n=6). Statistical significance was performed by Wilcoxon matched pairs signed rank test, *p < 0.05. **H** Densitometric analysis of β-actin-normalized PrP^{Sc} levels in shRNA-CTRL and shRNA-Serpina3n transfected cells relative to ScN2a RML cells transfected with Effectene only (n=6). Statistical significance was performed by Wilcoxon matched pairs signed rank test, *p < 0.05.

4.7 Molecular characterization of SerpinA3n$^{-/-}$ mice

The modification of SerpinA3n sequence present in SerpinA3n$^{-/-}$ mice consisted in a deletion of 402 bp and an insertion of 8 bp (ACAGTGTA) in intron 3 at chromosome 12 positive strand position 104,411,059 bp (TAACTGAGGAGAAGGTGGAGTCTCTG in GRCm38) and ending after CTGTTCTGTCCTCAGCCTAAGGCC at position 104,411,460 bp in intron 4. This mutation resulted in the deletion of exon 3 and an aminoacidic change after residue 212 and early truncation 1 amino acid later. PCR Genotyping was performed from tail snip or ear punch samples. Each genotype was determined by the presence of one or two bands at different height depending on the length of wild-type and/or mutant alleles: wild-type mice characterized by one band at 232 bp in, knockout mice showed one band at 488 bp in, hence both bands were present in heterozygous mice (**Figure 4.14A**).

In order to characterize KO animals, SerpinA3n transcript and protein levels were assessed in mouse brain tissue of SerpinA3n$^{+/+}$, SerpinA3n$^{+/-}$, SerpinA3n$^{-/-}$ samples. For RT-qPCR analysis, $C_T \geq 35$ was chosen as threshold level of expression, as previously used in literature (Vanni et al., 2017). Results normalized to three different reference genes (*Actb, Gapdh*, *Tubb3*) demonstrated a total depletion of *SerpinA3n* mRNA in SerpinA3n$^{-/-}$ mice when compared to WT mice (**Figure 4.14B-D**). To assess the absence of SerpinA3n at protein level in KO mice, WB on SerpinA3n$^{+/+}$, SerpinA3n$^{+/-}$ and SerpinA3n$^{-/-}$ mouse brain homogenates was performed. As expected no signal was detected in SerpinA3n$^{-/-}$ brain (**Figure 4.14E**) and densitometric analysis revealed a statistical significance difference between SerpinA3n$^{+/+}$ and SerpinA3n$^{-/-}$ (**Figure 4.14F**). SerpinA3n WB signal revealed two distinct bands 55 kDa, and one around 60 kDa, as previously observed in CD1 mice RML-infected (Vanni et al., 2017). As for immortalized cell line secreted SerpinA3n, its glycosylation state has been assessed via PNGase F treatment. One single band, at the same height of recombinant protein ($\cong$ 47 kDa) was detectable for SerpinA3n in WT animals while no bands were detectable in KO mice. (**Figure 4.14G**). Furthermore, the expression levels of other brain expressed *Serpin* transcripts was assessed on SerpinA3n$^{+/+}$, SerpinA3n$^{+/-}$ and SerpinA3n$^{-/-}$ samples. No brain expressed *Serpins* varied significantly in SerpinA3n$^{+/-}$ or SerpinA3n$^{-/-}$ compared to wild type mice (data not shown), except *SerpinI1* which showed an upregulation in SerpinA3n$^{-/-}$ animals (**Figure 4.14H-L**).

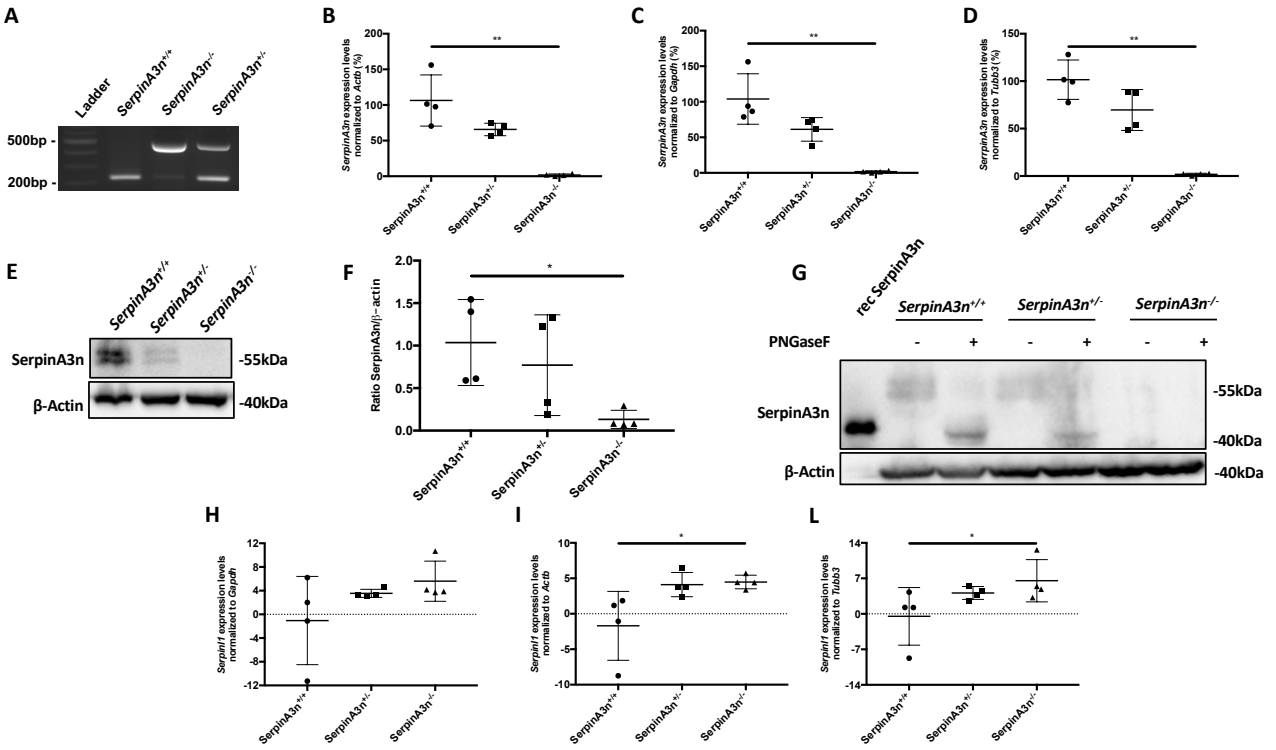

Figure 4.14. SerpinA3n DNA, RNA, protein and *SerpinI1* levels in SerpinA3n$^{-/-}$ mice. A Agarose gel of PCR products from tail biopsy of SerpinA3n$^{+/+}$, SerpinA3n$^{+/-}$ and SerpinA3n$^{-/-}$ mice. DNA base pair lengths was shown on the left (bp). **B, C, D** RT-qPCR analysis for *SerpinA3n* mRNA expression in SerpinA3n$^{+/+}$ (n=4), SerpinA3n$^{+/-}$ (n=4) and SerpinA3n$^{-/-}$ (n=4) mouse brain samples normalized to *Actb* (B), *Tubb3* (C) and *Gapdh* (D) as reference genes. The relative expression ratio was represented as percentage of expression compared to wild type animals. Statistical analysis was performed with Kruskal-Wallis with Dunn's multiple comparisons test, *p* value **<0.01. **E** Representative WB image of brain expressed SerpinA3n on SerpinA3n$^{+/+}$, SerpinA3n$^{+/-}$ and SerpinA3n$^{-/-}$ samples. β-actin was used as protein loading control was developed on the same membrane of SerpinA3n. WB image has been cropped to improve clarity of the signal. Molecular weight was represented on the right (kDa). **F** Densitometric analysis of WB of brain expressed SerpinA3n levels normalized on β-actin in SerpinA3n$^{+/+}$ (n=4), SerpinA3n$^{+/-}$ (n=4) and SerpinA3n$^{-/-}$ (n=4). Statistical analysis was performed with Kruskal-Wallis with Dunn's multiple comparisons test, *p* value *<0.05. **G** Representative WB image of SerpinA3n in SerpinA3n$^{+/+}$, SerpinA3n$^{+/-}$ and SerpinA3n$^{-/-}$ mouse brains with or without PNGase F treatment. Recombinant SerpinA3n was used as control for banding pattern. WB image has been cropped to improve clarity of the signal. Molecular weight was represented on the right (kDa). **H, I, L** RT-qPCR analysis for *SerpinI1* transcript expression in SerpinA3n$^{+/+}$ (n=4), SerpinA3n$^{+/-}$ (n=4) and SerpinA3n$^{-/-}$ (n=4) mouse brain samples normalized to *Actb* (H), *Tubb3* (I) and *Gapdh* (L) as reference genes. Statistical analysis was performed with Kruskal-Wallis with Dunn's multiple comparisons test, *p* value *<0.05.

4.8 Prion inoculation of SerpinA3n$^{-/-}$ mice

To assess the potential role of SerpinA3n in modifying the course of prion disease *in vivo*, SerpinA3n$^{-/-}$ and SerpinA3n$^{+/+}$ mice were inoculated with three different prion strains (RML, 139A, and ME7). One 139A-inoculated SerpinA3n$^{-/-}$ succumbed few days after the intracerebral injection. Regardless of the genetic background (SerpinA3n$^{-/-}$ or SerpinA3n$^{+/+}$), all the animals developed prion pathology with similar incubation (average IT RML-inoculated SerpinA3n$^{-/-}$ = 134 and SerpinA3n$^{+/+}$ = 164, average IT 139A-inoculated SerpinA3n$^{-/-}$ = 192 and SerpinA3n$^{+/+}$ = 192, average IT ME7-inoculated SerpinA3n$^{-/-}$ = 190 and SerpinA3n$^{+/+}$ = 201) (**Figure 4.15A-C**) and survival times (average ST RML-inoculated SerpinA3n$^{-/-}$ = 169 and SerpinA3n$^{+/+}$ = 182, average IT 139A-inoculated SerpinA3n$^{-/-}$ = 217 and SerpinA3n$^{+/+}$ = 210, average IT ME7-inoculated SerpinA3n$^{-/-}$ = 218 and SerpinA3n$^{+/+}$ = 221) (**Figure 4.15D-F**). Log rank test analysis confirmed that survival times between groups did not reach statistically significant differences.

Brain homogenates of SerpinA3n$^{-/-}$ and SerpinA3n$^{+/+}$ mice injected with RML strain were treated with PK and analyzed by means of WB. Similar levels and banding pattern of PK-resistant PrP^{Sc} were detected in both RML-injected SerpinA3n$^{-/-}$ and SerpinA3n$^{+/+}$ mice (**Figure 4.15G-H**).

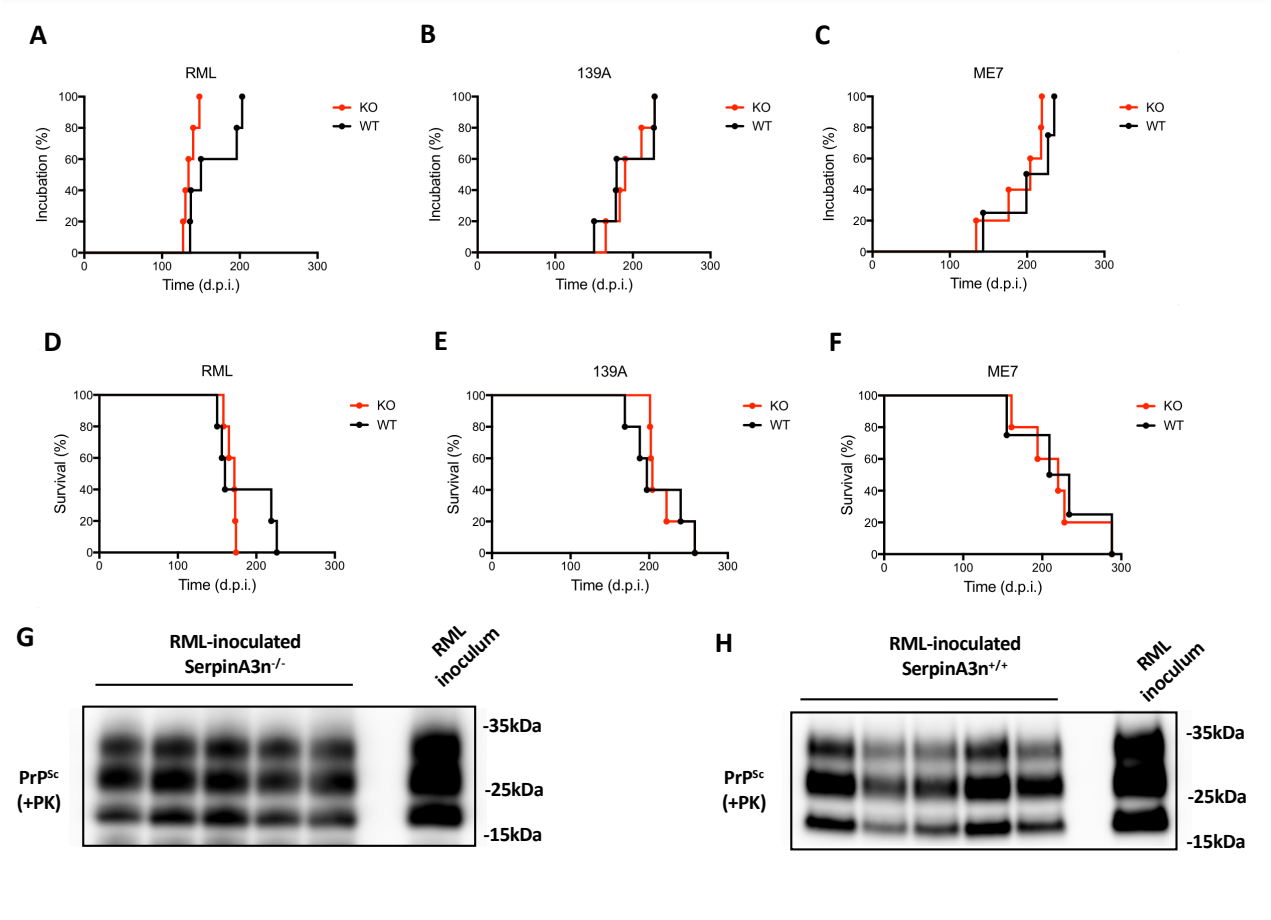

Figure 4.15. Incubation, survival times and PrP^{Sc} levels in SerpinA3n$^{-/-}$ and SerpinA3n$^{+/+}$ mice injected with prions. **A**, **B**, **C** Incubation times (as days post inoculation, d.p.i) between SerpinA3n$^{-/-}$ and SerpinA3n$^{+/+}$ mice injected with the three different prion strain (RML, 139A, ME7). Log rank test has been performed to assess statistically significant differences (IT RML p = 0.0554, IT 139A p = 0.2701, IT ME7 p = 0.8701). **D**, **E, F** Survival times (as days post inoculation, d.p.i) between SerpinA3n$^{-/-}$ and SerpinA3n$^{+/+}$ mice injected with the three different prion strain (RML, 139A, ME7). Log-rank test has been performed to assess statistically significant differences (ST RML p = 0.8217, ST 139A p = 0.8086, ST ME7 p = 0.7174). **G, H** WB analysis of PrP^{Sc} signals from RML-injected SerpinA3n$^{-/-}$ and SerpinA3n$^{+/+}$ brain homogenates. Each lane corresponded to a single animal. PK-treatment of RML-inoculum was included as control. Molecular weight was represented on the right (kDa).

5. DISCUSSION

Research in prion field makes extensive use of transcriptomics and proteomics analysis, which are based on comprehensive, high-throughput tools, useful to identify mechanism at the basis of neurodegeneration, dysregulated pathways, or susceptibility factors (Vanni, 2017).

In 2014, Barbisin and colleagues carried on a microarray-based study revealing changes in the expression levels of more than 300 transcripts in samples from BSE-infected macaque brains. Among them, *SERPINA3* was found to be eighteen-fold overexpressed (Barbisin et al., 2014). Most recently, a strong upregulation of SERPINA3 has been observed in prion-affected human samples, both at the mRNA and protein level (Vanni et al., 2017). The relation between SERPINA3 and prionopathies highlights the necessity to clarify the cellular events which modulate prion conversion and aggregation. Considering PrP^{C}-to-PrP^{Sc} conversion event, the accumulation of scrapie prion isoform may induce the activation of cellular pathways responsible for the production of SERPINA3. SERPINA3 could hinder one or more specific protease(s), responsible for PrP^{Sc} clearance. In such a way, the overexpression of SERPINA3 would strongly repress the activity of the above-mentioned protease(s), allowing further accumulation of PrP^{Sc}.

Firstly, to address whether other members of the serpin superfamily, besides the already known prion-related upregulation of SERPINA3 (Vanni, Moda et al. 2017), are differentially expressed in prion pathology, RT-qPCR analysis has been performed on post-mortem human frontal cortex samples.

Online available RNA sequencing datasets have been examined to understand which serpin superfamily members are expressed in brain tissue. A gold standard criterion does not exist for what concerns the setting of an arbitrary threshold to discriminate the expression of a particular transcript in a given tissue sample. However, Rasmköld and colleagues, investigating a set of core genes active in particular tissues, compared the expression level of exonic and intergenic regions to establish a threshold for detectable expression (Ramskold, Wang et al. 2009). They found that RPKM value of 0.3 balances the presence of false positive and negative results. However, analyzing each individual sample, this threshold was found to have subtle variations, oscillating between 0.2 and 0.8, confirming the uncertainty related to arbitrary threshold setting for all the analyzed samples. Hebenstreit and collaborators, instead, chose a cut-off RPKM value of 1 to discriminate between the presence or absence of a particular transcript (Hebenstreit, Fang et al. 2011).

Another useful parameter used in RNA-Sequencing experiments is TPM. To distinguish between expressed and non-expressed genes in a dataset, TPM ≥ 2 was identified as a threshold to consider a gene as highly transcribed (Wagner, Kin et al. 2012). Interestingly, this criterion was also consistent with RPKM value of 1, identified by Hebenstreit and collaborators (Hebenstreit, Fang et al. 2011), thus confirming the coherence between the two cut-off values and the selection method set. Considering these observations, RPKM ≥ 1 or TPM ≥ 2 was used to select brain expressed serpins for further transcriptomic analysis. However, it has to be highlighted that threshold value variations towards lower levels could increase the number of serpins included in this analysis.

The use of three reference genes for normalization is now a gold standard to reduce experimental errors and tissue derived effects on RT-qPCR (Penna, Vella et al. 2011, Maltseva, Khaustova et al. 2013). Thus, *GAPDH*, *B2M* and *ACTB*, which displayed comparable expression levels across the analyzed groups (Vanni, Zattoni et al. 2018), has been selected as suitable reference genes to consolidate the relative gene expression levels in the analyzed brain samples.

Since *SERPINA8* is located on chromosome 1q42.2 (Heit, Jackson et al. 2013), *SERPINA3* appears to be the only clade A gene member located on chromosome 14q32.1, which is expressed in brain tissue, corroborating the astrocytic expression of *SERPINA3* observed more than 15 years ago (Gopalan, Kasza et al. 2005). The distal sub cluster containing *SERPINA3,* including also kallistatin (*SERPINA4*), proteinase C inhibitor (*SERPINA5*) and the kallistatin-like gene (*SERPINA13*), are highly expressed in the liver (Baker, Belbin et al. 2007). These observations suggest the presence of a tissue-specific promoter or enhancer of *SERPINA3*, which leads to its peculiar brain expression.

Together with the relevant upregulation of *SERPINA3* in sCJD frontal cortex, transcriptomic analysis revealed the presence of other dysregulated *SERPIN* members.

Similarly, to *SERPINA3*, *SERPINB1* was upregulated in sCJD cases with respect to age matched non-neurodegenerative affected controls. *SERPINB1* is a key regulator of neutrophil-programmed cell death, expressed in human brain at the level of microglia and macrophages (Cui, Liu et al. 2014). Despite the significant upregulation found in sCJD patients, the role of *SERPINB1* in prion disease is still undefined. Genetic variation of *SERPINB1* seems to be associated to amyloidosis in a sex specific manner (Deming, Dumitrescu et al. 2018) and additionally, its expression in prefrontal cortex has been related to amyloid burden (Frosch 2018), further supporting the possible involvement of *SERPINB1* in neurodegeneration.

Another member of clade B serpins, *SERPINB6,* was upregulated in sCJD patients. This transcript encodes for a widely expressed nucleocytoplasmic serpin, which exerts a protective role against

cells death induced by proteases ectopic release or internalization, typical of infection status or cerebral ischemia (Scarff, Ung et al. 2004). It was recently shown that pharmacological inhibition of proteasome in PC12 cells results in α-synuclein inclusion bodies formation and upregulation of *SERPINB6*, suggesting a role for this serpin in response to cell insults (Hu, Zhang et al. 2014). Given that the ubiquitin proteasome system activity is fundamental in preventing the accumulation of misfolded proteins (Sweeney, Park et al. 2017), it is possible that *SERPINB6* dysregulations may also have a function in other neurodegenerative diseases. However, further studies are needed to better elucidate the function of this serpin member in proteasome activation.

Brain tissue from sCJD affected patients revealed a slight downregulation of *SERPINE2* compared to control group. SERPINE2, also known as glia-derived nexin of protease nexin 1, is known to regulate extracellular matrix by inhibiting fibrinolysis involved proteases (Boulaftali, Ho-Tin-Noe et al. 2011) Although SERPINE2 may exert protective activity in AD pathological progression (Vaughan, Su et al. 1994), it has been never associated to other neurodegenerative disorders, especially prion diseases. A decrease expression of SERPINE2 in sCJD affected brain samples is consistent with its reduced activity found in post mortem samples of patients with AD, where dysregulation of thrombin and SERPINE2 could lead to neuronal activity alterations contributing to neurodegeneration (Wagner, Geddes et al. 1989, Vaughan, Su et al. 1994).

sCJD patients showed an upregulation of *SERPING1,* which is a complement I esterase inhibitor, expressed in blood, liver, kidney, lung, heart, and brain (Heit, Jackson et al. 2013) and a marker of the A1 states of astrocytes (Makarava, Chang et al. 2019). A1 state can be associated with loss of astrocytes ability in promoting neuronal survival and with the induction of neurons and oligodendrocyte cell death (Liddelow and Barres 2017). Indeed, when the induction of A1 phenotype is prevented, astrocytes assume a neuroprotective role in neurodegeneration, (Makarava, Chang et al. 2019). A significant increase in expression of A1 markers, including *SERPING1*, was observed in cortex and hippocampus of prion-infected mice (Makarava, Chang et al. 2019). In view of this, considering the strict relationship between inflammation and neurodegeneration, Crespo and collaborators identified core regulatory genes, most of which involved in immune response, and can activate a larger network of genes differentially expressed in prion diseases (Crespo, Roomp et al. 2012). *SERPING1* ended up being a member of this huge network, with a role in PrP^{Sc} replication and accumulation.

Chronic neuroinflammation is also characterized by reactive microgliosis (Makarava, Chang et al. 2019). *SERPINH1*, upregulated in the frontal cortex from sCJD patients, was proposed as marker of

microglial activation since it was upregulated in Aβ-stimulated human microglial cells (Yoo, Byun et al. 2015). Considering the key role of microglia in neurodegeneration-related inflammatory responses, SERPINH1 may also act as microglia activator in prion pathology. In addition, *SERPINH1* expression was found to be increased in both AD and PD, indicating that its overexpression may correlate with different neurodegenerative diseases (Ebbert, Ross et al. 2017).

Among the nine analyzed human *SERPIN* transcripts, *SERPINI1* was consistently downregulated in sCJD patients. SERPINI1, known as neuroserpin, is an inhibitor of trypsin-like serine proteases widely expressed throughout the nervous system (Lee, Tsang et al. 2015). Despite the absence of any correlation between *SERPINI1* and prion disease, *SERPINI1* involvement in other neurodegenerative diseases has already been shown. SERPINI1 has been associated with a particular form of dementia, called FENIB, in which mutant neuroserpin polymers accumulate intracellularly, forming inclusions bodies in cortical and subcortical neurons and causing neuronal degeneration (Miranda, Romisch et al. 2004). Moreover, controversial evidence concerning the role of SERPINI1 in AD exists. Indeed, neuroserpin can bind to Aβ and alter its oligomerization, thus exerting a neuroprotective role (Kinghorn, Crowther et al. 2006), or it may represent a detrimental factor by reducing Aβ clearance (Fabbro, Schaller et al. 2011). In light of the aforementioned observations and the role of neuroserpin in neuroprotection and neurodegeneration (Lee, Tsang et al. 2015), *SERPINI1* may be involved in prion disease as well as in other neurodegenerative diseases; whether its involvement is beneficial or detrimental remains to be understood. Furthermore, *SerpinI1* was downregulated in symptomatic RML-infected CD1 mice, when normalized to *Gapdh* (**Figure 4.8**), corroborating the hypothetical role of this serpin in prion pathology.

Given the high sequence homology between human and mouse Serpins (Horvath, Forsyth et al. 2004), a possible correlation in differentially expressed serpins in human and mouse has been taking into account. Thus, transcriptomic analysis in brain of RML-infected CD1 mice, a widely used murine model of prion diseases (Chandler 1961), was performed.

Although *SerpinA3n* resulted to be one of the most upregulated transcripts in prion-infected brain, a significant upregulation of *SerpinF2* in RML-infected mouse brain was observed. SerpinF2, also known as α_2-antiplasmin, is an inhibitor of plasmin (Baker, Chen et al. 2018). Plasmin is a serine protease formed upon the proteolytic cleavage of its precursor, plasminogen, by tissue-type plasminogen activator (t-PA) or by the urokinase-type plasminogen activator. This system is controlled by several inhibitors such as the direct inhibitor of plasmin SerpinF2, or the plasminogen activator inhibitor SerpinI1 (Vingtdeux, Dreses-Werringloer et al. 2008). Of note, all the components

of plasmin cascade are present in the CNS and, although this system is traditionally studied for fibrinolysis, several works reported its involvement in neurodegeneration, particularly in AD.

However, few studies have explored the putative role of *SerpinF2* in prion diseases. Interestingly, both PrP^{C} and PrP^{Sc} can interact with t-PA and plasminogen and can stimulate plasmin formation (Ellis, Daniels et al. 2002). Furthermore, several *in vitro* studies have reported that interaction between PrP^{Sc} and plasminogen may favor PrP^{Sc} replication and propagation (Mays and Ryou 2011) and that t-PA displays higher expression and activity in mouse models of prion disease (Xanthopoulos, Paspaltsis et al. 2005). Despite the different hypotheses regarding the correlation between members of the plasmin cascade and prion diseases, none highlights a role for SerpinF2. The increased expression of *SerpinF2* could represent a cellular response to mitigate the strong effects of plasmin activity. Interestingly, plasmin system may also contribute to the degradation of extracellular protein aggregates, suggesting a possible involvement in neurodegeneration (Constantinescu, Brown et al. 2017). Therefore, direct inhibition of plasmin by SerpinF2 may counteract this process, favoring the accumulation of misfolded proteins.

The most intriguing aspect of this analysis is that, among the seventeen analyzed Serpins transcripts in the brain of prion-infected mice, *SerpinA3n* and *SerpinF2* were the only ones to be differentially upregulated in mouse brain. Given the absence of any significant dysregulation in the gene expression analysis performed using the other reference genes, the upregulation of *SerpinB6a* and the downregulation of *SerpinE1*, observed at symptomatic stage of prion disease, normalizing data with *Actb* (**Figure 4.8**) and *Tubb3* (**Figure 4.9**), respectively, can be attributed to variations among the group analyzed.

If we consider serpin homologies between human and mouse, SERPINA3/*SerpinA3n* is the one differentially expressed in both human and mouse brain. Conversely, the human orthologue of *SerpinF2*, *SERPINF2*, was not even included in the analysis because of its weak expression in the brain under physiological condition. However, it may be possible that *SERPINF2* expression could be induced only during pathological conditions (Barker, Kehoe et al. 2012). Recently, it has been shown that another member of the serpin superfamily, *SERPINA1*, is not expressed at high levels in normal brain tissue (Ebbert, Ross et al. 2017), but it is overexpressed in AD, frontotemporal lobar degeneration and CJD, suggesting that its expression may be detrimental for neuronal function(Abu-Rumeileh, Halbgebauer et al. 2020). For this reason, differential expression of *SERPINF2* in neurodegenerative-affected human brain cannot be excluded, even if further work is required to verify this hypothesis.

Overall, these results show that several members of the serpin superfamily are dysregulated in prion pathology, even if their implication in neurodegeneration is far from being completely elucidated.
It should also be considered that all other differentially expressed serpins, as well as *SERPINA3*/*SerpinA3n*, may represent a tight correlation with an inflammatory response, confirming the relevant role played by inflammation in neurodegeneration. Whether serpins could drive or mitigate the pathology through the modulation of neuroinflammation or whether their dysregulation is only a downstream effect should be further clarified.
Before performing any *in vitro* experiments to test whether prion formation could be influenced by SerpinA3n modulation, its transcript and protein expression levels have been assessed in prion-infected GT1 and N2a cells.
The marked fold change gene expression levels observed between both RML- and 22L-infected GT1 and N2a cells can be explained by the barely detectable levels ($C_T \geq 35$) of *SerpinA3n* in uninfected cells. It is plausible that both GT1 and N2a cells do not activate the transcriptional machinery involved in SerpinA3n expression, probably for the lack of transcription factors landing on SerpinA3n promoter. Prion infection seems to convey the factors needed for SerpinA3n expression, maybe through the activation of inflammatory pathways which play an important role in prion pathogenesis (Carroll, Striebel et al. 2015). However, RML- and 22L-infected cell lines are chronically infected with prions, so to prove whether prions presence is responsible for this peculiar up-regulation, RT-qPCR analysis on *de novo* prion-infected cells will be fundamental to establish a prion-dependent SerpinA3n transcriptional activation.
Although prion diseases are considered rapidly progressive disorders, some forms are characterized by very long incubation period during which prions continuously accumulate in the CNS of affected patients (Tee, Longoria Ibarrola et al. 2018). The SERPINA3 high transcript levels found in human patients with different form of prion disease (Vanni, Moda et al. 2017), which die, in some cases, years after putative start of prion accumulation, together with the high SerpinA3n upregulation found in GT1 and N2a chronically prion-infected cells suggest that SERPINA3/SerpinA3n transcript levels increase over time. Thus, SERPINA3/SerpinA3n upregulation could be associated to secondary pathways activated during the course of prion pathogenesis (e.g., inflammation) instead of a direct and prion-dependent activation.
SerpinA3n transcript upregulation is paralleled by its high protein levels in prion-infected cells, and the most striking results come from medium of GT1 and N2a infected cells. SerpinA3n is a secreted protein (Sipione, Simmen et al. 2006, Gueugneau, d'Hose et al. 2018, Sergi, Campbell et al. 2018),

therefore CM from RML- and 22L- infected GT1 and N2a cells has been collected and analysed to evaluate SerpinA3n levels (Gueugneau, d'Hose et al. 2018). Three to four-fold increase of SerpinA3n protein levels can be observed in GT1 and N2a cells infected with two different prion strains, compared to uninfected cells. Although without reaching statistical significance difference, a slight increase of intracellular SerpinA3n was present in prion-infected cells. This discrepancy could be attributed to the faint signal obtained from WB analysis, which is due to the detection of various non-specific bands observed in membrane probed with the SerpinA3n antibody used. Either a different antibody or a different protocol for cell lysis could be tested in order to obtain clearer results.

Secreted SerpinA3n WB signals revealed the presence of two bands around 55 and 70 kDa. It is known that SERPINA3 has several glycosylation sites (Ianni, Manerba et al. 2010) and having assessed the presence of three sites for glycosylation even in SerpinA3n protein sequence (https://www.uniprot.org/uniprot/Q91WP6), PNGase F treatment has been performed in CM from uninfected and infected cells. This enzyme is able to cleave the glycan between the innermost N-Acetylglucosamine and the asparagine, leaving aspartic acid in place of the asparagine (Maley, Trimble et al. 1989). Results, either from N2a and GT1 cells, showed the shift of the bands at the same molecular weight of recombinant SerpinA3n. However, rather than two different SerpinA3n glycoforms, the two bands observed in CM of prion-infected cells could be associated to two different proteins. At a careful observation, it is possible to appreciate that the lower band was not always detectable in uninfected cells (**Figure 4.10D**-**4.11D**) and, moreover, even after PNGase F treatment, the molecular weight of the most intense lower band had a similar migratory pattern of recombinant SerpinA3n.

These results suggested that SerpinA3n signal could be relative only to the 55kDa band (Vicuña, Strochlic et al. 2015). This is supported by the WB analysis performed in genetically modified N2a expressing SerpinA3n, where it was possible to appreciate the presence of a more intense signal coming from the lower band at 55kDa (**Figure 4.12C**), and from SerpinA3n transcriptional inhibition of SerpinA3n in ScN2a RML where, upon SerpinA3n targeting siRNA and shRNA transfections, the signal from 55kDa band almost disappeared. Given the high sequence similarity among the clade A murine serpins (Forsyth, Horvath et al. 2003), it is plausible that the SerpinA3n antibody used for these experiment is able to recognize other serpins besides SerpinA3n.

However, WB signal from SerpinA3n$^{-/-}$ mice did not reveal the appearance of any bands even after PNGase F treatment (Figure **4.14G**), suggesting that both bands visible either in wild-type and

heterozygous mice have to be associated to SerpinA3n. Therefore, the two signal bands observed in mouse brains can be explained by the different cellular population analysed (including also astrocytes and glial cells) compared to immortalized neuronal cell lines. Given the lack of clarity concerning the band relative to SerpinA3n signal, all densitometric analysis have been performed considering both bands from SerpinA3n WB experiments.

To test the hypothesis according to which increased SerpinA3n levels would lead to a further accumulation of prions, either N2a-SerpinA3n conditioned medium and recombinant SerpinA3n treatment have been performed. Firstly, the activity of N2a secreted and recombinant Serpina3n has been tested using chymotrypsin, one of its known target proteases (Horvath, Irving et al. 2005). Either recombinant and glycosylated, N2a-derived, SerpinA3n demonstrated their ability to form an SDS-stable complex with their cognate proteases (Horvath, Irving et al. 2005, Law, Zhang et al. 2006) resulting in the appearance of a band corresponding to the sum of SerpinA3n (47 kDa, for recombinant and around 55 kDa, for N2a overexpressing SerpinA3n CM) and chymotrypsin (25 kDa) molecular weight (**Figure 4.12D-E**).

ScN2a RML treatment with CM from SerpinA3n overexpressing N2a led to a 40% average increase of PrP^{Sc} signal compared to CM from empty-vector carrying N2a treatment (**Figure 4.13B**). The evaluation of the effect of CM coming from empty-vector carrying cells was essential to exclude any possible bias given by the transfection procedure on N2a cells, which would have affected prion accumulation. To test whether SerpinA3n effect on prion accumulation was limited to PrP^{Sc}, N2a-SerpinA3n CM treatment on N2a cells. Only a trend of PrP^{C} increase was visible in cells treated with N2a-SerpinA3n CM compared to N2a EV CM-treated cells (data not shown), suggesting a PrP^{Sc}-directed effect of N2a-secreted SerpinA3n on prion accumulation.

Similarly, 1μM recombinant SerpinA3n was responsible for an increased accumulation of prion in ScN2a RML cells compared to the vehicle treated ones. Since 0.5μM led to a slight increase in prion accumulation (**Figure 4.13D**), a titration experiment is needed to understand whether a SerpinA3n dose-dependent effect is responsible for PrP^{Sc} increase.

To further test SerpinA3n-prion relationship, PrP^{Sc} changes upon SerpinA3n transcriptional inhibition were evaluated. Either siRNA or shRNA transfection led to a reduction of prions compared to control cells. Although SerpinA3n-directed siRNA transfection was responsible for a strong, even not statistically significant, reduction of PrP^{Sc} compared to siRNA-EGFP transfection, only a 5% average reduction compared to Lipofectamine treated cells (**Figure 4.13F**) has been observed, suggesting that siRNA-mediated SerpinA3n reduction is not sufficient to reduce prion accumulation.

The lack of consistency in prion load reduction, between the two transfection methods, could be explained by an higher potency and sustainable effects characterizing shRNA transfection compared to siRNA one (Rao, Vorhies et al. 2009).

Although without any striking PrP^{Sc} changes, it seems that modulation of SerpinA3n could have an effect on prion accumulation. The hypothesis explaining this phenomenon resides in a SerpinA3n inhibition of protease(s) presumably involved in prion clearance. Therefore, increased Serpina3n levels (obtained through N2a-Serpina3n CM or recombinant SerpinA3n treatment) would lead to increase inhibition of protease(s) responsible for prion elimination, leading to a further pathological accumulation of the latter. Conversely, SerpinA3n reduction (*i.e*. at transcriptional levels) will free protease(s) ability to act and cleave pathological PrP^{Sc} aggregates.

Interestingly, the majority of prion and non-prion neurodegenerative disorders manifests symptoms in adulthood. This implies that the amount of pathologic proteins has to exceed a threshold for the pathologic process to be unabated (Prusiner 2012, Jucker and Walker 2013). Thus, probably, the clearance machine would be saturated during aging by the excess of protein aggregates or the age-dependent increase expression of protease inhibitor, such as SERPINA3 (Vanni, Colini Baldeschi et al. 2020), could reduce the protease(s)-dependent protein clearance.

However, to prove a SerpinA3n involvement in prion pathogenesis, *in vivo* model of prion diseases is required. Therefore, intracerebral injection of three different prion strains has been performed in $SerpinA3n^{-/-}$ and $SerpinA3n^{+/+}$ mice and their incubation and survival times has been observed. The absence of differences in incubation, survival times and prion accumulation between KO and WT mice suggested that SerpinA3n ablation is not sufficient to convey resistance to prion infection.

Compared to prion-infected immortalized cell, animals' prion-inoculation represents a more comprehensive model to study the disease and to test the effective role of putative players in the pathology. The prion reduction observed in SerpinA3n transcriptional-inhibited cells is not paralleled by a reduced prion accumulation in inoculated $SerpinA3n^{-/-}$ mice, suggesting that prion disease course is not altered in the absence of SerpinA3n. The biological complexity of genetically modified mice suggests that some compensatory mechanisms, not observed in immortalized cells, would take place in order to restore the balance upon depletion of SerpinA3n. Indeed, while brain expressed *Serpin* revealed no changes at transcript levels, *SerpinI1* showed a mild upregulation in $SerpinA3n^{-/-}$ mice compared to WT animals. Although the physiological explanation of this effect remains to be determined, *SerpinI1* slight upregulation may suggest a compensatory effect to rescue *SerpinA3n* absence in KO mice.

Future transcriptomic analysis in the brain of prion-infected SerpinA3n$^{-/-}$ animals will help to understand whether *SerpinI1* increased levels are present even in infected mice or if it is downregulated as observed in the brain of human and wild type mice infected with prion.

6. CONCLUSION

According to previous studies, *SERPINA3* transcript has been found significantly upregulated in prion-infected cynomolgus macaques (Barbisin et al., 2014). In addition, a striking up-regulation of SERPINA3, both at mRNA and protein level, was previously demonstrated also in different types of human prion diseases (Vanni et al., 2017).

Among brain expressed SERPINs, only *SERPINA3*/*SerpinA3n* showed a marked dysregulation both in prion-infected human samples and animal models of the diseases suggesting its involvement in prion-related neurodegeneration and its potential consideration as therapeutic target. However, future studies are needed to clarify the role of other differentially expressed serpins in neurodegenerative disorders.

According to the most intriguing hypothesis, SERPINA3/SerpinA3n might play a crucial role in prion clearance. It is likely that SERPINA3/SerpinA3n overexpression favours prion accumulation by inhibiting proteases presumably involved in PrP^{Sc} degradation, while SERPINA3/SerpinA3n inhibition is responsible for a prion reduction.

In vitro experiment on prion-infected cells demonstrated a SerpinA3n-dependent PrP^{Sc} changes. However, *in vivo* SerpinA3n ablation was not sufficient to convey resistance to prion infection. This could be explained by a brain expressed serpins, *SerpinI1,* upregulation characterizing SerpinA3n KO mice, which may compensate the absence of SerpinA3n.

Although SERPINA3/SerpinA3n puzzling traits in prion diseases have yet to be dissected, these findings, together with previous data, clearly identify SERPINA3 as an attractive therapeutic target paving the way for future medicaments aimed to boost the clearance of PrP^{Sc} aggregates responsible for prion diseases.

7. BIBLIOGRAPHY

Abraham, C. R. (2001). "Reactive astrocytes and alpha1-antichymotrypsin in Alzheimer's disease." Neurobiol Aging **22**(6): 931-936.

Abraham, C. R., D. J. Selkoe and H. Potter (1988). "Immunochemical identification of the serine protease inhibitor alpha 1-antichymotrypsin in the brain amyloid deposits of Alzheimer's disease." Cell **52**(4): 487-501.

Abrams, J. Y., L. B. Schonberger, E. D. Belay, R. A. Maddox, E. W. Leschek, J. L. Mills, D. K. Wysowski and J. E. Fradkin (2011). "Lower risk of Creutzfeldt-Jakob disease in pituitary growth hormone recipients initiating treatment after 1977." J Clin Endocrinol Metab **96**(10): E1666-1669.

Abskharon, R. N., G. Giachin, A. Wohlkonig, S. H. Soror, E. Pardon, G. Legname and J. Steyaert (2014). "Probing the N-terminal beta-sheet conversion in the crystal structure of the human prion protein bound to a nanobody." J Am Chem Soc **136**(3): 937-944.

Abu-Rumeileh, S., S. Halbgebauer, P. Steinacker, S. Anderl-Straub, B. Polischi, A. C. Ludolph, S. Capellari, P. Parchi and M. Otto (2020). "CSF SerpinA1 in Creutzfeldt-Jakob disease and frontotemporal lobar degeneration." Ann Clin Transl Neurol **7**(2): 191-199.

Aguzzi, A. and A. M. Calella (2009). "Prions: protein aggregation and infectious diseases." Physiol Rev **89**(4): 1105-1152.

Aguzzi, A., M. Heikenwalder and M. Polymenidou (2007). "Insights into prion strains and neurotoxicity." Nat Rev Mol Cell Biol **8**(7): 552-561.

Ali, T., S. Hannaoui, S. Nemani, W. Tahir, I. Zemlyankina, P. Cherry, S. Y. Shim, V. Sim, H. M. Schaetzl and S. Gilch (2021). "Oral administration of repurposed drug targeting Cyp46A1 increases survival times of prion infected mice." Acta Neuropathol Commun **9**(1): 58.

Almeida, L. M., U. Basu, B. Khaniya, M. Taniguchi, J. L. Williams, S. S. Moore and L. L. Guan (2011). "Gene expression in the medulla following oral infection of cattle with bovine spongiform encephalopathy." J Toxicol Environ Health A **74**(2-4): 110-126.

Alper, T., W. A. Cramp, D. A. Haig and M. C. Clarke (1967). "Does the agent of scrapie replicate without nucleic acid?" Nature **214**(5090): 764-766.

Altmeppen, H. C., J. Prox, B. Puig, M. A. Kluth, C. Bernreuther, D. Thurm, E. Jorissen, B. Petrowitz, U. Bartsch, B. De Strooper, P. Saftig and M. Glatzel (2011). "Lack of a-disintegrin-and-metalloproteinase ADAM10 leads to intracellular accumulation and loss of shedding of the cellular prion protein in vivo." Mol Neurodegener **6**: 36.

Altmeppen, H. C., B. Puig, F. Dohler, D. K. Thurm, C. Falker, S. Krasemann and M. Glatzel (2012). "Proteolytic processing of the prion protein in health and disease." Am J Neurodegener Dis **1**(1): 15-31.

Anderson, R. M., C. A. Donnelly, N. M. Ferguson, M. E. Woolhouse, C. J. Watt, H. J. Udy, S. MaWhinney, S. P. Dunstan, T. R. Southwood, J. W. Wilesmith, J. B. Ryan, L. J. Hoinville, J. E. Hillerton, A. R. Austin and G. A. Wells (1996). "Transmission dynamics and epidemiology of BSE in British cattle." Nature **382**(6594): 779-788.

Andrasfay, T. and N. Goldman (2021). "Reductions in 2020 US life expectancy due to COVID-19 and the disproportionate impact on the Black and Latino populations." Proc Natl Acad Sci U S A **118**(5).

Arai, T., M. Hasegawa, H. Akiyama, K. Ikeda, T. Nonaka, H. Mori, D. Mann, K. Tsuchiya, M. Yoshida, Y. Hashizume and T. Oda (2006). "TDP-43 is a component of ubiquitin-positive tau-negative inclusions in frontotemporal lobar degeneration and amyotrophic lateral sclerosis." Biochem Biophys Res Commun **351**(3): 602-611.

Arvanitakis, Z., R. C. Shah and D. A. Bennett (2019). "Diagnosis and Management of Dementia: Review." JAMA **322**(16): 1589-1599.

Ascari, L. M., S. C. Rocha, P. B. Gonçalves, T. C. R. G. Vieira and Y. Cordeiro (2020). "Challenges and Advances in Antemortem Diagnosis of Human Transmissible Spongiform Encephalopathies." Front Bioeng Biotechnol **8**: 585896.
Aslam, M. S. and L. Yuan (2019). "Serpina3n: Potential drug and challenges, mini review." J Drug Target: 1-11.
Atarashi, R., J. M. Wilham, L. Christensen, A. G. Hughson, R. A. Moore, L. M. Johnson, H. A. Onwubiko, S. A. Priola and B. Caughey (2008). "Simplified ultrasensitive prion detection by recombinant PrP conversion with shaking." Nat Methods **5**(3): 211-212.
Atkinson, C. J., K. Zhang, A. L. Munn, A. Wiegmans and M. Q. Wei (2016). "Prion protein scrapie and the normal cellular prion protein." Prion **10**(1): 63-82.
Avar, M., D. Heinzer, N. Steinke, B. Dogancay, R. Moos, S. Lugan, C. Cosenza, S. Hornemann, O. Andreoletti and A. Aguzzi (2020). "Prion infection, transmission, and cytopathology modeled in a low-biohazard human cell line." Life Sci Alliance **3**(8).
Babelhadj, B., M. A. Di Bari, L. Pirisinu, B. Chiappini, S. B. S. Gaouar, G. Riccardi, S. Marcon, U. Agrimi, R. Nonno and G. Vaccari (2018). "Prion Disease in Dromedary Camels, Algeria." Emerg Infect Dis **24**(6): 1029-1036.
Baker, C., O. Belbin, N. Kalsheker and K. Morgan (2007). "SERPINA3 (aka alpha-1-antichymotrypsin)." Front Biosci **12**: 2821-2835.
Baker, H. F., L. W. Duchen, J. M. Jacobs and R. M. Ridley (1990). "Spongiform encephalopathy transmitted experimentally from Creutzfeldt-Jakob and familial Gerstmann-Sträussler-Scheinker diseases." Brain **113 (Pt 6)**: 1891-1909.
Baker, S. K., Z. L. Chen, E. H. Norris, A. S. Revenko, A. R. MacLeod and S. Strickland (2018). "Blood-derived plasminogen drives brain inflammation and plaque deposition in a mouse model of Alzheimer's disease." Proc Natl Acad Sci U S A **115**(41): E9687-E9696.
Barbisin, M., S. Vanni, A. C. Schmadicke, J. Montag, D. Motzkus, L. Opitz, G. Salinas-Riester and G. Legname (2014). "Gene expression profiling of brains from bovine spongiform encephalopathy (BSE)-infected cynomolgus macaques." BMC Genomics **15**: 434.
Barker, R., P. G. Kehoe and S. Love (2012). "Activators and inhibitors of the plasminogen system in Alzheimer's disease." J Cell Mol Med **16**(4): 865-876.
Barret, A., F. Tagliavini, G. Forloni, C. Bate, M. Salmona, L. Colombo, A. De Luigi, L. Limido, S. Suardi, G. Rossi, F. Auvré, K. T. Adjou, N. Salès, A. Williams, C. Lasmézas and J. P. Deslys (2003). "Evaluation of quinacrine treatment for prion diseases." J Virol **77**(15): 8462-8469.
Barria, M. A., A. Balachandran, M. Morita, T. Kitamoto, R. Barron, J. Manson, R. Knight, J. W. Ironside and M. W. Head (2014). "Molecular barriers to zoonotic transmission of prions." Emerg Infect Dis **20**(1): 88-97.
Bartz, J. C. (2016). "Prion Strain Diversity." Cold Spring Harb Perspect Med **6**(12).
Bateman, D., D. Hilton, S. Love, M. Zeidler, J. Beck and J. Collinge (1995). "Sporadic Creutzfeldt-Jakob disease in a 18-year-old in the UK." Lancet **346**(8983): 1155-1156.
Beck, J. A., S. Mead, T. A. Campbell, A. Dickinson, D. P. Wientjens, E. A. Croes, C. M. Van Duijn and J. Collinge (2001). "Two-octapeptide repeat deletion of prion protein associated with rapidly progressive dementia." Neurology **57**(2): 354-356.
Bendheim, P. E., H. R. Brown, R. D. Rudelli, L. J. Scala, N. L. Goller, G. Y. Wen, R. J. Kascsak, N. R. Cashman and D. C. Bolton (1992). "Nearly ubiquitous tissue distribution of the scrapie agent precursor protein." Neurology **42**(1): 149-156.
Benestad, S. L., J. N. Arsac, W. Goldmann and M. Nöremark (2008). "Atypical/Nor98 scrapie: properties of the agent, genetics, and epidemiology." Vet Res **39**(4): 19.

Benetti, F., S. Gustincich and G. Legname (2012). "Gene expression profiling and therapeutic interventions in neurodegenerative diseases: a comprehensive study on potentiality and limits." Expert Opin Drug Discov **7**(3): 245-259.
Beraldo, F. H., C. P. Arantes, T. G. Santos, C. F. Machado, M. Roffe, G. N. Hajj, K. S. Lee, A. C. Magalhães, F. A. Caetano, G. L. Mancini, M. H. Lopes, T. A. Américo, M. H. Magdesian, S. S. Ferguson, R. Linden, M. A. Prado and V. R. Martins (2011). "Metabotropic glutamate receptors transduce signals for neurite outgrowth after binding of the prion protein to laminin γ1 chain." FASEB J **25**(1): 265-279.
Beraldo, F. H., C. P. Arantes, T. G. Santos, N. G. Queiroz, K. Young, R. J. Rylett, R. P. Markus, M. A. Prado and V. R. Martins (2010). "Role of alpha7 nicotinic acetylcholine receptor in calcium signaling induced by prion protein interaction with stress-inducible protein 1." J Biol Chem **285**(47): 36542-36550.
Beringue, V., D. Vilette, G. Mallinson, F. Archer, M. Kaisar, M. Tayebi, G. S. Jackson, A. R. Clarke, H. Laude, J. Collinge and S. Hawke (2004). "PrPSc binding antibodies are potent inhibitors of prion replication in cell lines." J Biol Chem **279**(38): 39671-39676.
Bernacka, K., A. Kuryliszyn-Moskal and P. A. Klimiuk (1993). "Serum alpha-1-antitrypsin and alpha-1-antichymotrypsin after surgical treatment and during postoperative clinical course of human gastric cancer." Neoplasma **40**(2): 111-116.
Bernardi, L. and A. C. Bruni (2019). "Mutations in Prion Protein Gene: Pathogenic Mechanisms in C-Terminal vs. N-Terminal Domain, a Review." Int J Mol Sci **20**(14).
Bieschke, J., P. Weber, N. Sarafoff, M. Beekes, A. Giese and H. Kretzschmar (2004). "Autocatalytic self-propagation of misfolded prion protein." Proc Natl Acad Sci U S A **101**(33): 12207-12211.
Bonda, D. J., S. Manjila, P. Mehndiratta, F. Khan, B. R. Miller, K. Onwuzulike, G. Puoti, M. L. Cohen, L. B. Schonberger and I. Cali (2016). "Human prion diseases: surgical lessons learned from iatrogenic prion transmission." Neurosurg Focus **41**(1): E10.
Booth, S., C. Bowman, R. Baumgartner, G. Sorensen, C. Robertson, M. Coulthart, C. Phillipson and R. L. Somorjai (2004). "Identification of central nervous system genes involved in the host response to the scrapie agent during preclinical and clinical infection." J Gen Virol **85**(Pt 11): 3459-3471.
Borchelt, D. R., M. Rogers, N. Stahl, G. Telling and S. B. Prusiner (1993). "Release of the cellular prion protein from cultured cells after loss of its glycoinositol phospholipid anchor." Glycobiology **3**(4): 319-329.
Bougard, D., J. P. Brandel, M. Belondrade, V. Beringue, C. Segarra, H. Fleury, J. L. Laplanche, C. Mayran, S. Nicot, A. Green, A. Welaratne, D. Narbey, C. Fournier-Wirth, R. Knight, R. Will, P. Tiberghien, S. Haik and J. Coste (2016). "Detection of prions in the plasma of presymptomatic and symptomatic patients with variant Creutzfeldt-Jakob disease." Sci Transl Med **8**(370): 370ra182.
Boulaftali, Y., B. Ho-Tin-Noe, A. Pena, S. Loyau, L. Venisse, D. François, B. Richard, V. Arocas, J. P. Collet, M. Jandrot-Perrus and M. C. Bouton (2011). "Platelet protease nexin-1, a serpin that strongly influences fibrinolysis and thrombolysis." Circulation **123**(12): 1326-1334.
Braak, H., I. Alafuzoff, T. Arzberger, H. Kretzschmar and K. Del Tredici (2006). "Staging of Alzheimer disease-associated neurofibrillary pathology using paraffin sections and immunocytochemistry." Acta Neuropathol **112**(4): 389-404.
Braak, H., K. Del Tredici, U. Rüb, R. A. de Vos, E. N. Jansen Steur and E. Braak (2003). "Staging of brain pathology related to sporadic Parkinson's disease." Neurobiol Aging **24**(2): 197-211.
Brandner, S., S. Isenmann, A. Raeber, M. Fischer, A. Sailer, Y. Kobayashi, S. Marino, C. Weissmann and A. Aguzzi (1996). "Normal host prion protein necessary for scrapie-induced neurotoxicity." Nature **379**(6563): 339-343.

Brandner, S. and Z. Jaunmuktane (2017). "Prion disease: experimental models and reality." Acta Neuropathol **133**(2): 197-222.
Bremer, J., F. Baumann, C. Tiberi, C. Wessig, H. Fischer, P. Schwarz, A. D. Steele, K. V. Toyka, K. A. Nave, J. Weis and A. Aguzzi (2010). "Axonal prion protein is required for peripheral myelin maintenance." Nat Neurosci **13**(3): 310-318.
Britton, T. C., S. al-Sarraj, C. Shaw, T. Campbell and J. Collinge (1995). "Sporadic Creutzfeldt-Jakob disease in a 16-year-old in the UK." Lancet **346**(8983): 1155.
Brown, K. and J. A. Mastrianni (2010). "The prion diseases." J Geriatr Psychiatry Neurol **23**(4): 277-298.
Brown, P., J. P. Brandel, T. Sato, Y. Nakamura, J. MacKenzie, R. G. Will, A. Ladogana, M. Pocchiari, E. W. Leschek and L. B. Schonberger (2012). "Iatrogenic Creutzfeldt-Jakob disease, final assessment." Emerg Infect Dis **18**(6): 901-907.
Brown, P., L. G. Goldfarb, W. R. McCombie, A. Nieto, D. Squillacote, W. Sheremata, B. W. Little, M. S. Godec, C. J. Gibbs and D. C. Gajdusek (1992). "Atypical Creutzfeldt-Jakob disease in an American family with an insert mutation in the PRNP amyloid precursor gene." Neurology **42**(2): 422-427.
Bruce, M. E., R. G. Will, J. W. Ironside, I. McConnell, D. Drummond, A. Suttie, L. McCardle, A. Chree, J. Hope, C. Birkett, S. Cousens, H. Fraser and C. J. Bostock (1997). "Transmissions to mice indicate that 'new variant' CJD is caused by the BSE agent." Nature **389**(6650): 498-501.
Bruijn, L. I., M. K. Houseweart, S. Kato, K. L. Anderson, S. D. Anderson, E. Ohama, A. G. Reaume, R. W. Scott and D. W. Cleveland (1998). "Aggregation and motor neuron toxicity of an ALS-linked SOD1 mutant independent from wild-type SOD1." Science **281**(5384): 1851-1854.
Bueler, H., A. Aguzzi, A. Sailer, R. A. Greiner, P. Autenried, M. Aguet and C. Weissmann (1993). "Mice devoid of PrP are resistant to scrapie." Cell **73**(7): 1339-1347.
Burthem, J., B. Urban, A. Pain and D. J. Roberts (2001). "The normal cellular prion protein is strongly expressed by myeloid dendritic cells." Blood **98**(13): 3733-3738.
Butler, D. A., M. R. Scott, J. M. Bockman, D. R. Borchelt, A. Taraboulos, K. K. Hsiao, D. T. Kingsbury and S. B. Prusiner (1988). "Scrapie-infected murine neuroblastoma cells produce protease-resistant prion proteins." J Virol **62**(5): 1558-1564.
Béringue, V., J. L. Vilotte and H. Laude (2008). "Prion agent diversity and species barrier." Vet Res **39**(4): 47.
Caiati, M. D., V. F. Safiulina, G. Fattorini, S. Sivakumaran, G. Legname and E. Cherubini (2013). "PrPC controls via protein kinase A the direction of synaptic plasticity in the immature hippocampus." J Neurosci **33**(7): 2973-2983.
Campbell, I. L., M. Eddleston, P. Kemper, M. B. Oldstone and M. V. Hobbs (1994). "Activation of cerebral cytokine gene expression and its correlation with onset of reactive astrocyte and acute-phase response gene expression in scrapie." J Virol **68**(4): 2383-2387.
Capellari, S., R. Strammiello, D. Saverioni, H. Kretzschmar and P. Parchi (2011). "Genetic Creutzfeldt-Jakob disease and fatal familial insomnia: insights into phenotypic variability and disease pathogenesis." Acta Neuropathol **121**(1): 21-37.
Carroll, J. A., J. F. Striebel, B. Race, K. Phillips and B. Chesebro (2015). "Prion infection of mouse brain reveals multiple new upregulated genes involved in neuroinflammation or signal transduction." J Virol **89**(4): 2388-2404.
Castilla, J., R. Morales, P. Saa, M. Barria, P. Gambetti and C. Soto (2008). "Cell-free propagation of prion strains." EMBO J **27**(19): 2557-2566.
Caughey, B., R. E. Race, D. Ernst, M. J. Buchmeier and B. Chesebro (1989). "Prion protein biosynthesis in scrapie-infected and uninfected neuroblastoma cells." J Virol **63**(1): 175-181.

Caughey, B., G. J. Raymond, D. Ernst and R. E. Race (1991). "N-terminal truncation of the scrapie-associated form of PrP by lysosomal protease(s): implications regarding the site of conversion of PrP to the protease-resistant state." J Virol **65**(12): 6597-6603.
Chandler, R. L. (1961). "Encephalopathy in mice produced by inoculation with scrapie brain material." Lancet **1**(7191): 1378-1379.
Charles, J. F., F. Coury, R. Sulyanto, D. Sitara, J. Wu, N. Brady, K. Tsang, K. Sigrist, D. M. Tollefsen, L. He, D. Storm and A. O. Aliprantis (2012). "The collection of NFATc1-dependent transcripts in the osteoclast includes numerous genes non-essential to physiologic bone resorption." Bone **51**(5): 902-912.
Chen, C., X. F. Xu, R. Q. Zhang, Y. Ma, Y. Lv, J. L. Li, Q. Shi, K. Xiao, J. Sun, X. D. Yang and X. P. Dong (2017). "Remarkable increases of alpha1-antichymotrypsin in brain tissues of rodents during prion infection." Prion **11**(5): 338-351.
Chen, J. M., N. Chuzhanova, P. D. Stenson, C. Férec and D. N. Cooper (2005). "Meta-analysis of gross insertions causing human genetic disease: novel mutational mechanisms and the role of replication slippage." Hum Mutat **25**(2): 207-221.
Chen, S. G., D. B. Teplow, P. Parchi, J. K. Teller, P. Gambetti and L. Autilio-Gambetti (1995). "Truncated forms of the human prion protein in normal brain and in prion diseases." J Biol Chem **270**(32): 19173-19180.
Cho, H. J. (1976). "Is the scrapie agent a virus?" Nature **262**(5567): 411-412.
Clavaguera, F., T. Bolmont, R. A. Crowther, D. Abramowski, S. Frank, A. Probst, G. Fraser, A. K. Stalder, M. Beibel, M. Staufenbiel, M. Jucker, M. Goedert and M. Tolnay (2009). "Transmission and spreading of tauopathy in transgenic mouse brain." Nat Cell Biol **11**(7): 909-913.
Colby, D. W. and S. B. Prusiner (2011). "Prions." Cold Spring Harb Perspect Biol **3**(1): a006833.
Colby, D. W., Q. Zhang, S. Wang, D. Groth, G. Legname, D. Riesner and S. B. Prusiner (2007). "Prion detection by an amyloid seeding assay." Proc Natl Acad Sci U S A **104**(52): 20914-20919.
Colini Baldeschi, A., S. Vanni, M. Zattoni and G. Legname (2020). "Novel regulators of PrP." Expert Opin Ther Targets **24**(8): 759-776.
Collinge, J., M. S. Palmer, K. C. Sidle, I. Gowland, R. Medori, J. Ironside and P. Lantos (1995). "Transmission of fatal familial insomnia to laboratory animals." Lancet **346**(8974): 569-570.
Collins, S., C. A. McLean and C. L. Masters (2001). "Gerstmann-Straussler-Scheinker syndrome,fatal familial insomnia, and kuru: a review of these less common human transmissible spongiform encephalopathies." J Clin Neurosci **8**(5): 387-397.
Comoy, E. E., J. Mikol, S. Luccantoni-Freire, E. Correia, N. Lescoutra-Etchegaray, V. Durand, C. Dehen, O. Andreoletti, C. Casalone, J. A. Richt, J. J. Greenlee, T. Baron, S. L. Benestad, P. Brown and J. P. Deslys (2015). "Transmission of scrapie prions to primate after an extended silent incubation period." Sci Rep **5**: 11573.
Concha-Marambio, L., S. Pritzkow, F. Moda, F. Tagliavini, J. W. Ironside, P. E. Schulz and C. Soto (2016). "Detection of prions in blood from patients with variant Creutzfeldt-Jakob disease." Sci Transl Med **8**(370): 370ra183.
Constantinescu, P., R. A. Brown, A. R. Wyatt, M. Ranson and M. R. Wilson (2017). "Amorphous protein aggregates stimulate plasminogen activation, leading to release of cytotoxic fragments that are clients for extracellular chaperones." J Biol Chem **292**(35): 14425-14437.
Crespo, I., K. Roomp, W. Jurkowski, H. Kitano and A. del Sol (2012). "Gene regulatory network analysis supports inflammation as a key neurodegeneration process in prion disease." BMC Syst Biol **6**: 132.
Cronier, S., H. Laude and J. M. Peyrin (2004). "Prions can infect primary cultured neurons and astrocytes and promote neuronal cell death." Proc Natl Acad Sci U S A **101**(33): 12271-12276.

Cui, X., Y. Liu, C. Wan, C. Lu, J. Cai, S. He, T. Ni, J. Zhu, L. Wei, Y. Zhang and H. Qian (2014). "Decreased expression of SERPINB1 correlates with tumor invasion and poor prognosis in hepatocellular carcinoma." J Mol Histol **45**(1): 59-68.
Dadras, S. S., R. J. Lin, G. Razavi, A. Kawakami, J. Du, E. Feige, D. A. Milner, M. F. Loda, S. R. Granter, M. Detmar, H. R. Widlund, M. A. Horstmann and D. E. Fisher (2015). "A novel role for microphthalmia-associated transcription factor-regulated pigment epithelium-derived factor during melanoma progression." Am J Pathol **185**(1): 252-265.
Dandoy-Dron, F., L. Benboudjema, F. Guillo, A. Jaegly, C. Jasmin, D. Dormont, M. G. Tovey and M. Dron (2000). "Enhanced levels of scrapie responsive gene mRNA in BSE-infected mouse brain." Brain Res Mol Brain Res **76**(1): 173-179.
Das, S. and H. Potter (1995). "Expression of the Alzheimer amyloid-promoting factor antichymotrypsin is induced in human astrocytes by IL-1." Neuron **14**(2): 447-456.
Davies, M. J. and D. A. Lomas (2008). "The molecular aetiology of the serpinopathies." Int J Biochem Cell Biol **40**(6-7): 1273-1286.
Deming, Y., L. Dumitrescu, L. L. Barnes, M. Thambisetty, B. Kunkle, K. A. Gifford, W. S. Bush, L. B. Chibnik, S. Mukherjee, P. L. De Jager, W. Kukull, M. Huentelman, P. K. Crane, S. M. Resnick, C. D. Keene, T. J. Montine, G. D. Schellenberg, J. L. Haines, H. Zetterberg, K. Blennow, E. B. Larson, S. C. Johnson, M. Albert, A. Moghekar, J. L. Del Aguila, M. V. Fernandez, J. Budde, J. Hassenstab, A. M. Fagan, M. Riemenschneider, R. C. Petersen, L. Minthon, M. J. Chao, V. M. Van Deerlin, V. M. Lee, L. M. Shaw, J. Q. Trojanowski, E. R. Peskind, G. Li, L. K. Davis, J. M. Sealock, N. J. Cox, I. Alzheimer's Disease Neuroimaging, C. Alzheimer Disease Genetics, A. M. Goate, D. A. Bennett, J. A. Schneider, A. L. Jefferson, C. Cruchaga and T. J. Hohman (2018). "Sex-specific genetic predictors of Alzheimer's disease biomarkers." Acta Neuropathol **136**(6): 857-872.
Denny, R. A., L. K. Gavrin and E. Saiah (2013). "Recent developments in targeting protein misfolding diseases." Bioorg Med Chem Lett **23**(7): 1935-1944.
Detwiler, L. A. and M. Baylis (2003). "The epidemiology of scrapie." Rev Sci Tech **22**(1): 121-143.
DiFiglia, M., E. Sapp, K. O. Chase, S. W. Davies, G. P. Bates, J. P. Vonsattel and N. Aronin (1997). "Aggregation of huntingtin in neuronal intranuclear inclusions and dystrophic neurites in brain." Science **277**(5334): 1990-1993.
Ducrot, C., M. Arnold, A. de Koeijer, D. Heim and D. Calavas (2008). "Review on the epidemiology and dynamics of BSE epidemics." Vet Res **39**(4): 15.
Duffy, P., J. Wolf, G. Collins, A. G. DeVoe, B. Streeten and D. Cowen (1974). "Letter: Possible person-to-person transmission of Creutzfeldt-Jakob disease." N Engl J Med **290**(12): 692-693.
Dyer, C. (2018). "British man with CJD gets experimental treatment in world first." BMJ **363**: k4608.
Ebbert, M. T. W., C. A. Ross, L. J. Pregent, R. J. Lank, C. Zhang, R. B. Katzman, K. Jansen-West, Y. Song, E. L. da Rocha, C. Palmucci, P. Desaro, A. E. Robertson, A. M. Caputo, D. W. Dickson, K. B. Boylan, R. Rademakers, T. Ordog, H. Li and V. V. Belzil (2017). "Conserved DNA methylation combined with differential frontal cortex and cerebellar expression distinguishes C9orf72-associated and sporadic ALS, and implicates SERPINA1 in disease." Acta Neuropathol **134**(5): 715-728.
Ellis, V., M. Daniels, R. Misra and D. R. Brown (2002). "Plasminogen activation is stimulated by prion protein and regulated in a copper-dependent manner." Biochemistry **41**(22): 6891-6896.
Fabbro, S., K. Schaller and N. W. Seeds (2011). "Amyloid-beta levels are significantly reduced and spatial memory defects are rescued in a novel neuroserpin-deficient Alzheimer's disease transgenic mouse model." J Neurochem **118**(5): 928-938.
Falsig, J., C. Julius, I. Margalith, P. Schwarz, F. L. Heppner and A. Aguzzi (2008). "A versatile prion replication assay in organotypic brain slices." Nat Neurosci **11**(1): 109-117.

Figgie, M. P. and B. S. Appleby (2021). "Clinical Use of Improved Diagnostic Testing for Detection of Prion Disease." Viruses **13**(5).
Filali, H., I. Martin-Burriel, F. Harders, L. Varona, C. Serrano, C. Acín, J. J. Badiola, A. Bossers and R. Bolea (2012). "Medulla oblongata transcriptome changes during presymptomatic natural scrapie and their association with prion-related lesions." BMC Genomics **13**: 399.
Filali, H., E. Vidal, R. Bolea, M. Márquez, P. Marco, A. Vargas, M. Pumarola, I. Martin-Burriel and J. J. Badiola (2013). "Gene and protein patterns of potential prion-related markers in the central nervous system of clinical and preclinical infected sheep." Vet Res **44**: 14.
Fluharty, B. R., E. Biasini, M. Stravalaci, A. Sclip, L. Diomede, C. Balducci, P. La Vitola, M. Messa, L. Colombo, G. Forloni, T. Borsello, M. Gobbi and D. A. Harris (2013). "An N-terminal fragment of the prion protein binds to amyloid-β oligomers and inhibits their neurotoxicity in vivo." J Biol Chem **288**(11): 7857-7866.
Forloni, G., M. Tettamanti, U. Lucca, Y. Albanese, E. Quaglio, R. Chiesa, A. Erbetta, F. Villani, V. Redaelli, F. Tagliavini, V. Artuso and I. Roiter (2015). "Preventive study in subjects at risk of fatal familial insomnia: Innovative approach to rare diseases." Prion **9**(2): 75-79.
Forsyth, S., A. Horvath and P. Coughlin (2003). "A review and comparison of the murine alpha1-antitrypsin and alpha1-antichymotrypsin multigene clusters with the human clade A serpins." Genomics **81**(3): 336-345.
Frosch, M. P. (2018). ""When sex influences the brain: implications for Alzheimer disease"." Acta Neuropathol **136**(6): 855-856.
Frosh, A., L. C. Smith, C. J. Jackson, J. M. Linehan, S. Brandner, J. D. Wadsworth and J. Collinge (2004). "Analysis of 2000 consecutive UK tonsillectomy specimens for disease-related prion protein." Lancet **364**(9441): 1260-1262.
Furiya, Y., M. Hirano, N. Kurumatani, T. Nakamuro, R. Matsumura, N. Futamura and S. Ueno (2005). "Alpha-1-antichymotrypsin gene polymorphism and susceptibility to multiple system atrophy (MSA)." Brain Res Mol Brain Res **138**(2): 178-181.
Gajdusek, D. C., C. J. Gibbs and M. Alpers (1966). "Experimental transmission of a Kuru-like syndrome to chimpanzees." Nature **209**(5025): 794-796.
Gambetti, P., I. Cali, S. Notari, Q. Kong, W. Q. Zou and W. K. Surewicz (2011). "Molecular biology and pathology of prion strains in sporadic human prion diseases." Acta Neuropathol **121**(1): 79-90.
Gambetti, P., Z. Dong, J. Yuan, X. Xiao, M. Zheng, A. Alshekhlee, R. Castellani, M. Cohen, M. A. Barria, D. Gonzalez-Romero, E. D. Belay, L. B. Schonberger, K. Marder, C. Harris, J. R. Burke, T. Montine, T. Wisniewski, D. W. Dickson, C. Soto, C. M. Hulette, J. A. Mastrianni, Q. Kong and W. Q. Zou (2008). "A novel human disease with abnormal prion protein sensitive to protease." Ann Neurol **63**(6): 697-708.
Gambetti, P., Q. Kong, W. Zou, P. Parchi and S. G. Chen (2003). "Sporadic and familial CJD: classification and characterisation." Br Med Bull **66**: 213-239.
Gasperini, L., E. Meneghetti, B. Pastore, F. Benetti and G. Legname (2015). "Prion protein and copper cooperatively protect neurons by modulating NMDA receptor through S-nitrosylation." Antioxid Redox Signal **22**(9): 772-784.
Geschwind, M. D. (2015). "Prion Diseases." Continuum (Minneap Minn) **21**(6 Neuroinfectious Disease): 1612-1638.
Gettins, P. G. (2002). "Serpin structure, mechanism, and function." Chem Rev **102**(12): 4751-4804.
Gettins, P. G. and S. T. Olson (2016). "Inhibitory serpins. New insights into their folding, polymerization, regulation and clearance." Biochem J **473**(15): 2273-2293.
Gibbs, C. J., D. C. Gajdusek, D. M. Asher, M. P. Alpers, E. Beck, P. M. Daniel and W. B. Matthews (1968). "Creutzfeldt-Jakob disease (spongiform encephalopathy): transmission to the chimpanzee." Science **161**(3839): 388-389.

Gill, O. N., Y. Spencer, A. Richard-Loendt, C. Kelly, R. Dabaghian, L. Boyes, J. Linehan, M. Simmons, P. Webb, P. Bellerby, N. Andrews, D. A. Hilton, J. W. Ironside, J. Beck, M. Poulter, S. Mead and S. Brandner (2013). "Prevalent abnormal prion protein in human appendixes after bovine spongiform encephalopathy epizootic: large scale survey." BMJ **347**: f5675.
Giri, R. K., R. Young, R. Pitstick, S. J. DeArmond, S. B. Prusiner and G. A. Carlson (2006). "Prion infection of mouse neurospheres." Proc Natl Acad Sci U S A **103**(10): 3875-3880.
Glenner, G. G. and C. W. Wong (1984). "Alzheimer's disease: initial report of the purification and characterization of a novel cerebrovascular amyloid protein." Biochem Biophys Res Commun **120**(3): 885-890.
Glynn, C., M. R. Sawaya, P. Ge, M. Gallagher-Jones, C. W. Short, R. Bowman, M. Apostol, Z. H. Zhou, D. S. Eisenberg and J. A. Rodriguez (2020). "Cryo-EM structure of a human prion fibril with a hydrophobic, protease-resistant core." Nat Struct Mol Biol **27**(5): 417-423.
Goldfarb, L. G., R. B. Petersen, M. Tabaton, P. Brown, A. C. LeBlanc, P. Montagna, P. Cortelli, J. Julien, C. Vital, W. W. Pendelbury and et al. (1992). "Fatal familial insomnia and familial Creutzfeldt-Jakob disease: disease phenotype determined by a DNA polymorphism." Science **258**(5083): 806-808.
Gopalan, S., A. Kasza, W. Xu, D. L. Kiss, K. M. Wilczynska, R. E. Rydel and T. Kordula (2005). "Astrocyte- and hepatocyte-specific expression of genes from the distal serpin subcluster at 14q32.1 associates with tissue-specific chromatin structures." J Neurochem **94**(3): 763-773.
Gossner, A. G. and J. Hopkins (2014). "Transcriptome analysis of CNS immediately before and after the detection of PrP(Sc) in SSBP/1 sheep scrapie." Vet Microbiol **173**(3-4): 201-207.
Groveman, B. R., N. C. Ferreira, S. T. Foliaki, R. O. Walters, C. W. Winkler, B. Race, A. G. Hughson, G. Zanusso and C. L. Haigh (2021). "Human cerebral organoids as a therapeutic drug screening model for Creutzfeldt-Jakob disease." Sci Rep **11**(1): 5165.
Groveman, B. R., S. T. Foliaki, C. D. Orru, G. Zanusso, J. A. Carroll, B. Race and C. L. Haigh (2019). "Sporadic Creutzfeldt-Jakob disease prion infection of human cerebral organoids." Acta Neuropathol Commun **7**(1): 90.
Gueugneau, M., D. d'Hose, C. Barbe, M. de Barsy, P. Lause, D. Maiter, L. B. Bindels, N. M. Delzenne, L. Schaeffer, Y. G. Gangloff, C. Chambon, C. Coudy-Gandilhon, D. Bechet and J. P. Thissen (2018). "Increased Serpina3n release into circulation during glucocorticoid-mediated muscle atrophy." J Cachexia Sarcopenia Muscle **9**(5): 929-946.
Haik, S., G. Marcon, A. Mallet, M. Tettamanti, A. Welaratne, G. Giaccone, S. Azimi, V. Pietrini, J. R. Fabreguettes, D. Imperiale, P. Cesaro, C. Buffa, C. Aucan, U. Lucca, L. Peckeu, S. Suardi, C. Tranchant, I. Zerr, C. Houillier, V. Redaelli, H. Vespignani, A. Campanella, F. Sellal, A. Krasnianski, D. Seilhean, U. Heinemann, F. Sedel, M. Canovi, M. Gobbi, G. Di Fede, J. L. Laplanche, M. Pocchiari, M. Salmona, G. Forloni, J. P. Brandel and F. Tagliavini (2014). "Doxycycline in Creutzfeldt-Jakob disease: a phase 2, randomised, double-blind, placebo-controlled trial." Lancet Neurol **13**(2): 150-158.
Hainfellner, J. A., S. Brantner-Inthaler, L. Cervenáková, P. Brown, T. Kitamoto, J. Tateishi, H. Diringer, P. P. Liberski, H. Regele and M. Feucht (1995). "The original Gerstmann-Sträussler-Scheinker family of Austria: divergent clinicopathological phenotypes but constant PrP genotype." Brain Pathol **5**(3): 201-211.
Halliez, S., B. Passet, S. Martin-Lannerée, J. Hernandez-Rapp, H. Laude, S. Mouillet-Richard, J. L. Vilotte and V. Béringue (2014). "To develop with or without the prion protein." Front Cell Dev Biol **2**: 58.
Head, M. W. and J. W. Ironside (2012). "Review: Creutzfeldt-Jakob disease: prion protein type, disease phenotype and agent strain." Neuropathol Appl Neurobiol **38**(4): 296-310.

Hebenstreit, D., M. Fang, M. Gu, V. Charoensawan, A. van Oudenaarden and S. A. Teichmann (2011). "RNA sequencing reveals two major classes of gene expression levels in metazoan cells." Mol Syst Biol **7**: 497.
Heit, C., B. C. Jackson, M. McAndrews, M. W. Wright, D. C. Thompson, G. A. Silverman, D. W. Nebert and V. Vasiliou (2013). "Update of the human and mouse SERPIN gene superfamily." Hum Genomics **7**: 22.
Heutinck, K. M., J. Kassies, S. Florquin, I. J. ten Berge, J. Hamann and A. T. Rowshani (2012). "SerpinB9 expression in human renal tubular epithelial cells is induced by triggering of the viral dsRNA sensors TLR3, MDA5 and RIG-I." Nephrol Dial Transplant **27**(7): 2746-2754.
Hill, A. F., M. Desbruslais, S. Joiner, K. C. Sidle, I. Gowland, J. Collinge, L. J. Doey and P. Lantos (1997). "The same prion strain causes vCJD and BSE." Nature **389**(6650): 448-450, 526.
Hilton, D. A. and J. W. Ironside (2003). "Screening for variant Creutzfeldt-Jakob disease." J Neurol Neurosurg Psychiatry **74**(6): 828-829.
Horvath, A. J., S. L. Forsyth and P. B. Coughlin (2004). "Expression patterns of murine antichymotrypsin-like genes reflect evolutionary divergence at the Serpina3 locus." J Mol Evol **59**(4): 488-497.
Horvath, A. J., J. A. Irving, J. Rossjohn, R. H. Law, S. P. Bottomley, N. S. Quinsey, R. N. Pike, P. B. Coughlin and J. C. Whisstock (2005). "The murine orthologue of human antichymotrypsin: a structural paradigm for clade A3 serpins." J Biol Chem **280**(52): 43168-43178.
Hou, Y., X. Dan, M. Babbar, Y. Wei, S. G. Hasselbalch, D. L. Croteau and V. A. Bohr (2019). "Ageing as a risk factor for neurodegenerative disease." Nat Rev Neurol **15**(10): 565-581.
Houston, F. and O. Andréoletti (2018). "The zoonotic potential of animal prion diseases." Handb Clin Neurol **153**: 447-462.
Hu, X., H. Zhang, Y. Zhang, Y. Zhang, L. Bai, Q. Chen, J. Wu and L. Zhang (2014). "Differential protein profile of PC12 cells exposed to proteasomal inhibitor lactacystin." Neurosci Lett **575**: 25-30.
Huntington, J. A. (2011). "Serpin structure, function and dysfunction." J Thromb Haemost **9 Suppl 1**: 26-34.
Hwang, D., I. Y. Lee, H. Yoo, N. Gehlenborg, J. H. Cho, B. Petritis, D. Baxter, R. Pitstick, R. Young, D. Spicer, N. D. Price, J. G. Hohmann, S. J. Dearmond, G. A. Carlson and L. E. Hood (2009). "A systems approach to prion disease." Mol Syst Biol **5**: 252.
Hwang, S. R., B. Steineckert, A. Kohn, M. Palkovits and V. Y. Hook (1999). "Molecular studies define the primary structure of alpha1-antichymotrypsin (ACT) protease inhibitor in Alzheimer's disease brains. Comparison of act in hippocampus and liver." J Biol Chem **274**(3): 1821-1827.
Hölscher, C., H. Delius and A. Bürkle (1998). "Overexpression of nonconvertible PrPc delta114-121 in scrapie-infected mouse neuroblastoma cells leads to trans-dominant inhibition of wild-type PrP(Sc) accumulation." J Virol **72**(2): 1153-1159.
Iadanza, M. G., M. P. Jackson, E. W. Hewitt, N. A. Ranson and S. E. Radford (2018). "A new era for understanding amyloid structures and disease." Nat Rev Mol Cell Biol **19**(12): 755-773.
Ianni, M., M. Manerba, G. Di Stefano, E. Porcellini, M. Chiappelli, I. Carbone and F. Licastro (2010). "Altered glycosylation profile of purified plasma ACT from Alzheimer's disease." Immun Ageing **7 Suppl 1**: S6.
Imran, M. and S. Mahmood (2011). "An overview of animal prion diseases." Virol J **8**: 493.
Imran, M. and S. Mahmood (2011). "An overview of human prion diseases." Virol J **8**: 559.
Irving, J. A., R. N. Pike, A. M. Lesk and J. C. Whisstock (2000). "Phylogeny of the serpin superfamily: implications of patterns of amino acid conservation for structure and function." Genome Res **10**(12): 1845-1864.

Ishibashi, M. (2006). "Standardization of prostate-specific antigen (PSA) assays: can interchangeability of PSA measurements be improved?" Clin Chem **52**(1): 1-2.
Jaul, E. and J. Barron (2017). "Age-Related Diseases and Clinical and Public Health Implications for the 85 Years Old and Over Population." Front Public Health **5**: 335.
Jendroska, K., F. P. Heinzel, M. Torchia, L. Stowring, H. A. Kretzschmar, A. Kon, A. Stern, S. B. Prusiner and S. J. DeArmond (1991). "Proteinase-resistant prion protein accumulation in Syrian hamster brain correlates with regional pathology and scrapie infectivity." Neurology **41**(9): 1482-1490.
Jiménez-Huete, A., P. M. Lievens, R. Vidal, P. Piccardo, B. Ghetti, F. Tagliavini, B. Frangione and F. Prelli (1998). "Endogenous proteolytic cleavage of normal and disease-associated isoforms of the human prion protein in neural and non-neural tissues." Am J Pathol **153**(5): 1561-1572.
Jucker, M. and L. C. Walker (2013). "Self-propagation of pathogenic protein aggregates in neurodegenerative diseases." Nature **501**(7465): 45-51.
Jucker, M. and L. C. Walker (2018). "Propagation and spread of pathogenic protein assemblies in neurodegenerative diseases." Nat Neurosci **21**(10): 1341-1349.
Kalsheker, N. A. (1996). "Alpha 1-antichymotrypsin." Int J Biochem Cell Biol **28**(9): 961-964.
Kamboh, M. I., D. K. Sanghera, R. E. Ferrell and S. T. DeKosky (1995). "APOE*4-associated Alzheimer's disease risk is modified by alpha 1-antichymotrypsin polymorphism." Nat Genet **10**(4): 486-488.
Kanaani, J., S. B. Prusiner, J. Diacovo, S. Baekkeskov and G. Legname (2005). "Recombinant prion protein induces rapid polarization and development of synapses in embryonic rat hippocampal neurons in vitro." J Neurochem **95**(5): 1373-1386.
Kane, M. D., W. J. Lipinski, M. J. Callahan, F. Bian, R. A. Durham, R. D. Schwarz, A. E. Roher and L. C. Walker (2000). "Evidence for seeding of beta -amyloid by intracerebral infusion of Alzheimer brain extracts in beta -amyloid precursor protein-transgenic mice." J Neurosci **20**(10): 3606-3611.
Kanemaru, K., B. Meckelein, D. C. Marshall, J. D. Sipe and C. R. Abraham (1996). "Synthesis and secretion of active alpha 1-antichymotrypsin by murine primary astrocytes." Neurobiol Aging **17**(5): 767-771.
Kim, M. O., L. T. Takada, K. Wong, S. A. Forner and M. D. Geschwind (2018). "Genetic PrP Prion Diseases." Cold Spring Harb Perspect Biol **10**(5).
Kimberlin, R. H. and C. A. Walker (1986). "Pathogenesis of scrapie (strain 263K) in hamsters infected intracerebrally, intraperitoneally or intraocularly." J Gen Virol **67 (Pt 2)**: 255-263.
Kinghorn, K. J., D. C. Crowther, L. K. Sharp, C. Nerelius, R. L. Davis, H. T. Chang, C. Green, D. C. Gubb, J. Johansson and D. A. Lomas (2006). "Neuroserpin binds Abeta and is a neuroprotective component of amyloid plaques in Alzheimer disease." J Biol Chem **281**(39): 29268-29277.
Knight, R. (2010). "The risk of transmitting prion disease by blood or plasma products." Transfus Apher Sci **43**(3): 387-391.
Kobayashi, A., K. Teruya, Y. Matsuura, T. Shirai, Y. Nakamura, M. Yamada, H. Mizusawa, S. Mohri and T. Kitamoto (2015). "The influence of PRNP polymorphisms on human prion disease susceptibility: an update." Acta Neuropathol **130**(2): 159-170.
Koo, E. H., C. R. Abraham, H. Potter, L. C. Cork and D. L. Price (1991). "Developmental expression of alpha 1-antichymotrypsin in brain may be related to astrogliosis." Neurobiol Aging **12**(5): 495-501.
Kordower, J. H., Y. Chu, R. A. Hauser, T. B. Freeman and C. W. Olanow (2008). "Lewy body-like pathology in long-term embryonic nigral transplants in Parkinson's disease." Nat Med **14**(5): 504-506.
Kordula, T., M. Bugno, R. E. Rydel and J. Travis (2000). "Mechanism of interleukin-1- and tumor necrosis factor alpha-dependent regulation of the alpha 1-antichymotrypsin gene in human astrocytes." J Neurosci **20**(20): 7510-7516.

Kordula, T., R. E. Rydel, E. F. Brigham, F. Horn, P. C. Heinrich and J. Travis (1998). "Oncostatin M and the interleukin-6 and soluble interleukin-6 receptor complex regulate alpha1-antichymotrypsin expression in human cortical astrocytes." J Biol Chem **273**(7): 4112-4118.
Kosik, K. S., C. L. Joachim and D. J. Selkoe (1986). "Microtubule-associated protein tau (tau) is a major antigenic component of paired helical filaments in Alzheimer disease." Proc Natl Acad Sci U S A **83**(11): 4044-4048.
Kovacs, G. G. and H. Budka (2009). "Molecular pathology of human prion diseases." Int J Mol Sci **10**(3): 976-999.
Kovacs, G. G., J. Seguin, I. Quadrio, R. Höftberger, I. Kapás, N. Streichenberger, A. G. Biacabe, D. Meyronet, R. Sciot, R. Vandenberghe, K. Majtenyi, L. László, T. Ströbel, H. Budka and A. Perret-Liaudet (2011). "Genetic Creutzfeldt-Jakob disease associated with the E200K mutation: characterization of a complex proteinopathy." Acta Neuropathol **121**(1): 39-57.
Kovács, G. G., M. Puopolo, A. Ladogana, M. Pocchiari, H. Budka, C. van Duijn, S. J. Collins, A. Boyd, A. Giulivi, M. Coulthart, N. Delasnerie-Laupretre, J. P. Brandel, I. Zerr, H. A. Kretzschmar, J. de Pedro-Cuesta, M. Calero-Lara, M. Glatzel, A. Aguzzi, M. Bishop, R. Knight, G. Belay, R. Will, E. Mitrova and EUROCJD (2005). "Genetic prion disease: the EUROCJD experience." Hum Genet **118**(2): 166-174.
Kraus, A., F. Hoyt, C. L. Schwartz, B. Hansen, E. Artikis, A. G. Hughson, G. J. Raymond, B. Race, G. S. Baron and B. Caughey (2021). "High-resolution structure and strain comparison of infectious mammalian prions." Mol Cell.
Krem, M. M. and E. Di Cera (2003). "Conserved Ser residues, the shutter region, and speciation in serpin evolution." J Biol Chem **278**(39): 37810-37814.
Kretzschmar, H. A., M. Neumann and D. Stavrou (1995). "Codon 178 mutation of the human prion protein gene in a German family (Backer family): sequencing data from 72-year-old celloidin-embedded brain tissue." Acta Neuropathol **89**(1): 96-98.
Kuwata, K., N. Nishida, T. Matsumoto, Y. O. Kamatari, J. Hosokawa-Muto, K. Kodama, H. K. Nakamura, K. Kimura, M. Kawasaki, Y. Takakura, S. Shirabe, J. Takata, Y. Kataoka and S. Katamine (2007). "Hot spots in prion protein for pathogenic conversion." Proc Natl Acad Sci U S A **104**(29): 11921-11926.
Lasmézas, C. I., J. P. Deslys, R. Demaimay, K. T. Adjou, F. Lamoury, D. Dormont, O. Robain, J. Ironside and J. J. Hauw (1996). "BSE transmission to macaques." Nature **381**(6585): 743-744.
Laurén, J., D. A. Gimbel, H. B. Nygaard, J. W. Gilbert and S. M. Strittmatter (2009). "Cellular prion protein mediates impairment of synaptic plasticity by amyloid-beta oligomers." Nature **457**(7233): 1128-1132.
Law, R. H., Q. Zhang, S. McGowan, A. M. Buckle, G. A. Silverman, W. Wong, C. J. Rosado, C. G. Langendorf, R. N. Pike, P. I. Bird and J. C. Whisstock (2006). "An overview of the serpin superfamily." Genome Biol **7**(5): 216.
Lawson, V. A., S. J. Collins, C. L. Masters and A. F. Hill (2005). "Prion protein glycosylation." J Neurochem **93**(4): 793-801.
Le Pichon, C. E., M. T. Valley, M. Polymenidou, A. T. Chesler, B. T. Sagdullaev, A. Aguzzi and S. Firestein (2009). "Olfactory behavior and physiology are disrupted in prion protein knockout mice." Nat Neurosci **12**(1): 60-69.
Lebeurrier, N., S. Launay, R. Macrez, E. Maubert, H. Legros, A. Leclerc, S. P. Jamin, J. Y. Picard, S. Marret, V. Laudenbach, P. Berger, P. Sonderegger, C. Ali, N. di Clemente and D. Vivien (2008). "Anti-Mullerian-hormone-dependent regulation of the brain serine-protease inhibitor neuroserpin." J Cell Sci **121**(Pt 20): 3357-3365.

Lee, T. W., V. W. Tsang and N. P. Birch (2015). "Physiological and pathological roles of tissue plasminogen activator and its inhibitor neuroserpin in the nervous system." Front Cell Neurosci **9**: 396.
Legname, G. (2017). "Elucidating the function of the prion protein." PLoS Pathog **13**(8): e1006458.
Leinonen, J., T. Lovgren, T. Vornanen and U. H. Stenman (1993). "Double-label time-resolved immunofluorometric assay of prostate-specific antigen and of its complex with alpha 1-antichymotrypsin." Clin Chem **39**(10): 2098-2103.
Lewis, V., V. A. Johanssen, P. J. Crouch, G. M. Klug, N. M. Hooper and S. J. Collins (2016). "Prion protein "gamma-cleavage": characterizing a novel endoproteolytic processing event." Cell Mol Life Sci **73**(3): 667-683.
Li, J. Y., E. Englund, J. L. Holton, D. Soulet, P. Hagell, A. J. Lees, T. Lashley, N. P. Quinn, S. Rehncrona, A. Björklund, H. Widner, T. Revesz, O. Lindvall and P. Brundin (2008). "Lewy bodies in grafted neurons in subjects with Parkinson's disease suggest host-to-graft disease propagation." Nat Med **14**(5): 501-503.
Liberski, P. P. (2012). "Historical overview of prion diseases: a view from afar." Folia Neuropathol **50**(1): 1-12.
Licastro, F., I. L. Campbell, C. Kincaid, I. Veinbergs, E. Van Uden, E. Rockenstein, M. Mallory, J. R. Gilbert and E. Masliah (1999). "A role for apoE in regulating the levels of alpha-1-antichymotrypsin in the aging mouse brain and in Alzheimer's disease." Am J Pathol **155**(3): 869-875.
Liddelow, S. A. and B. A. Barres (2017). "Reactive Astrocytes: Production, Function, and Therapeutic Potential." Immunity **46**(6): 957-967.
Lino, M. M., S. Atanasoski, M. Kvajo, B. Fayard, E. Moreno, H. R. Brenner, U. Suter and D. Monard (2007). "Mice lacking protease nexin-1 show delayed structural and functional recovery after sciatic nerve crush." J Neurosci **27**(14): 3677-3685.
Linsenmeier, L., H. C. Altmeppen, S. Wetzel, B. Mohammadi, P. Saftig and M. Glatzel (2017). "Diverse functions of the prion protein - Does proteolytic processing hold the key?" Biochim Biophys Acta Mol Cell Res **1864**(11 Pt B): 2128-2137.
Livak, K. J. and T. D. Schmittgen (2001). "Analysis of relative gene expression data using real-time quantitative PCR and the 2(-Delta Delta C(T)) Method." Methods **25**(4): 402-408.
Lomas, D. A., D. L. Evans, J. T. Finch and R. W. Carrell (1992). "The mechanism of Z alpha 1-antitrypsin accumulation in the liver." Nature **357**(6379): 605-607.
Lugaresi, E., R. Medori, P. Montagna, A. Baruzzi, P. Cortelli, A. Lugaresi, P. Tinuper, M. Zucconi and P. Gambetti (1986). "Fatal familial insomnia and dysautonomia with selective degeneration of thalamic nuclei." N Engl J Med **315**(16): 997-1003.
Mackay, G. A., R. S. Knight and J. W. Ironside (2011). "The molecular epidemiology of variant CJD." Int J Mol Epidemiol Genet **2**(3): 217-227.
Maiti, N. R. and W. K. Surewicz (2001). "The role of disulfide bridge in the folding and stability of the recombinant human prion protein." J Biol Chem **276**(4): 2427-2431.
Makarava, N., J. C. Chang, R. Kushwaha and I. V. Baskakov (2019). "Region-Specific Response of Astrocytes to Prion Infection." Front Neurosci **13**: 1048.
Maley, F., R. B. Trimble, A. L. Tarentino and T. H. Plummer (1989). "Characterization of glycoproteins and their associated oligosaccharides through the use of endoglycosidases." Anal Biochem **180**(2): 195-204.
Maltseva, D. V., N. A. Khaustova, N. N. Fedotov, E. O. Matveeva, A. E. Lebedev, M. U. Shkurnikov, V. V. Galatenko, U. Schumacher and A. G. Tonevitsky (2013). "High-throughput identification of reference genes for research and clinical RT-qPCR analysis of breast cancer samples." J Clin Bioinforma **3**(1): 13.

Mammana, A., S. Baiardi, M. Rossi, A. Franceschini, V. Donadio, S. Capellari, B. Caughey and P. Parchi (2020). "Detection of prions in skin punch biopsies of Creutzfeldt-Jakob disease patients." Ann Clin Transl Neurol **7**(4): 559-564.
Manix, M., P. Kalakoti, M. Henry, J. Thakur, R. Menger, B. Guthikonda and A. Nanda (2015). "Creutzfeldt-Jakob disease: updated diagnostic criteria, treatment algorithm, and the utility of brain biopsy." Neurosurg Focus **39**(5): E2.
Manni, G., V. Lewis, M. Senesi, G. Spagnolli, F. Fallarino, S. J. Collins, S. Mouillet-Richard and E. Biasini (2020). "The cellular prion protein beyond prion diseases." Swiss Med Wkly **150**: w20222.
Mastrianni, J. A., M. T. Curtis, J. C. Oberholtzer, M. M. Da Costa, S. DeArmond, S. B. Prusiner and J. Y. Garbern (1995). "Prion disease (PrP-A117V) presenting with ataxia instead of dementia." Neurology **45**(11): 2042-2050.
Matsuzaki, S., K. Iwamura, M. Itakura, H. Kamiguchi and T. Katsunuma (1981). "A clinical evaluation of serum alpha-1-antichymotrypsin levels in liver disease and cancers." Gastroenterol Jpn **16**(6): 582-591.
Mays, C. E. and C. Ryou (2011). "Plasminogen: A cellular protein cofactor for PrPSc propagation." Prion **5**(1): 22-27.
McDonald, A. J., J. P. Dibble, E. G. Evans and G. L. Millhauser (2014). "A new paradigm for enzymatic control of α-cleavage and β-cleavage of the prion protein." J Biol Chem **289**(2): 803-813.
McMahon, H. E., A. Mangé, N. Nishida, C. Créminon, D. Casanova and S. Lehmann (2001). "Cleavage of the amino terminus of the prion protein by reactive oxygen species." J Biol Chem **276**(3): 2286-2291.
Mead, S. (2006). "Prion disease genetics." Eur J Hum Genet **14**(3): 273-281.
Mead, S., J. Whitfield, M. Poulter, P. Shah, J. Uphill, T. Campbell, H. Al-Dujaily, H. Hummerich, J. Beck, C. A. Mein, C. Verzilli, J. Whittaker, M. P. Alpers and J. Collinge (2009). "A novel protective prion protein variant that colocalizes with kuru exposure." N Engl J Med **361**(21): 2056-2065.
Merz, P. A., R. A. Somerville, H. M. Wisniewski, L. Manuelidis and E. E. Manuelidis (1983). "Scrapie-associated fibrils in Creutzfeldt-Jakob disease." Nature **306**(5942): 474-476.
Miele, G., H. Seeger, D. Marino, R. Eberhard, M. Heikenwalder, K. Stoeck, M. Basagni, R. Knight, A. Green, F. Chianini, R. P. Wuthrich, C. Hock, I. Zerr and A. Aguzzi (2008). "Urinary alpha1-antichymotrypsin: a biomarker of prion infection." PLoS One **3**(12): e3870.
Mills, J. D., M. Ward, W. S. Kim, G. M. Halliday and M. Janitz (2016). "Strand-specific RNA-sequencing analysis of multiple system atrophy brain transcriptome." Neuroscience **322**: 234-250.
Minikel, E. V., S. M. Vallabh, M. Lek, K. Estrada, K. E. Samocha, J. F. Sathirapongsasuti, C. Y. McLean, J. Y. Tung, L. P. Yu, P. Gambetti, J. Blevins, S. Zhang, Y. Cohen, W. Chen, M. Yamada, T. Hamaguchi, N. Sanjo, H. Mizusawa, Y. Nakamura, T. Kitamoto, S. J. Collins, A. Boyd, R. G. Will, R. Knight, C. Ponto, I. Zerr, T. F. Kraus, S. Eigenbrod, A. Giese, M. Calero, J. de Pedro-Cuesta, S. Haïk, J. L. Laplanche, E. Bouaziz-Amar, J. P. Brandel, S. Capellari, P. Parchi, A. Poleggi, A. Ladogana, A. H. O'Donnell-Luria, K. J. Karczewski, J. L. Marshall, M. Boehnke, M. Laakso, K. L. Mohlke, A. Kähler, K. Chambert, S. McCarroll, P. F. Sullivan, C. M. Hultman, S. M. Purcell, P. Sklar, S. J. van der Lee, A. Rozemuller, C. Jansen, A. Hofman, R. Kraaij, J. G. van Rooij, M. A. Ikram, A. G. Uitterlinden, C. M. van Duijn, M. J. Daly, D. G. MacArthur and E. A. C. (ExAC) (2016). "Quantifying prion disease penetrance using large population control cohorts." Sci Transl Med **8**(322): 322ra329.
Miranda, E., K. Romisch and D. A. Lomas (2004). "Mutants of neuroserpin that cause dementia accumulate as polymers within the endoplasmic reticulum." J Biol Chem **279**(27): 28283-28291.
Moda, F., P. Gambetti, S. Notari, L. Concha-Marambio, M. Catania, K. W. Park, E. Maderna, S. Suardi, S. Haïk, J. P. Brandel, J. Ironside, R. Knight, F. Tagliavini and C. Soto (2014). "Prions in the urine of patients with variant Creutzfeldt-Jakob disease." N Engl J Med **371**(6): 530-539.

Mok, T., Z. Jaunmuktane, S. Joiner, T. Campbell, C. Morgan, B. Wakerley, F. Golestani, P. Rudge, S. Mead, H. R. Jager, J. D. Wadsworth, S. Brandner and J. Collinge (2017). "Variant Creutzfeldt-Jakob Disease in a Patient with Heterozygosity at PRNP Codon 129." N Engl J Med **376**(3): 292-294.
Monari, L., S. G. Chen, P. Brown, P. Parchi, R. B. Petersen, J. Mikol, F. Gray, P. Cortelli, P. Montagna and B. Ghetti (1994). "Fatal familial insomnia and familial Creutzfeldt-Jakob disease: different prion proteins determined by a DNA polymorphism." Proc Natl Acad Sci U S A **91**(7): 2839-2842.
Moore, R. A., I. Vorberg and S. A. Priola (2005). "Species barriers in prion diseases--brief review." Arch Virol Suppl(19): 187-202.
Morales, R. (2017). "Prion strains in mammals: Different conformations leading to disease." PLoS Pathog **13**(7): e1006323.
Morales, R., K. Abid and C. Soto (2007). "The prion strain phenomenon: molecular basis and unprecedented features." Biochim Biophys Acta **1772**(6): 681-691.
Mottonen, J., A. Strand, J. Symersky, R. M. Sweet, D. E. Danley, K. F. Geoghegan, R. D. Gerard and E. J. Goldsmith (1992). "Structural basis of latency in plasminogen activator inhibitor-1." Nature **355**(6357): 270-273.
Mouillet-Richard, S., M. Ermonval, C. Chebassier, J. L. Laplanche, S. Lehmann, J. M. Launay and O. Kellermann (2000). "Signal transduction through prion protein." Science **289**(5486): 1925-1928.
Muthukumar, T., R. Ding, D. Dadhania, M. Medeiros, B. Li, V. K. Sharma, C. Hartono, D. Serur, S. V. Seshan, H. D. Volk, P. Reinke, S. Kapur and M. Suthanthiran (2003). "Serine proteinase inhibitor-9, an endogenous blocker of granzyme B/perforin lytic pathway, is hyperexpressed during acute rejection of renal allografts." Transplantation **75**(9): 1565-1570.
Nagai, N., M. Hosokawa, S. Itohara, E. Adachi, T. Matsushita, N. Hosokawa and K. Nagata (2000). "Embryonic lethality of molecular chaperone hsp47 knockout mice is associated with defects in collagen biosynthesis." J Cell Biol **150**(6): 1499-1506.
Nemani, S. K., J. L. Myskiw, L. Lamoureux, S. A. Booth and V. L. Sim (2020). "Exposure Risk of Chronic Wasting Disease in Humans." Viruses **12**(12).
Neumann, M., D. M. Sampathu, L. K. Kwong, A. C. Truax, M. C. Micsenyi, T. T. Chou, J. Bruce, T. Schuck, M. Grossman, C. M. Clark, L. F. McCluskey, B. L. Miller, E. Masliah, I. R. Mackenzie, H. Feldman, W. Feiden, H. A. Kretzschmar, J. Q. Trojanowski and V. M. Lee (2006). "Ubiquitinated TDP-43 in frontotemporal lobar degeneration and amyotrophic lateral sclerosis." Science **314**(5796): 130-133.
Nishida, N., D. A. Harris, D. Vilette, H. Laude, Y. Frobert, J. Grassi, D. Casanova, O. Milhavet and S. Lehmann (2000). "Successful transmission of three mouse-adapted scrapie strains to murine neuroblastoma cell lines overexpressing wild-type mouse prion protein." J Virol **74**(1): 320-325.
Nonno, R., M. A. Di Bari, F. Cardone, G. Vaccari, P. Fazzi, G. Dell'Omo, C. Cartoni, L. Ingrosso, A. Boyle, R. Galeno, M. Sbriccoli, H. P. Lipp, M. Bruce, M. Pocchiari and U. Agrimi (2006). "Efficient transmission and characterization of Creutzfeldt-Jakob disease strains in bank voles." PLoS Pathog **2**(2): e12.
Notari, S., B. S. Appleby and P. Gambetti (2018). "Variably protease-sensitive prionopathy." Handb Clin Neurol **153**: 175-190.
Nuvolone, M., N. Schmid, G. Miele, S. Sorce, R. Moos, C. Schori, R. R. Beerli, M. Bauer, P. Saudan, K. Dietmeier, I. Lachmann, M. Linnebank, R. Martin, U. Kallweit, V. Kana, E. J. Rushing, H. Budka and A. Aguzzi (2017). "Cystatin F is a biomarker of prion pathogenesis in mice." PLoS One **12**(2): e0171923.
Olson, S. T. and P. G. Gettins (2011). "Regulation of proteases by protein inhibitors of the serpin superfamily." Prog Mol Biol Transl Sci **99**: 185-240.

Orr, H. T., M. Y. Chung, S. Banfi, T. J. Kwiatkowski, A. Servadio, A. L. Beaudet, A. E. McCall, L. A. Duvick, L. P. Ranum and H. Y. Zoghbi (1993). "Expansion of an unstable trinucleotide CAG repeat in spinocerebellar ataxia type 1." Nat Genet **4**(3): 221-226.
Orrú, C. D., M. Bongianni, G. Tonoli, S. Ferrari, A. G. Hughson, B. R. Groveman, M. Fiorini, M. Pocchiari, S. Monaco, B. Caughey and G. Zanusso (2014). "A test for Creutzfeldt-Jakob disease using nasal brushings." N Engl J Med **371**(6): 519-529.
Orrú, C. D., J. Yuan, B. S. Appleby, B. Li, Y. Li, D. Winner, Z. Wang, Y. A. Zhan, M. Rodgers, J. Rarick, R. E. Wyza, T. Joshi, G. X. Wang, M. L. Cohen, S. Zhang, B. R. Groveman, R. B. Petersen, J. W. Ironside, M. E. Quiñones-Mateu, J. G. Safar, Q. Kong, B. Caughey and W. Q. Zou (2017). "Prion seeding activity and infectivity in skin samples from patients with sporadic Creutzfeldt-Jakob disease." Sci Transl Med **9**(417).
Osterholm, M. T., C. J. Anderson, M. D. Zabel, J. M. Scheftel, K. A. Moore and B. S. Appleby (2019). "Chronic Wasting Disease in Cervids: Implications for Prion Transmission to Humans and Other Animal Species." mBio **10**(4).
Padmanabhan, J., M. Levy, D. W. Dickson and H. Potter (2006). "Alpha1-antichymotrypsin, an inflammatory protein overexpressed in Alzheimer's disease brain, induces tau phosphorylation in neurons." Brain **129**(Pt 11): 3020-3034.
Pan, K. M., M. Baldwin, J. Nguyen, M. Gasset, A. Serban, D. Groth, I. Mehlhorn, Z. Huang, R. J. Fletterick, F. E. Cohen and et al. (1993). "Conversion of alpha-helices into beta-sheets features in the formation of the scrapie prion proteins." Proc Natl Acad Sci U S A **90**(23): 10962-10966.
Papadimitriou, C. S., H. Stein and N. X. Papacharalampous (1980). "Presence of alpha1-antichymotrypsin and alpha1-antitrypsin in haematopoietic and lymphoid tissue cells as revealed by the immunoperoxidase method." Pathol Res Pract **169**(3-4): 287-297.
Pappalardo, E., L. C. Zingale and M. Cicardi (2004). "C1 inhibitor gene expression in patients with hereditary angioedema: quantitative evaluation by means of real-time RT-PCR." J Allergy Clin Immunol **114**(3): 638-644.
Parchi, P., R. Castellani, P. Cortelli, P. Montagna, S. G. Chen, R. B. Petersen, V. Manetto, C. L. Vnencak-Jones, M. J. McLean and J. R. Sheller (1995). "Regional distribution of protease-resistant prion protein in fatal familial insomnia." Ann Neurol **38**(1): 21-29.
Parchi, P., A. Giese, S. Capellari, P. Brown, W. Schulz-Schaeffer, O. Windl, I. Zerr, H. Budka, N. Kopp, P. Piccardo, S. Poser, A. Rojiani, N. Streichemberger, J. Julien, C. Vital, B. Ghetti, P. Gambetti and H. Kretzschmar (1999). "Classification of sporadic Creutzfeldt-Jakob disease based on molecular and phenotypic analysis of 300 subjects." Ann Neurol **46**(2): 224-233.
Pasternack, J. M., C. R. Abraham, B. J. Van Dyke, H. Potter and S. G. Younkin (1989). "Astrocytes in Alzheimer's disease gray matter express alpha 1-antichymotrypsin mRNA." Am J Pathol **135**(5): 827-834.
Patterson C, “World Alzheimer report 2018.” Alzheimer's Disease International, London, 2018
Pattison, J. (1998). "The emergence of bovine spongiform encephalopathy and related diseases." Emerg Infect Dis **4**(3): 390-394.
Peng, C., J. Q. Trojanowski and V. M. Lee (2020). "Protein transmission in neurodegenerative disease." Nat Rev Neurol **16**(4): 199-212.
Penna, I., S. Vella, A. Gigoni, C. Russo, R. Cancedda and A. Pagano (2011). "Selection of candidate housekeeping genes for normalization in human postmortem brain samples." Int J Mol Sci **12**(9): 5461-5470.
Perini, F., R. Vidal, B. Ghetti, F. Tagliavini, B. Frangione and F. Prelli (1996). "PrP27-30 is a normal soluble prion protein fragment released by human platelets." Biochem Biophys Res Commun **223**(3): 572-577.

Petsch, B., A. Müller-Schiffmann, A. Lehle, E. Zirdum, I. Prikulis, F. Kuhn, A. J. Raeber, J. W. Ironside, C. Korth and L. Stitz (2011). "Biological effects and use of PrPSc- and PrP-specific antibodies generated by immunization with purified full-length native mouse prions." J Virol **85**(9): 4538-4546.
Porcellini, E., E. J. Davis, M. Chiappelli, E. Ianni, G. Di Stefano, P. Forti, G. Ravaglia and F. Licastro (2008). "Elevated plasma levels of alpha-1-anti-chymotrypsin in age-related cognitive decline and Alzheimer's disease: a potential therapeutic target." Curr Pharm Des **14**(26): 2659-2664.
Prusiner, S. B. (1982). "Novel proteinaceous infectious particles cause scrapie." Science **216**(4542): 136-144.
Prusiner, S. B. (1991). "Molecular biology of prion diseases." Science **252**(5012): 1515-1522.
Prusiner, S. B. (1998). "Prions." Proc Natl Acad Sci U S A **95**(23): 13363-13383.
Prusiner, S. B. (2012). "Cell biology. A unifying role for prions in neurodegenerative diseases." Science **336**(6088): 1511-1513.
Prusiner, S. B. (2013). "Biology and genetics of prions causing neurodegeneration." Annu Rev Genet **47**: 601-623.
Prusiner, S. B., M. P. McKinley, K. A. Bowman, D. C. Bolton, P. E. Bendheim, D. F. Groth and G. G. Glenner (1983). "Scrapie prions aggregate to form amyloid-like birefringent rods." Cell **35**(2 Pt 1): 349-358.
Puckett, C., P. Concannon, C. Casey and L. Hood (1991). "Genomic structure of the human prion protein gene." Am J Hum Genet **49**(2): 320-329.
Puoti, G., A. Bizzi, G. Forloni, J. G. Safar, F. Tagliavini and P. Gambetti (2012). "Sporadic human prion diseases: molecular insights and diagnosis." Lancet Neurol **11**(7): 618-628.
Race, B., K. Williams, C. D. Orru, A. G. Hughson, L. Lubke and B. Chesebro (2018). "Lack of Transmission of Chronic Wasting Disease to Cynomolgus Macaques." J Virol **92**(14).
Ramskold, D., E. T. Wang, C. B. Burge and R. Sandberg (2009). "An abundance of ubiquitously expressed genes revealed by tissue transcriptome sequence data." PLoS Comput Biol **5**(12): e1000598.
Rao, D. D., J. S. Vorhies, N. Senzer and J. Nemunaitis (2009). "siRNA vs. shRNA: similarities and differences." Adv Drug Deliv Rev **61**(9): 746-759.
Rau, J. C., C. Deans, M. R. Hoffman, D. B. Thomas, G. T. Malcom, A. W. Zieske, J. P. Strong, G. G. Koch and F. C. Church (2009). "Heparin cofactor II in atherosclerotic lesions from the Pathobiological Determinants of Atherosclerosis in Youth (PDAY) study." Exp Mol Pathol **87**(3): 178-183.
Raymond, G. J., H. T. Zhao, B. Race, L. D. Raymond, K. Williams, E. E. Swayze, S. Graffam, J. Le, T. Caron, J. Stathopoulos, R. O'Keefe, L. L. Lubke, A. G. Reidenbach, A. Kraus, S. L. Schreiber, C. Mazur, D. E. Cabin, J. B. Carroll, E. V. Minikel, H. Kordasiewicz, B. Caughey and S. M. Vallabh (2019). "Antisense oligonucleotides extend survival of prion-infected mice." JCI Insight **5**.
Reis, P. P., L. Waldron, R. S. Goswami, W. Xu, Y. Xuan, B. Perez-Ordonez, P. Gullane, J. Irish, I. Jurisica and S. Kamel-Reid (2011). "mRNA transcript quantification in archival samples using multiplexed, color-coded probes." BMC Biotechnol **11**: 46.
Resenberger, U. K., A. Harmeier, A. C. Woerner, J. L. Goodman, V. Müller, R. Krishnan, R. M. Vabulas, H. A. Kretzschmar, S. Lindquist, F. U. Hartl, G. Multhaup, K. F. Winklhofer and J. Tatzelt (2011). "The cellular prion protein mediates neurotoxic signalling of β-sheet-rich conformers independent of prion replication." EMBO J **30**(10): 2057-2070.
Rieger, R., F. Edenhofer, C. I. Lasmézas and S. Weiss (1997). "The human 37-kDa laminin receptor precursor interacts with the prion protein in eukaryotic cells." Nat Med **3**(12): 1383-1388.

Riemer, C., S. Neidhold, M. Burwinkel, A. Schwarz, J. Schultz, J. Kratzschmar, U. Monning and M. Baier (2004). "Gene expression profiling of scrapie-infected brain tissue." Biochem Biophys Res Commun **323**(2): 556-564.
Ritchie, D. L. and M. A. Barria (2021). "Prion Diseases: A Unique Transmissible Agent or a Model for Neurodegenerative Diseases?" Biomolecules **11**(2).
Saborio, G. P., B. Permanne and C. Soto (2001). "Sensitive detection of pathological prion protein by cyclic amplification of protein misfolding." Nature **411**(6839): 810-813.
Safdar, H., K. L. Cheung, H. L. Vos, F. J. Gonzalez, P. H. Reitsma, Y. Inoue and B. J. van Vlijmen (2012). "Modulation of mouse coagulation gene transcription following acute in vivo delivery of synthetic small interfering RNAs targeting HNF4alpha and C/EBPalpha." PLoS One **7**(6): e38104.
Sanfilippo, C., A. Longo, F. Lazzara, D. Cambria, G. Distefano, M. Palumbo, A. Cantarella, L. Malaguarnera and M. Di Rosa (2017). "CHI3L1 and CHI3L2 overexpression in motor cortex and spinal cord of sALS patients." Mol Cell Neurosci **85**: 162-169.
Santuccione, A., V. Sytnyk, I. Leshchyns'ka and M. Schachner (2005). "Prion protein recruits its neuronal receptor NCAM to lipid rafts to activate p59fyn and to enhance neurite outgrowth." J Cell Biol **169**(2): 341-354.
Sarkar, A. and P. L. Wintrode (2011). "Effects of glycosylation on the stability and flexibility of a metastable protein: the human serpin α(1)-antitrypsin." Int J Mass Spectrom **302**(1-3): 69-75.
Scarff, K. L., K. S. Ung, H. Nandurkar, P. J. Crack, C. H. Bird and P. I. Bird (2004). "Targeted disruption of SPI3/Serpinb6 does not result in developmental or growth defects, leukocyte dysfunction, or susceptibility to stroke." Mol Cell Biol **24**(9): 4075-4082.
Schmitt-Ulms, G., G. Legname, M. A. Baldwin, H. L. Ball, N. Bradon, P. J. Bosque, K. L. Crossin, G. M. Edelman, S. J. DeArmond, F. E. Cohen and S. B. Prusiner (2001). "Binding of neural cell adhesion molecules (N-CAMs) to the cellular prion protein." J Mol Biol **314**(5): 1209-1225.
Schmitz, M., K. Dittmar, F. Llorens, E. Gelpi, I. Ferrer, W. J. Schulz-Schaeffer and I. Zerr (2016). "Hereditary Human Prion Diseases: an Update." Mol Neurobiol.
Schätzl, H. M., L. Laszlo, D. M. Holtzman, J. Tatzelt, S. J. DeArmond, R. I. Weiner, W. C. Mobley and S. B. Prusiner (1997). "A hypothalamic neuronal cell line persistently infected with scrapie prions exhibits apoptosis." J Virol **71**(11): 8821-8831.
Sergi, D., F. M. Campbell, C. Grant, A. C. Morris, E. M. Bachmair, C. Koch, F. H. McLean, A. Muller, N. Hoggard, B. de Roos, B. Porteiro, M. V. Boekschoten, F. C. McGillicuddy, D. Kahn, P. Nicol, J. Benzler, C. D. Mayer, J. E. Drew, H. M. Roche, M. Muller, R. Nogueiras, C. Dieguez, A. Tups and L. M. Williams (2018). "SerpinA3N is a novel hypothalamic gene upregulated by a high-fat diet and leptin in mice." Genes Nutr **13**: 28.
Silveira, J. R., G. J. Raymond, A. G. Hughson, R. E. Race, V. L. Sim, S. F. Hayes and B. Caughey (2005). "The most infectious prion protein particles." Nature **437**(7056): 257-261.
Silverman, G. A., P. I. Bird, R. W. Carrell, F. C. Church, P. B. Coughlin, P. G. Gettins, J. A. Irving, D. A. Lomas, C. J. Luke, R. W. Moyer, P. A. Pemberton, E. Remold-O'Donnell, G. S. Salvesen, J. Travis and J. C. Whisstock (2001). "The serpins are an expanding superfamily of structurally similar but functionally diverse proteins. Evolution, mechanism of inhibition, novel functions, and a revised nomenclature." J Biol Chem **276**(36): 33293-33296.
Sipione, S., K. C. Simmen, S. J. Lord, B. Motyka, C. Ewen, I. Shostak, G. R. Rayat, J. M. Dufour, G. S. Korbutt, R. V. Rajotte and R. C. Bleackley (2006). "Identification of a novel human granzyme B inhibitor secreted by cultured sertoli cells." J Immunol **177**(8): 5051-5058.
Slapšak, U., G. Salzano, L. Amin, R. N. Abskharon, G. Ilc, B. Zupančič, I. Biljan, J. Plavec, G. Giachin and G. Legname (2016). "The N Terminus of the Prion Protein Mediates Functional Interactions with the Neuronal Cell Adhesion Molecule (NCAM) Fibronectin Domain." J Biol Chem **291**(42): 21857-21868.

Smith, H. L., O. J. Freeman, A. J. Butcher, S. Holmqvist, I. Humoud, T. Schätzl, D. T. Hughes, N. C. Verity, D. P. Swinden, J. Hayes, L. de Weerd, D. H. Rowitch, R. J. M. Franklin and G. R. Mallucci (2020). "Astrocyte Unfolded Protein Response Induces a Specific Reactivity State that Causes Non-Cell-Autonomous Neuronal Degeneration." Neuron **105**(5): 855-866.e855.
Spagnolli, G., M. Rigoli, S. Orioli, A. M. Sevillano, P. Faccioli, H. Wille, E. Biasini and J. R. Requena (2019). "Full atomistic model of prion structure and conversion." PLoS Pathog **15**(7): e1007864.
Spencer, M. D., R. S. Knight and R. G. Will (2002). "First hundred cases of variant Creutzfeldt-Jakob disease: retrospective case note review of early psychiatric and neurological features." BMJ **324**(7352): 1479-1482.
Spillantini, M. G., R. A. Crowther, R. Jakes, N. J. Cairns, P. L. Lantos and M. Goedert (1998). "Filamentous alpha-synuclein inclusions link multiple system atrophy with Parkinson's disease and dementia with Lewy bodies." Neurosci Lett **251**(3): 205-208.
Stahl, N., D. R. Borchelt, K. Hsiao and S. B. Prusiner (1987). "Scrapie prion protein contains a phosphatidylinositol glycolipid." Cell **51**(2): 229-240.
Steele, A. D., J. G. Emsley, P. H. Ozdinler, S. Lindquist and J. D. Macklis (2006). "Prion protein (PrPc) positively regulates neural precursor proliferation during developmental and adult mammalian neurogenesis." Proc Natl Acad Sci U S A **103**(9): 3416-3421.
Stopschinski, B. E. and M. I. Diamond (2017). "The prion model for progression and diversity of neurodegenerative diseases." Lancet Neurol **16**(4): 323-332.
Stratikos, E. and P. G. Gettins (1999). "Formation of the covalent serpin-proteinase complex involves translocation of the proteinase by more than 70 A and full insertion of the reactive center loop into beta-sheet A." Proc Natl Acad Sci U S A **96**(9): 4808-4813.
Sweeney, P., H. Park, M. Baumann, J. Dunlop, J. Frydman, R. Kopito, A. McCampbell, G. Leblanc, A. Venkateswaran, A. Nurmi and R. Hodgson (2017). "Protein misfolding in neurodegenerative diseases: implications and strategies." Transl Neurodegener **6**: 6.
Tachikawa, H., M. Tsuda, K. Onoe, M. Ueno, S. Takagi and Y. Shinohara (2001). "alpha-1-Antichymotrypsin gene A1252G variant (ACT Isehara-1) is associated with a lacunar type of ischemic cerebrovascular disease." J Hum Genet **46**(1): 45-47.
Tagliavini, F., F. Prelli, M. Porro, M. Salmona, O. Bugiani and B. Frangione (1992). "A soluble form of prion protein in human cerebrospinal fluid: implications for prion-related encephalopathies." Biochem Biophys Res Commun **184**(3): 1398-1404.
Tahir, W., B. Abdulrahman, D. H. Abdelaziz, S. Thapa, R. Walia and H. M. Schatzl (2020). "An astrocyte cell line that differentially propagates murine prions." J Biol Chem **295**(33): 11572-11583.
Takada, L. T., M. O. Kim, S. Metcalf, I. Gala and M. D. Geschwind (2018). "Prion disease." Handb Clin Neurol **148**: 441-464.
Takada, S., M. Tsuda, M. Matsumoto, S. Fujinami, M. Yamamura and T. Katsunuma (1988). "Incorporation of alpha-1-antichymotrypsin into human stomach adenocarcinoma cell nuclei and inhibition of DNA primase activity." Tokai J Exp Clin Med **13**(6): 321-327.
Tamgüney, G., K. Giles, E. Bouzamondo-Bernstein, P. J. Bosque, M. W. Miller, J. Safar, S. J. DeArmond and S. B. Prusiner (2006). "Transmission of elk and deer prions to transgenic mice." J Virol **80**(18): 9104-9114.
Tang, Y., W. Xiang, L. Terry, H. A. Kretzschmar and O. Windl (2010). "Transcriptional analysis implicates endoplasmic reticulum stress in bovine spongiform encephalopathy." PLoS One **5**(12): e14207.
Taylor, D. R., E. T. Parkin, S. L. Cocklin, J. R. Ault, A. E. Ashcroft, A. J. Turner and N. M. Hooper (2009). "Role of ADAMs in the ectodomain shedding and conformational conversion of the prion protein." J Biol Chem **284**(34): 22590-22600.

Tee, B. L., E. M. Longoria Ibarrola and M. D. Geschwind (2018). "Prion Diseases." Neurol Clin **36**(4): 865-897.
Thal, D. R., U. Rüb, M. Orantes and H. Braak (2002). "Phases of A beta-deposition in the human brain and its relevance for the development of AD." Neurology **58**(12): 1791-1800.
Tobler, I., S. E. Gaus, T. Deboer, P. Achermann, M. Fischer, T. Rulicke, M. Moser, B. Oesch, P. A. McBride and J. C. Manson (1996). "Altered circadian activity rhythms and sleep in mice devoid of prion protein." Nature **380**(6575): 639-642.
Urbach, H., J. Klisch, H. K. Wolf, D. Brechtelsbauer, S. Gass and L. Solymosi (1998). "MRI in sporadic Creutzfeldt-Jakob disease: correlation with clinical and neuropathological data." Neuroradiology **40**(2): 65-70.
United Nations, Department of Economic and Social Affairs, Population Division (2019). World Population Ageing 2019: Highlights (ST/ESA/SER.A/430)).
van Duijn, C. M., N. Delasnerie-Lauprêtre, C. Masullo, I. Zerr, R. de Silva, D. P. Wientjens, J. P. Brandel, T. Weber, V. Bonavita, M. Zeidler, A. Alpérovitch, S. Poser, E. Granieri, A. Hofman and R. G. Will (1998). "Case-control study of risk factors of Creutzfeldt-Jakob disease in Europe during 1993-95. European Union (EU) Collaborative Study Group of Creutzfeldt-Jakob disease (CJD)." Lancet **351**(9109): 1081-1085.
Vanni, S. (2017). "Omics of Prion Diseases." Prog Mol Biol Transl Sci **150**: 409-431.
Vanni, S., A. Colini Baldeschi, M. Zattoni and G. Legname (2020). "Brain aging: A Ianus-faced player between health and neurodegeneration." J Neurosci Res **98**(2): 299-311.
Vanni, S., F. Moda, M. Zattoni, E. Bistaffa, E. De Cecco, M. Rossi, G. Giaccone, F. Tagliavini, S. Haik, J. P. Deslys, G. Zanusso, J. W. Ironside, I. Ferrer, G. G. Kovacs and G. Legname (2017). "Differential overexpression of SERPINA3 in human prion diseases." Sci Rep **7**(1): 15637.
Vanni, S., M. Zattoni, F. Moda, G. Giaccone, F. Tagliavini, S. Haik, J. P. Deslys, G. Zanusso, J. W. Ironside, M. Carmona, I. Ferrer, G. G. Kovacs and G. Legname (2018). "Hemoglobin mRNA Changes in the Frontal Cortex of Patients with Neurodegenerative Diseases." Front Neurosci **12**: 8.
Vaughan, P. J., J. Su, C. W. Cotman and D. D. Cunningham (1994). "Protease nexin-1, a potent thrombin inhibitor, is reduced around cerebral blood vessels in Alzheimer's disease." Brain Res **668**(1-2): 160-170.
Vicente, C. P., L. He, M. S. Pavao and D. M. Tollefsen (2004). "Antithrombotic activity of dermatan sulfate in heparin cofactor II-deficient mice." Blood **104**(13): 3965-3970.
Victoria, G. S., A. Arkhipenko, S. Zhu, S. Syan and C. Zurzolo (2016). "Astrocyte-to-neuron intercellular prion transfer is mediated by cell-cell contact." Sci Rep **6**: 20762.
Vicuña, L., D. E. Strochlic, A. Latremoliere, K. K. Bali, M. Simonetti, D. Husainie, S. Prokosch, P. Riva, R. S. Griffin, C. Njoo, S. Gehrig, M. A. Mall, B. Arnold, M. Devor, C. J. Woolf, S. D. Liberles, M. Costigan and R. Kuner (2015). "The serine protease inhibitor SerpinA3N attenuates neuropathic pain by inhibiting T cell-derived leukocyte elastase." Nat Med **21**(5): 518-523.
Vilette, D. (2008). "Cell models of prion infection." Vet Res **39**(4): 10.
Vincent, B., E. Paitel, P. Saftig, Y. Frobert, D. Hartmann, B. De Strooper, J. Grassi, E. Lopez-Perez and F. Checler (2001). "The disintegrins ADAM10 and TACE contribute to the constitutive and phorbol ester-regulated normal cleavage of the cellular prion protein." J Biol Chem **276**(41): 37743-37746.
Vingtdeux, V., U. Dreses-Werringloer, H. Zhao, P. Davies and P. Marambaud (2008). "Therapeutic potential of resveratrol in Alzheimer's disease." BMC Neurosci **9 Suppl 2**: S6.
Visentin, C., L. Broggini, B. M. Sala, R. Russo, A. Barbiroli, C. Santambrogio, S. Nonnis, A. Dubnovitsky, M. Bolognesi, E. Miranda, A. Achour and S. Ricagno (2020). "Glycosylation Tunes Neuroserpin Physiological and Pathological Properties." Int J Mol Sci **21**(9).

Vázquez-Fernández, E., M. R. Vos, P. Afanasyev, L. Cebey, A. M. Sevillano, E. Vidal, I. Rosa, L. Renault, A. Ramos, P. J. Peters, J. J. Fernández, M. van Heel, H. S. Young, J. R. Requena and H. Wille (2016). "The Structural Architecture of an Infectious Mammalian Prion Using Electron Cryomicroscopy." PLoS Pathog **12**(9): e1005835.
Wagner, G. P., K. Kin and V. J. Lynch (2012). "Measurement of mRNA abundance using RNA-seq data: RPKM measure is inconsistent among samples." Theory Biosci **131**(4): 281-285.
Wagner, S. L., J. W. Geddes, C. W. Cotman, A. L. Lau, D. Gurwitz, P. J. Isackson and D. D. Cunningham (1989). "Protease nexin-1, an antithrombin with neurite outgrowth activity, is reduced in Alzheimer disease." Proc Natl Acad Sci U S A **86**(21): 8284-8288.
Walker, L. C. and M. Jucker (2015). "Neurodegenerative diseases: expanding the prion concept." Annu Rev Neurosci **38**: 87-103.
Walmsley, A. R., N. T. Watt, D. R. Taylor, W. S. Perera and N. M. Hooper (2009). "alpha-cleavage of the prion protein occurs in a late compartment of the secretory pathway and is independent of lipid rafts." Mol Cell Neurosci **40**(2): 242-248.
Walter, E. D., D. J. Stevens, M. P. Visconte and G. L. Millhauser (2007). "The prion protein is a combined zinc and copper binding protein: Zn2+ alters the distribution of Cu2+ coordination modes." J Am Chem Soc **129**(50): 15440-15441.
Wang, L. Q., K. Zhao, H. Y. Yuan, Q. Wang, Z. Guan, J. Tao, X. N. Li, Y. Sun, C. W. Yi, J. Chen, D. Li, D. Zhang, P. Yin, C. Liu and Y. Liang (2020). "Cryo-EM structure of an amyloid fibril formed by full-length human prion protein." Nat Struct Mol Biol **27**(6): 598-602.
Watts, J. C., K. Giles, S. Patel, A. Oehler, S. J. DeArmond and S. B. Prusiner (2014). "Evidence that bank vole PrP is a universal acceptor for prions." PLoS Pathog **10**(4): e1003990.
Westergard, L., J. A. Turnbaugh and D. A. Harris (2011). "A naturally occurring C-terminal fragment of the prion protein (PrP) delays disease and acts as a dominant-negative inhibitor of PrPSc formation." J Biol Chem **286**(51): 44234-44242.
Whisstock, J. C., R. N. Pike, L. Jin, R. Skinner, X. Y. Pei, R. W. Carrell and A. M. Lesk (2000). "Conformational changes in serpins: II. The mechanism of activation of antithrombin by heparin." J Mol Biol **301**(5): 1287-1305.
Whisstock, J. C., G. A. Silverman, P. I. Bird, S. P. Bottomley, D. Kaiserman, C. J. Luke, S. C. Pak, J. M. Reichhart and J. A. Huntington (2010). "Serpins flex their muscle: II. Structural insights into target peptidase recognition, polymerization, and transport functions." J Biol Chem **285**(32): 24307-24312.
Widmer, C., J. M. Gebauer, E. Brunstein, S. Rosenbaum, F. Zaucke, C. Drogemuller, T. Leeb and U. Baumann (2012). "Molecular basis for the action of the collagen-specific chaperone Hsp47/SERPINH1 and its structure-specific client recognition." Proc Natl Acad Sci U S A **109**(33): 13243-13247.
Wieser, H. G., K. Schindler and D. Zumsteg (2006). "EEG in Creutzfeldt-Jakob disease." Clin Neurophysiol **117**(5): 935-951.
Wilesmith, J. W., J. B. Ryan and M. J. Atkinson (1991). "Bovine spongiform encephalopathy: epidemiological studies on the origin." Vet Rec **128**(9): 199-203.
Wilham, J. M., C. D. Orrú, R. A. Bessen, R. Atarashi, K. Sano, B. Race, K. D. Meade-White, L. M. Taubner, A. Timmes and B. Caughey (2010). "Rapid end-point quantitation of prion seeding activity with sensitivity comparable to bioassays." PLoS Pathog **6**(12): e1001217.
Will, R. G. (2003). "Acquired prion disease: iatrogenic CJD, variant CJD, kuru." Br Med Bull **66**: 255-265.
Will, R. G., J. W. Ironside, M. Zeidler, S. N. Cousens, K. Estibeiro, A. Alperovitch, S. Poser, M. Pocchiari, A. Hofman and P. G. Smith (1996). "A new variant of Creutzfeldt-Jakob disease in the UK." Lancet **347**(9006): 921-925.

Williams, E. S. and S. Young (1980). "Chronic wasting disease of captive mule deer: a spongiform encephalopathy." J Wildl Dis **16**(1): 89-98.
Wroe, S. J., S. Pal, D. Siddique, H. Hyare, R. Macfarlane, S. Joiner, J. M. Linehan, S. Brandner, J. D. Wadsworth, P. Hewitt and J. Collinge (2006). "Clinical presentation and pre-mortem diagnosis of variant Creutzfeldt-Jakob disease associated with blood transfusion: a case report." Lancet **368**(9552): 2061-2067.
Xanthopoulos, K., I. Paspaltsis, V. Apostolidou, S. Petrakis, C. J. Siao, A. Kalpatsanidis, N. Grigoriadis, A. Tsaftaris, S. E. Tsirka and T. Sklaviadis (2005). "Tissue plasminogen activator in brain tissues infected with transmissible spongiform encephalopathies." Neurobiol Dis **20**(2): 519-527.
Xerxa, E., M. Barbisin, M. N. Chieppa, H. Krmac, E. Vallino Costassa, P. Vatta, M. Simmons, M. Caramelli, C. Casalone, C. Corona and G. Legname (2016). "Whole Blood Gene Expression Profiling in Preclinical and Clinical Cattle Infected with Atypical Bovine Spongiform Encephalopathy." PLoS One **11**(4): e0153425.
Xiang, W., M. Hummel, G. Mitteregger, C. Pace, O. Windl, U. Mansmann and H. A. Kretzschmar (2007). "Transcriptome analysis reveals altered cholesterol metabolism during the neurodegeneration in mouse scrapie model." J Neurochem **102**(3): 834-847.
Xiang, W., O. Windl, G. Wunsch, M. Dugas, A. Kohlmann, N. Dierkes, I. M. Westner and H. A. Kretzschmar (2004). "Identification of differentially expressed genes in scrapie-infected mouse brains by using global gene expression technology." J Virol **78**(20): 11051-11060.
Xiao, X., J. Yuan, L. Qing, I. Cali, J. Mikol, M. B. Delisle, E. Uro-Coste, L. Zeng, M. Abouelsaad, D. Gazgalis, M. C. Martinez, G. X. Wang, P. Brown, J. W. Ironside, P. Gambetti, Q. Kong and W. Q. Zou (2014). "Comparative Study of Prions in Iatrogenic and Sporadic Creutzfeldt-Jakob Disease." J Clin Cell Immunol **5**(4).
Yamada, M. (2002). "Risk factors for cerebral amyloid angiopathy in the elderly." Ann N Y Acad Sci **977**: 37-44.
Yamaguchi, K., Y. O. Kamatari, F. Ono, H. Shibata, T. Fuse, A. E. Elhelaly, M. Fukuoka, T. Kimura, J. Hosokawa-Muto, T. Ishikawa, M. Tobiume, Y. Takeuchi, Y. Matsuyama, D. Ishibashi, N. Nishida and K. Kuwata (2019). "A designer molecular chaperone against transmissible spongiform encephalopathy slows disease progression in mice and macaques." Nat Biomed Eng **3**(3): 206-219.
Yamamoto, M., I. Kondo, N. Ogawa, M. Asanuma, Y. Yamashita and Y. Mizuno (1997). "Genetic association between susceptibility to Parkinson's disease and alpha1-antichymotrypsin polymorphism." Brain Res **759**(1): 153-155.
Ying, Y. S., R. G. Anderson and K. G. Rothberg (1992). "Each caveola contains multiple glycosyl-phosphatidylinositol-anchored membrane proteins." Cold Spring Harb Symp Quant Biol **57**: 593-604.
Yoo, Y., K. Byun, T. Kang, D. Bayarsaikhan, J. Y. Kim, S. Oh, Y. H. Kim, S. Y. Kim, W. I. Chung, S. U. Kim, B. Lee and Y. M. Park (2015). "Amyloid-beta-activated human microglial cells through ER-resident proteins." J Proteome Res **14**(1): 214-223.
Zahn, R., A. Liu, T. Luhrs, R. Riek, C. von Schroetter, F. Lopez Garcia, M. Billeter, L. Calzolai, G. Wider and K. Wuthrich (2000). "NMR solution structure of the human prion protein." Proc Natl Acad Sci U S A **97**(1): 145-150.
Zattoni, M. and G. Legname (2021). "Tackling prion diseases: a review of the patent landscape." Expert Opin Ther Pat.
Zerr, I., K. Kallenberg, D. M. Summers, C. Romero, A. Taratuto, U. Heinemann, M. Breithaupt, D. Varges, B. Meissner, A. Ladogana, M. Schuur, S. Haik, S. J. Collins, G. H. Jansen, G. B. Stokin, J. Pimentel, E. Hewer, D. Collie, P. Smith, H. Roberts, J. P. Brandel, C. van Duijn, M. Pocchiari, C. Begue, P. Cras, R. G. Will and P. Sanchez-Juan (2009). "Updated clinical diagnostic criteria for sporadic Creutzfeldt-Jakob disease." Brain **132**(Pt 10): 2659-2668.

Zhao, N., Y. Ren, Y. Yamazaki, W. Qiao, F. Li, L. M. Felton, S. Mahmoudiandehkordi, A. Kueider-Paisley, B. Sonoustoun, M. Arnold, F. Shue, J. Zheng, O. N. Attrebi, Y. A. Martens, Z. Li, L. Bastea, A. D. Meneses, K. Chen, J. W. Thompson, L. St John-Williams, M. Tachibana, T. Aikawa, H. Oue, L. Job, A. Yamazaki, C. C. Liu, P. Storz, Y. W. Asmann, N. Ertekin-Taner, T. Kanekiyo, R. Kaddurah-Daouk and G. Bu (2020). "Alzheimer's Risk Factors Age, APOE Genotype, and Sex Drive Distinct Molecular Pathways." Neuron **106**(5): 727-742.e726.
Zhou, Y., W. M. Song, P. S. Andhey, A. Swain, T. Levy, K. R. Miller, P. L. Poliani, M. Cominelli, S. Grover, S. Gilfillan, M. Cella, T. K. Ulland, K. Zaitsev, A. Miyashita, T. Ikeuchi, M. Sainouchi, A. Kakita, D. A. Bennett, J. A. Schneider, M. R. Nichols, S. A. Beausoleil, J. D. Ulrich, D. M. Holtzman, M. N. Artyomov and M. Colonna (2020). "Human and mouse single-nucleus transcriptomics reveal TREM2-dependent and TREM2-independent cellular responses in Alzheimer's disease." Nat Med **26**(1): 131-142.
Zou, Z., A. Anisowicz, M. J. Hendrix, A. Thor, M. Neveu, S. Sheng, K. Rafidi, E. Seftor and R. Sager (1994). "Maspin, a serpin with tumor-suppressing activity in human mammary epithelial cells." Science **263**(5146): 526-529.